

# Università degli Studi di Padova

Dipartimento di Scienze Chirurgiche Oncologiche  
Gastroenterologiche

Corso di Dottorato in Oncologia Clinica e Sperimentale e  
Immunologia – XXXII ciclo

## **Therapeutic targeting of Hedgehog signalling pathway in T-cell acute lymphoblastic leukemia (T-ALL)**

*Coordinatrice:* Chiar.ma Prof.ssa Paola Zanovello

*Supervisore:* Dr. Erich Piovan

*Dottoranda:* Deborah Bongiovanni



# Index

SUMMARY .....	1
RIASSUNTO .....	3
1. INTRODUCTION .....	6
1.1 T-CELL ACUTE LYMPHOBLASTIC LEUKEMIA .....	7
1.1.1 Molecular pathogenesis .....	7
1.1.1.1 The genetic landscape of T-ALL .....	7
1.1.1.2 Oncogenic signalling pathways .....	9
1.1.2 T-ALL classification .....	15
1.1.3 Treatment of T-ALL .....	17
1.1.3.1 Opportunities for targeted therapies .....	19
1.2. HEDGEHOG SIGNALLING PATHWAY .....	23
1.2.1 Canonical pathway activation .....	23
1.2.2 Hedgehog pathway activation and cancer: .....	26
1.2.3. SHH signalling in T-cell maturation .....	32
1.2.4. SHH signalling in hematological malignancies .....	33
2. AIM OF THE THESIS .....	36
3. MATERIALS AND METHODS .....	39
3.1 CELL LINES AND PRIMARY T-ALL XENOGRAFTS .....	40
3.2 DRUG TREATMENTS .....	41
3.3 CELL VIABILITY ASSAY .....	41
3.4 APOPTOSIS AND CELL CYCLE ANALYSIS .....	42
3.5 PLASMIDS .....	42
3.6 RETROVIRUS PRODUCTION .....	43
3.7 RNA EXTRACTION, REVERSE-TRANSCRIPTION AND QUANTITATIVE REAL TIME PCR .....	43
3.8 WESTERN BLOT ANALYSIS .....	45

3.9 CELLULAR FRACTIONATION, IMMUNOPRECIPITATION ANALYSIS AND PROTEIN HALF-LIFE DETERMINATION .....	46
3.10 DUAL LUCIFERASE REPORTER ASSAY .....	47
3.11 STATISTICAL ANALYSIS.....	48
4. RESULTS.....	50
4.1 EXPRESSION OF HEDGEHOG PATHWAY COMPONENTS IN T-ALL.....	51
4.2 ASSESSMENT OF THE EFFECTS OF HEDGEHOG INHIBITION ON T-ALL CELLS IN VITRO.....	58
4.3 GANT61 AND DEXAMETHASONE SHOW A SYNERGISTIC ANTI-LEUKEMIC EFFECT IN VITRO.....	61
4.4 DEXAMETHASONE IMPAIRS GLI1 FUNCTION.....	69
4.5 DEXAMETHASONE DOES NOT AFFECT GLI1 SUBCELLULAR LOCALIZATION .....	77
4.6 DEXAMETHASONE REDUCES GLI1 PROTEIN STABILITY .....	78
4.7 NR3C1 INTERACTS WITH GLI1 AND PROMOTES ITS ACETYLATION .....	80
5. DISCUSSION.....	86
6. REFERENCES.....	94
LIST OF FIGURES.....	114
LIST OF TABLES .....	115
LIST OF ABBREVIATIONS.....	116



# SUMMARY

T-cell acute lymphoblastic leukemia (T-ALL) is an aggressive hematological tumour arising from the malignant transformation of T-cell precursors. Notwithstanding intensified therapy, ~40% of adult and ~20% of pediatric patients face a dismal prognosis due to primary resistance to treatment and relapse, raising the need for more efficient and targeted therapies.

Hedgehog (HH) signalling is a major developmental pathway frequently deregulated in cancer, for which a role in T-ALL is recently emerging. The therapeutic targeting of HH signalling in T-ALL by specific inhibitors *in vitro* and *in vivo* was shown to be partially effective when used as monotherapy and seems to suggest an important role for the non-canonical activation of the pathway (*i.e.* independent of upstream Smoothed receptor). This non-canonical activation of GLI1 transcription factor, the main HH downstream effector, underscores the necessity of dissecting the complex regulatory network upstream of GLI1 in T-ALL.

In this study, we evaluated gene and protein expression of HH pathway components in T-ALL cell lines, patient-derived xenografts (PDX) and Notch1-dependent T-ALL murine models, confirming their expression in the majority of the tested samples. A significant fraction of T-ALL cell lines and PDX-derived cells were sensitive to HH pathway inhibition by GANT61 (GLI1/2 inhibitor), much less so to cyclopamine (Smoothed inhibitor).

Interestingly, in a Notch1-induced T-ALL murine model, pharmacological combinations targeting commonly deregulated oncogenic pathways in T-ALL revealed a therapeutically relevant synergism between GANT61 and glucocorticoids (GCs). Combined treatment of T-ALL cell lines and PDX-derived cells with GANT61 plus Dexamethasone (Dexa) showed a synergistic anti-leukemic effect, affecting both cell proliferation and survival. In order to gain mechanistic insights of the found crosstalk between the HH pathway and

the GC receptor pathway, we studied the impact of synthetic GCs on GLI1 function. GCs impaired GLI1 transcriptional activity in transfected HEK-293T cells stably expressing the GC receptor; however, gene expression data and Western blot analysis seemed to exclude a transcriptional effect of GCs on GLI1, but rather suggested a post-translational mechanism of action. Cell fractionation analysis did not reveal significant re-distribution of GLI1 upon Dexa treatment, while GLI1 stability was shown to be impaired, revealing a reduced protein half-life after treatment. Finally, GLI1 and the GC receptor were shown to interact, with the GC receptor recruiting the acetyltransferase PCAF and dissociating from the deacetylase HDAC1 upon Dexa treatment, thus putatively leading to GLI1 hyperacetylation and reduced transcriptional activity.

In conclusion, we demonstrated that HH pathway is active in a subset of T-ALLs and the differential sensitivity to HH inhibitors suggests a ligand-independent non-canonical mechanism of activation. We also collected evidence of a crosstalk between the GC receptor and HH pathway, with the GC receptor acting as a negative regulator of GLI1 transcription factor, setting the therapeutic rationale for combining GLI1 inhibitors and GCs.

# RIASSUNTO

La leucemia linfoblastica acuta a cellule T (T-ALL) è un tumore ematologico aggressivo che ha origine dalla trasformazione maligna dei precursori dei linfociti T. Nonostante la chemioterapia intensiva, il ~40% dei pazienti adulti e il ~20% dei pazienti pediatrici va incontro a prognosi infausta a causa di resistenza primaria alla terapia o di recidiva, sottolineando la necessità di terapie più mirate ed efficaci.

La via di segnalazione di Hedgehog (HH), essenziale per il normale sviluppo embrionale e dell'adulto, risulta essere frequentemente deregolata nel cancro e recentemente ne sta emergendo un ruolo anche nella T-ALL. L'inibizione mirata *in vitro* e *in vivo* della via di HH tramite specifici inibitori si è rivelata parzialmente efficace nella T-ALL se usata come monoterapia, evidenziando inoltre un ruolo importante dell'attivazione non canonica di HH, cioè indipendente dal recettore Smoothened. L'attivazione non canonica della via a livello del fattore di trascrizione GLI1, il principale effettore a valle di HH, indica la necessità di delucidare il complesso network di regolazione a monte di GLI1 nella T-ALL.

In questo studio, abbiamo valutato l'espressione genica e proteica dei componenti della via di HH nella T-ALL usando linee cellulari, cellule derivate da paziente xenotrapiantate in topo (PDX, patient-derived xenografts) e modelli murini Notch1-dipendenti, confermando la loro espressione nella maggioranza dei campioni in esame. Una frazione significativa delle linee cellulari e delle cellule derivate da PDX è risultata essere sensibile all'inibizione della via di HH tramite GANT61 (inibitore di GLI1/2) e in minor misura tramite ciclopamina (inibitore di Smoothened).

Inoltre, in un modello murino di T-ALL Notch1-dipendente, combinazioni di farmaci agenti su diversi pathway oncogenici comunemente deregolati nella



T-ALL hanno evidenziato un sinergismo rilevante dal punto di vista terapeutico fra GANT61 e i glucocorticoidi (GC). Il trattamento combinato di GANT61 e desametasone (Dexa) su linee cellulari e cellule derivate da PDX ha mostrato un effetto sinergico anti-leucemico, compromettendo proliferazione e sopravvivenza cellulari. Al fine di avere un quadro più meccanicistico dell'interazione osservata fra la via di HH e la via di segnalazione dei GC, abbiamo studiato l'effetto di GC sintetici sulla funzionalità di GLI1. I GC hanno compromesso l'attività trascrizionale di GLI1 in cellule HEK-293T stabilmente esprimenti il recettore dei GC; tuttavia, i dati di espressione genica e proteica sembrano escludere un effetto trascrizionale dei GC su GLI1, ma suggeriscono piuttosto un meccanismo d'azione post-traduzionale. L'analisi tramite frazionamento cellulare non ha evidenziato un'alterata distribuzione di GLI1 a seguito del trattamento con Dexa, mentre la stabilità di GLI1 è risultata essere compromessa, mostrando una ridotta emivita della proteina dopo trattamento. Infine, GLI1 e il recettore dei GC sono risultati interagire e il trattamento con Dexa ha determinato un reclutamento della acetiltrasferasi PCAF e una dissociazione della deacetilasi HDAC1 dal complesso, così promuovendo uno stato iperacetilato e meno attivo di GLI1.

In conclusione, abbiamo dimostrato che la via di HH è attiva in un sottogruppo di casi di T-ALL e la diversa sensibilità ai farmaci inibitori della via suggerisce un possibile meccanismo di attivazione non canonico e ligando-indipendente. Inoltre, abbiamo evidenziato un'interazione fra la via dei GC e la via di HH, in cui il recettore dei GC agisce da regolatore negativo del fattore di trascrizione GLI1, fornendo un razionale terapeutico per combinazioni di inibitori di GLI1 e GC.



# **1. Introduction**

## 1.1 T-cell acute lymphoblastic leukemia

T-cell acute lymphoblastic leukemia (T-ALL) is an aggressive hematologic tumor, accounting for 15% of pediatric and 25% of adult newly diagnosed ALL cases [1]. Clinically, T-ALL patients present with diffuse infiltration of the bone marrow by immature T-cell blasts, high white blood cell counts, and mediastinal and central nervous system (CNS) involvement. Compared to the more common B-cell lineage ALL (B-ALL), T-ALL is associated with unfavorable prognosis, with higher rates of relapse [2].

T-ALL results from the malignant transformation and uncontrolled clonal proliferation of an immature lymphoid cell committed to T-cell lineage. At the molecular level, T-ALL is a heterogeneous disease, where a wide spectrum of genetic lesions and micro-environmental factors cooperate to promote a multistep leukemogenic process, altering normal cell growth, survival, proliferation and differentiation during thymocyte development.

### 1.1.1 Molecular pathogenesis

#### 1.1.1.1 The genetic landscape of T-ALL

Recent improvements in genome-wide profiling and sequencing studies provided a more comprehensive view of major genetic aberrations involved in T-ALL pathogenesis, identifying ~20 genes that are recurrently mutated. Mutations do not occur randomly, but are grouped by clusters of frequently associated or mutually exclusive genes [3]. The most prominent genetic alteration in T-ALL (>70% of pediatric cases) is the deletion of the cyclin-dependent kinase inhibitor 2A (CDKN2A) locus on chromosome 9p21 affecting the expression of p16/INK4A and p14/ARF tumor suppressor

genes, which regulate cell cycle progression and p53-mediated apoptosis, respectively [4,5].

Additional frequent and characteristic events of T-ALL are chromosomal translocations of transcription factor genes to regulatory regions of T-cell receptor genes, leading to the aberrant expression of rearranged proto-oncogenes.

These transcription factors include:

- *basic helix-loop-helix (bHLH) transcription factors*: T-cell acute lymphoblastic leukemia 1 (TAL1) [6], TAL2 [7], lymphoblastic leukemia associated hematopoietic regulator 1 (LYL1) [8], and BHLHB1 [9];
- *LIM-only domain (LMO) transcription factors*: LMO1 and LMO2 [10]-[11];
- *homeobox (HOX) transcription factors*: T-cell leukemia homeobox 1 (TLX1/HOX11) [12], TLX3 (HOX11L2) [13], NK2 homeobox NKX2-1, NKX2-2 and NKX2-5 [14,15], and homeobox A (HOXA) cluster [16];
- *other proto-oncogenes*: avian myelocytomatosis viral oncogene homolog (MYC) [17] and myeloblastosis transcriptional activator (MYB) [18].

Deregulated transcription factors are associated with specific transcriptional profiles that define distinct molecular T-ALL subgroups (TAL1/LMO; TLX1; TLX3; HOXA subtypes).

Moreover, mutations and deletions in tumor suppressor genes such as Wilms Tumor 1 (WT1), Lymphoid Enhancer Binding Factor 1 (LEF1), ETS Variant 6 (ETV6), B-Cell CLL/Lymphoma 11B (BCL11B), Runt Related Transcription Factor 1 (RUNX1) and GATA Binding Protein 3 (GATA3) contribute to the overall transcriptional deregulation of T-ALL [19-23].

In addition, several genes encoding epigenetic regulators and chromatin modifiers are also recurrently mutated in T-ALL [24], including Enhancer of zeste homolog 2 (EZH2), suppressor of zeste 12 homolog (SUZ12) and embryonic ectoderm development (EED), the plant homeodomain factor gene

PHF6, the histone demethylase 6A (KDM6A) and ubiquitin specific peptidase 7 (USP7).

### 1.1.1.2 Oncogenic signalling pathways

The genetic landscape of T-ALL pathogenesis is further complicated by alterations in signalling pathways that are commonly shared across the different molecular subgroups and crosstalk to promote disease progression providing proliferative and survival advantages to T-ALL blasts. These signalling pathways, which are crucial to normal T-cell development, control a plethora of biological processes and offer numerous opportunities for targeted therapies (see Paragraph 1.1.3.1). Deregulated signalling pathways in T-ALL mainly result from cell intrinsic factors, such as genetic lesions in critical signalling components, or as a response to cell-extrinsic micro-environmental factors, such as nutrient availability, hypoxia, chemokines, and growth factors [25].

An overview of relevant signalling pathways in T-ALL pathogenesis is shown in Figure 1, adapted from Bongiovanni *et al.* [25]:

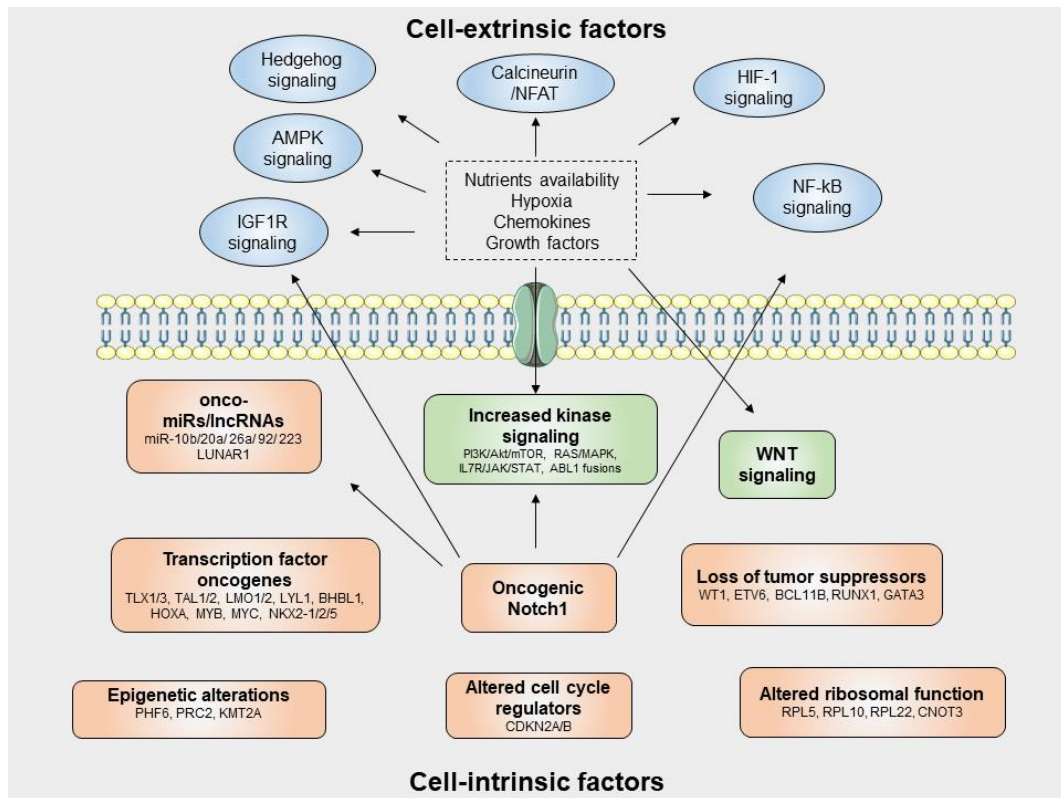


**Figure 1: Oncogenic pathways in T-ALL**

Schematic representation of cell-extrinsic (blue), cell-intrinsic (red) or mixed factors (green) contributing to T-ALL leukemogenic process. Adapted from *Bongiovanni et al.* [25]

## *NOTCH1 pathway*

Together with chromosomal rearrangements and loss of the CDKN2A locus, the most important hallmark of T-ALL is the oncogenic activation of NOTCH1 signalling, with over 60% of T-ALL patients harboring activating mutations in NOTCH1 [26]. The members of NOTCH protein family are essential regulators of early T-cell fate specification and thymocyte development [27]. NOTCH1 activating mutations lead to the ligand-independent release of the intracellular domain of NOTCH1 (ICN), which subsequently translocates to the nucleus where it acts as a transcription factor. Alternatively, NOTCH1 mutations in the proline, glutamic acid, serine,

threonine-rich (PEST) domain or inactivating mutations in F-box and WD repeat domain containing 7 (FBXW7) preserve ICN from ubiquitin-mediated degradation by the proteasome [28]. NOTCH1 can promote leukemia cell growth via direct transcriptional upregulation of anabolic pathways, including ribosome biosynthesis, protein translation and nucleotide and amino acid metabolism [4]. Moreover, NOTCH1-mediated transcriptional upregulation of MYC oncogene can further enhance these growth-promoting effects. In addition, NOTCH directly regulates Interleukin-7-receptor (IL-7R) [29] and Insulin-like growth factor (IGF1R) [30] genes, which both are important in T-ALL mediating survival and proliferative signals to foster the leukemogenic process.

### *PI3K/AKT/mTOR pathway*

Phosphoinositide 3-kinase (PI3K)/AKT pathway is aberrantly activated in >85% T-ALL cases [31]. Frequently, PI3K/AKT pathway is activated by deletions or loss of function mutations in phosphatase and tensin homolog (PTEN), a lipid phosphatase functioning as the main negative regulator of the pathway [31,32]. In addition, PTEN can be inactivated by transcriptional repression by NOTCH1 target hairy and enhancer of split-1 (HES1), by casein kinase 2 (CK2)-mediated phosphorylation or reactive oxygen species (ROS)-induced oxidation [31]. Moreover, PI3K/AKT/mammalian target of rapamycin (mTOR) pathway is activated downstream of IL-7R signalling [33] and IGF1R signalling [30]. Mutations affecting PTEN/PI3K/AKT pathway are highly prevalent in TAL1<sup>+</sup> cases, suggesting that TAL1 over-expression cooperates with mutations affecting the PI3K/AKT pathway (especially PTEN inactivation) to promote T-cell transformation.



### *IL-7R/JAK/STAT pathway*

IL-7 is an essential cytokine for normal T-cell development and homeostasis, promoting cell survival and cell cycle progression. In T-ALL, stromal cells of the tumor microenvironment (*i.e.* thymus and bone marrow) secrete IL-7 and favor disease progression [34,35]. Approximately 10% of T-ALL cases show gain of function mutations in IL-7R, resulting in constitutive Janus kinase/signal transducer and activator of transcription (JAK/STAT) signalling [36]. Gain of function mutations in JAK1, JAK3, STAT5 have also been detected in a variable fraction of T-ALL cases [21,37-39]. Mutations affecting IL-7R/JAK/STAT pathway are particularly enriched in TLX1/TLX3<sup>+</sup> and HOXA<sup>+</sup> T-ALL cases [36]. Moreover, IL7R is also a direct transcriptional target of NOTCH1, leading to hyperactivated IL7 signalling cascade also in the absence of mutations in IL-7R, JAK or STAT genes [29].

### *RAS/MAPK pathway*

Activating mutations in Kirsten/Harvey rat sarcoma viral oncogene homologs (KRAS, HRAS) and protein phosphatase non-receptor type 11 (PTPN11) oncogenes have been described in 5-10% of T-ALL, in particular in the early T-cell precursor ALL (ETP-ALL) subgroup (see Paragraph 1.1.2 for T-ALL classification) [21]. In addition, cryptic deletions and/or mutations in neurofibromin 1 (NF1) tumor suppressor gene, encoding a negative regulator of Ras pathway, occur in 3% of T-ALL [40].

### *Chimeric ABL1 fusion genes*

Aberrant rearrangements of Abelson murine leukemia viral oncogene homolog 1 (ABL1) tyrosine kinase occur in about 8% of T-ALL cases [41]. While breakpoint cluster region (BCR)-ABL1 fusion protein is a hallmark of chronic myeloid leukemia (CML), it is exceptionally rare in T-ALL [42]. The

most frequent and T-ALL specific ABL1 rearrangement is Nucleoporin 214 (NUP214)-ABL1 episomal amplification (6% cases) [43,44].

Additional pathogenic mechanisms reported to play a role in T-ALL as a result of genetic lesions include altered ribosomal function through mutations affecting ribosomal proteins (e.g. RPL5, RPL10, RPL22) [45] and altered expression of oncogenic miRNAs (e.g. miR-19b, miR-20a, miR-26a, miR-92, and miR-223) or long non-coding RNAs, such as leukemia-induced non coding activator RNA 1 (LUNAR1) [46].

The most common genetic lesions found in T-ALL patients are listed in Table 1, extracted from Belver *et al.* [4]:

**Table 1: Genetic alterations in T-ALL**

Gene	Genetic lesion	Frequency (%)	Refs
<i>Transcription factor oncogenes</i>			
TAL1	t(1;14)(p32;q11)	3	192
	t(1;7)(p32;q34)	<1	82
	5' super-enhancer generating mutations	5	61,62
	1p32 deletion	25	192
TAL2	t(7;9)(q34;q32)	1	7
LYL1	t(7;19)(q34;p13)	1	8
BHLHB1	t(14;21)(q11.2;q22)	1	9
LMO1	• t(11;14)(p15;q11)	1	11,87
	• t(7;11)(q34;p15)		
LMO2	t(11;14)(p13;q11)	6	10
	t(7;11)(q34;p13)	<1	193
	11p13 deletion	3	70
TLX1	t(10;14)(q24;q11)	5–10 (paediatric T-ALL)	24
	• t(7;10)(q35;q24)	30 (adult T-ALL)	89
	• del(10)(q24q26)		
TLX3	t(5;14)(q35;q32)	20–25 (paediatric T-ALL) and 5 (adult T-ALL)	14
HOXA	inv(7)(p15q34)	3	16,82
	t(7;7)(p15;q34)	3	194
PICALM–MLLT10	t(10;11)(p13;q14)	5–10	86
KMT2A–MLLT1 (also known as MLL–ENL)	t(11;19)(q23;p13)	5	195
SET–NUP214	9q34 deletion	3	87
NKX2-1	• inv(14)(q11.2q13) • inv(14)(q13q32.33) • t(7;14)(q34;q13)	5 (paediatric T-ALL)	15

# 1. Introduction

NKX2-2	t(14;20)(q11;p11)	1	15
ZEB2	t(2;14)(q22;q32)	<1	196
MYB	t(6;7)(q23;q34)	3	19
MYC	t(8;14)(q24;q11)	1	197
<b>NOTCH1 pathway</b>			
NOTCH1	t(7;9)(q34;q34.3)	<1	34
	Activating mutation	>60	4
FBXW7	Inactivating mutation	8–30	35,36
<b>Cell cycle</b>			
CDKN2A and CDKN2B	• 9p21 deletion • Methylation	>70	54
CCND2	• t(7;12)(q34;p13) • t(12;14)(p13;q11)	3	58
RB1	13q14.2 deletion	12 (paediatric T-ALL)	56
CDKN1B	12p13.2 deletion	12	57
<b>Transcription factor tumour suppressors</b>			
WT1	Inactivating mutation or deletion	10	97
LEF1	Inactivating mutation or deletion	10–15	129
ETV6	Inactivating mutation or deletion	13	26
BCL11B	Inactivating mutation or deletion	10	90,127
RUNX1	Inactivating mutation or deletion	10–20	95,198
GATA3	Inactivating mutation or deletion	5	27
<b>Signal transduction</b>			
PTEN	Inactivating mutation	10–15	145
	10q23 deletion	10–15	146,150
NUP214–ABL1	Episomal 9q34 amplification	5	99
EML1–ABL1	t(9;14)(q34;q32)	<1	199
ETV6–ABL1	t(9;12)(q34;p13)	<1	200
NRAS	Activating mutation	5	201,26
KRAS	Activating mutation	2	27
PTPN11	Mutation	3	27
NF1	Inactivating mutation or deletion	3	167
JAK1	Activating mutation	4–18	162,202
ETV6–JAK2	t(9;12)(p24;p13)	<1	153
JAK3	Activating mutation	7	27
FLT3	Activating mutation	5–10	27,203
IL7R	Activating mutation	10	154,155
IRS4	• t(X;7)(q22;q34) • t(X;14)(q22;q11.2)	<1	151
DNM2	Inactivating mutation	15	5,27
<b>Chromatin remodelling</b>			
EZH2	Inactivating mutation or deletion	10–15	27,140
SUZ12	Inactivating mutation or deletion	10	27
EED	Inactivating mutation or deletion	10	27
PHF6	Inactivating mutation or deletion	20–40	98
KDM6A	Inactivating mutation or deletion	5–15	141,143

(continued)

Ribosomal proteins and translation			
RPL10	Mutation	6 (paediatric T-ALL)	161
RPL11	Inactivating mutation	1	173
RPL5	Inactivating mutation	2	161
CNOT3	Mutation	10 (adult T-ALL)	161

*BHLHB1*, basic helix-loop-helix protein 1; *CCND2*, cyclin D2; *CDKN*, cyclin-dependent kinase inhibitor; *CNOT3*, CCR4–NOT transcription complex subunit 3; *DNM2*, DNA methylase 2; *EED*, embryonic ectoderm development; *EML1*, echinoderm microtubule associated protein like 1; *ETV6*, ETS variant 6; *EZH2*, enhancer of zeste 2; *FBXW7*, F-box and WD repeat domain containing 7; *FLT3*, fms related tyrosine kinase 3; *GATA3*, GATA binding protein 3; *HOXA*, homeobox A; *IL7R*, interleukin-7 receptor; *IRS4*, insulin receptor substrate 4; *JAK*, Janus kinase; *KDM6A*, lysine-specific demethylase 6A; *KMT2A*, histone-lysine N-methyltransferase 2A; *LEF1*, lymphoid enhancer factor 1; *LMO*, LIM domain only; *LYL1*, lymphoblastic leukaemia associated haematopoiesis regulator 1; *MLL*, mixed lineage leukaemia; *NF1*, neurofibromin; *NKX2*, NK2 homeobox; *NUP214*, nucleoporin 214; *PHF6*, PHD finger protein 6; *PICALM*, phosphatidylinositol-binding clathrin assembly protein; *PTPN11*, protein tyrosine phosphatase non-receptor type 11; *RB1*, retinoblastoma 1; *RPL*, ribosomal protein; *RUNX1*, runt related transcription factor 1; *SUZ12*, suppressor of zeste 12; T-ALL, T cell acute lymphoblastic leukaemia; *TAL*, T cell acute lymphocytic leukaemia; *TLX*, T cell leukaemia homeobox; *WT1*, Wilms tumour 1; *ZEB2*, zinc finger E-box binding homeobox 2.

## 1.1.2 T-ALL classification

T-ALL arises from the malignant transformation of immature progenitors primed towards T-cell development. As normal thymocytes mature, they are characterized by a changing pattern of cluster of differentiation (CD) markers; therefore, the constellation of CD markers in lymphoblasts can suggest the maturational stage at which the transformation occurs. Four immunophenotypic subgroups of T-ALL have been defined by the European Group for the Immunological Characterization of Leukemias (EGIL) [47,48]:

-*pro-T (T-I)*: CD3<sup>+</sup>/CD7<sup>+</sup>/CD2<sup>-</sup>/CD1a<sup>-</sup>/CD34<sup>+/-</sup>

-*pre-T (T-II)*: CD3<sup>+</sup>/CD7<sup>+</sup>/CD2<sup>+</sup>/CD1a<sup>-</sup>/CD34<sup>+/-</sup>

-*cortical T (T-III)*: CD3<sup>+</sup>/CD7<sup>+</sup>/CD2<sup>+</sup>/CD1a<sup>+</sup>/CD34<sup>-</sup>

-*mature T (T-IV)*: CD3<sup>+</sup>/CD7<sup>+</sup>/CD2<sup>+</sup>/CD1a<sup>-</sup>/CD34<sup>-</sup>/membrane CD3<sup>+</sup>.

The immature pro- and pre-T stages are double negative (DN) for CD4 and CD8 and the cortical T group is double positive (DP) for CD4 and CD8,

whereas the mature T group is single positive (SP) for CD4 or CD8 [49]. While pro- and pre- T-ALL subgroups tend to have a worse outcome, cortical and mature subtypes have a better prognosis [50].

Finally, the recently defined ETP-ALL, which accounts for 10% of pediatric and 40-50% of adult cases [51], present unique immunophenotypic features, which include lack of CD1a, CD4 and CD8 expression, weak CD5 expression, and expression of at least one myeloid and/or stem cell marker [52]. Initially ETP-ALL was associated with a very dismal outcome; however, in more recent studies intensified treatment strategies seemed to overcome the poor prognosis [53].

The immunophenotypic T-ALL subgroups are associated with distinct molecular subtypes showing unique transcriptional signatures, as a result of deregulated expression of specific transcription factor oncogenes (see Paragraph 1.1.1)

ETP-ALLs present an arrest at the earliest stages of T-cell differentiation and is associated with LYL1 overexpression. ETP-ALLs show a transcriptional program closely related to hematopoietic stem cells and myeloid progenitors, with predominant alterations in transcription factor genes regulating hematopoietic and T-cell fate development, such as RUNX1, GATA3 and ETV6 [52]. They have a lower prevalence of NOTCH1 mutations and frequently harbor mutations in genes commonly mutated in acute myeloid leukemia such as isocitrate dehydrogenase (IDH1), IDH2 and DNA methyltransferase 3A (DNMT3A) and fms related tyrosine kinase 3 (FLT3) [21,54,55].

Early cortical T-ALLs are arrested in the initial stages of cortical thymocyte maturation and are typically associated with activation of the TLX1, TLX3, NKX2-1 and NKX2-2 homeobox genes. They have the highest prevalence of NOTCH1 mutations and almost universally harbor deletions of the CDKN2A locus [14,56]. TLX1 and TLX3 specific cooperating mutations include

NUP214–ABL1 rearrangements and mutations in PHF6, WT1 and PTPN2 [51].

Late cortical leukemias typically present activation of the TAL1 oncogene, together with altered expression of LMO1 or LMO2. Frequent mutations in NOTCH1 and CDKN2A, and a high prevalence of PTEN mutations and deletions are also observed [56].

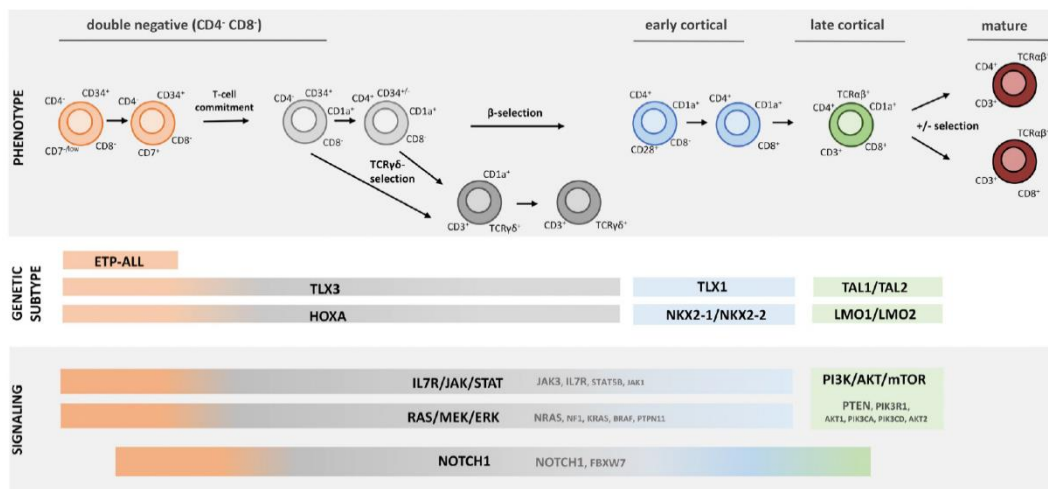


**Figure 2: Schematic representation of normal T-cell differentiation in humans in relation to the different T-ALL molecular subgroups**

Mutations that activate specific oncogenic signalling pathways are unequally enriched in T-ALL subgroups. The size of the font indicates the frequency of aberrations. Adapted from De Smedt *et al.* [57].

## 1.1.3 Treatment of T-ALL

The current standard treatment for T-ALL consists of high dose multi-agent chemotherapy, allowing 80% of pediatric and 40% of adult patients to achieve long-term remission [4]. The therapeutic protocols are designed according to risk stratification and criteria for treatment allocation are response-oriented, with Prednisone response and minimal residual disease

(MRD) analysis at different time points proven to be the strongest prognostic factors for T-ALL [50,58].

The Associazione Italiana di Emato-Oncologia Pediatrica (AIEOP)-Berlin-Frankfurt-Münster (BFM) study group traditionally evaluates the peripheral blood blast cell count after 7-day glucocorticoid pre-treatment to classify patients as Prednisone Good Responders (PGR,  $<1000/\mu\text{l}$  blasts on day 8) or Prednisone Poor Responders (PPR,  $\geq 1000/\mu\text{l}$  blasts), stratifying all PPR patients to the high risk group of treatment protocols [59].

After the initial Prednisone cytoreductive pre-phase, therapy of T-ALL is typically divided in three phases [59-62]:

- *Remission-induction phase*: the primary goal is to eradicate  $>99\%$  of the initial bulk of leukemic cells and achieve a rapid hematological recovery. Different combinations of drugs may be used, but they generally include a glucocorticoid (Dexamethasone or Prednisone) administered with vincristine, anthracyclines and l-asparaginase. For children in high-risk groups or adults, an additional dose of Cyclophosphamide (CPM) is typically added. As CNS involvement is a major clinical problem for T-ALL patients, CNS prophylaxis by intrathecal methotrexate (MTX) with or without cranial radiotherapy is usually started at induction and continued through the other phases.
- *Consolidation (intensification) phase*: once remission is achieved, intensification treatment with risk-based combinations of chemotherapeutics - including CPM, 6-Mercaptopurine (6-MP) and Cytarabine (ARA-C)- helps eradicating residual leukemic blasts and prevent the risk of relapse.
- *Maintenance- (continuation) phase*: after consolidation, the patient is generally put on a maintenance chemotherapy regimen for 2 years,

which is based on high dose MTX and 6-MP, often along with pulses of vincristine and steroids.

These aggressive regimens are often associated with acute toxicities and long-term side effects affecting bone development, fertility and the CNS [63]. Moreover, limited therapeutic options are available for primary resistant and relapsed patients, for which prognosis remains dismal.

Allogeneic hematopoietic stem cell transplantation is an option for persistent T-ALL at later times of treatment and represents the only curative option for the majority of relapsed/refractory cases [64,65].

While the treatment for relapsed B-ALL has been revolutionized by the recent approval of blinatumomab [66], inotuzumab ozagamicin [67] and anti-CD19 chimeric antigen receptor (CAR) T-cell therapy [68], treatment for refractory/relapsed T-ALL stalled since the approval of nelarabine in 2005 [69]. Indeed, Nelarabine, a pro-drug of ARA-G (9-beta-D-arabinofuranosylguanine) specifically cytotoxic to T-lymphoblasts [70], remains the only agent specifically approved for relapsed T-ALL to date.

### **1.1.3.1 Opportunities for targeted therapies**

Progress in our understanding of crucial genes, signalling pathways and molecular mechanisms underlying the pathobiology of T-ALL paved the way for novel targeted therapies, including immunotherapies and a number of small-molecule inhibitors targeting key drivers of the disease.

The most desirable target for T-ALL is NOTCH1, which would allow a therapeutic intervention in the over 60% of T-ALL patients harboring activating NOTCH1 mutations [26]. Several strategies to inhibit NOTCH1 signalling in T-ALL have been investigated, most notably gamma-secretase inhibitors (GSI). GSI block the cleavage of NOTCH1 from the cellular membrane, thereby preventing translocation of ICN1 to the nucleus and



NOTCH-mediated transcriptional activation [71]. Despite promising pre-clinical data, clinical trials were disappointing due to limited clinical efficacy and gastrointestinal toxicity. Moreover, several mechanisms of resistance to GSI have been reported, including loss of PTEN, FBXW7 mutations, NOTCH-independent MYC activation and epigenetic regulations [65]. Nevertheless, glucocorticoids were shown to have a protective effect against GSI-mediated gastro-intestinal toxicities [72], and in turn, GSI enhance the response to steroids such as dexamethasone [73]. Alternative strategies to target NOTCH1 pathway are being developed to improve selectivity and reduce off-target effects, including specific NOTCH1 inhibitory antibodies [74,75], stapled peptides that target NOTCH1 transcriptional complex [76], inhibitors of NOTCH1 target genes (*e.g.* IGF1R [30], HES1 [77], MYC [78]) and inhibitors of sarcoplasmic/endoplasmic reticulum calcium ATPase (SERCA) channels impairing NOTCH1 receptor protein processing [79].

A second strategy targeting a central genetic driver of T-ALL is to block deregulated cell cycle progression resulting from loss of the p16/INK4A tumor suppressor gene, which is present in about 70% T-ALL cases [4]. Palbociclib is an inhibitor of CDK4 and CDK6 which has been shown to inhibit cell cycle progression of T-ALL cells *in vitro* and to inhibit disease progression *in vivo* [80,81] and is now being investigated in phase I clinical trials (NCT03515200, NCT03132454).

Another interesting therapeutic target is the PI3K/AKT/mTOR signalling pathway, which is commonly constitutively activated in T-ALL, mainly via loss of PTEN tumor suppressor. Inhibition of PI3K/AKT/mTOR signalling pathway via different approaches - including pan-PI3K inhibitors, isotype-specific PI3K $\delta/\gamma$  inhibitors, AKT inhibitors, mTOR inhibitors or dual PI3K/mTOR inhibitors - produced convincing pre-clinical data in T-ALL [82-87], providing also multiple strategies to overcome resistance to glucocorticoids, GSI and chemotherapy [32,84,87]. Clinical efficacy of these

inhibitors proved to be disappointingly modest as monotherapy [88]; however, ongoing clinical trials are evaluating mTOR inhibitors everolimus (NCT01523977) and temsirolimus (NCT01614197) in combination with chemotherapy in children with relapsed T-ALL.

Additionally, another signalling pathway aberrantly activated in T-ALL and potentially targetable is IL-7R/JAK/STAT pathway, with several lines of evidence showing a role not only in leukemogenesis, but also in modulating steroid resistance [89-91]. JAK1/2 inhibition by ruxolitinib showed anti-leukemic activity in ETP-ALL patient xenografts *in vivo* independent of the presence of JAK/STAT mutations [92] and it is under investigation in combination with chemotherapy for relapsed ETP-ALL patients (NCT03613428).

Moreover, pharmacologic inhibition of the anti-apoptotic protein BCL-2 by Venetoclax has been suggested as a valuable approach in immature subtypes of human T-ALL, in particular in ETP-ALL, and it is now being evaluated in combinatorial regimens in phase I and Ib/II clinical trials (NCT03181126, NCT03504644).

As for immunotherapies, emerging approaches (NCT03081910, NCT03690011) include CAR T-cells targeting CD5 (which is expressed by the majority of T-ALL cells, but only by a subset of healthy T-cells), or CD7 prior CRISPR/CAS9- mediated ablation of CD7 on CAR T-cells to prevent fratricide effects [93,94]. Another potential target typically expressed on T-ALL cells is CD38, which can be targeted by monoclonal antibody Daratumumab [95] and is now under evaluation in combination with chemotherapy (NCT03384654). Moreover, inhibition of the C-X-C motif chemokine receptor 4 (CXCR4) decreases survival and proliferation of T-ALL cells *in vitro* and impairs homing to the bone marrow *in vivo* [96]. A CXCR4 peptide antagonist BL-8040 is now being studied in combination with nelarabine (NCT02763384).

A summary of selected ongoing clinical trials for relapsed T-ALL is shown in Table 2, extracted from McMahon *et al.* [97]:

**Table 2: Selected ongoing clinical trials for relapsed T-ALL**

Study	Target	Ph.	Patients	Intervention
Immunotherapeutic studies				
NCT03384654	CD38	II	1–30 years old with R/R T- or B-ALL	Daratumumab + chemotherapy
NCT03690011	CD7	I	≤75 years old with relapsed T-ALL or T cell lymphoma	CAR T cells targeting CD7
NCT03081910	CD5	I	≤75 years old with relapsed T-ALL or T cell lymphoma	CAR T cells targeting CD5
NCT02763384	CXCR4	I/IIa	≥18 years old with R/R T-ALL	BL-8040 + nelarabine
Targeted agents				
NCT03181126	BCL-2	I	≥4 years old with R/R T- or B-ALL	Venetoclax + navitoclax + chemotherapy
NCT03504644	BCL2	Ib/II	≥18 years old with R/R T- or B-ALL	Venetoclax + liposomal vincristine
NCT03132454	CDK4/6	I	≥15 years old with R/R T- or B-ALL	Palbociclib in combination with sorafenib, decitabine, or dex
NCT03515200	CDK4/6	I	≤21 years old with R/R T- or B-ALL	Palbociclib + chemotherapy
NCT01523977	mTOR	I	18 months–21 years old with relapsed T- or Ph-negative B-ALL	Everolimus + chemotherapy
NCT01614197	mTOR	I	1–21 years old with R/R T- or B-ALL	Temsirolimus + etoposide and cyclophosphamide
NCT03705507	MEK	I/II	All ages with R/R T- or B-ALL with Ras mutation	Selumetinib + dex
NCT03613428	JAK1/2	I	13–75 years old with R/R ETP-ALL	Ruxolitinib + chemotherapy
Other				
NCT02879643	Microtubule	I	1–21 years old with relapsed B- or T-ALL	Liposomal vincristine + chemotherapy
NCT02303821	Proteasome	Ib	1–21 years old with R/R T- or B-ALL	Carfilzomib + chemotherapy

*Ph.*, phase; *R/R*, relapsed and/or refractory; *CAR*, chimeric antigen receptor; *mTOR*, mammalian target of rapamycin; *ETP*, early T-precursor; *CDK*, cyclin-dependent kinase; *dex*, dexamethasone

In conclusion, huge progress has been made in the definition of the genetic and molecular landscape underlying T-ALL pathogenesis in the past decades; however, the therapeutic options for patients with relapsed/refractory T-ALL are still limited. Improved understanding of oncogenic cell-intrinsic factors as well as of aberrant signalling networks governing the interaction with the tumor micro-environment will help identifying novel targets and develop effective therapeutic strategies for T-ALL patients.

### 1.2. Hedgehog signalling pathway

Hedgehog (HH) gene was originally identified by Nusslein-Volhard and Wieschaus by genetic screening in *Drosophila melanogaster* for its role in larval segmentation [98]. Shortly thereafter, three mammalian Hedgehog ligands - Desert Hedgehog (DHH), Indian Hedgehog (IHH) and Sonic Hedgehog (SHH) - were found, sharing with their fruit fly paralog a key regulatory role in organogenesis, tissue regeneration and homeostasis. All HH proteins, despite the shared downstream signalling machinery and partially redundant function, differ for their expression patterns in various tissues [99]. Intriguingly, secreted HH ligands can trigger distinct cellular outcomes according to their concentration in exposed cells as a result of spatial and temporal gradients [100,101]. The regulation of the dorsoventral patterning of the neural tube and the anteroposterior patterning of the limbs are examples of the essential function of HH ligands as morphogens [102]. In line with its role of master developmental regulator, defects in HH signalling can cause severe congenital malformations, including holoprosencephaly, brachydactyly and polydactyly [103]. HH is also a mitogen and survival factor for adult stem cell populations across several tissues [104-106], thus it is of no surprise that aberrant activation of the pathway was reported to play a role in the tumorigenesis of different types of solid and hematological cancers [107].

#### 1.2.1 Canonical pathway activation

HH ligands are synthesized as a precursor protein of ~45 kDa, which undergoes auto-proteolytic cleavage generating a ~19 kDa amino-terminal (HH-N) and a ~25 kDa carboxy-terminal (HH-C) peptide. While HH-C is targeted to proteasomal degradation, HH-N is covalently modified by the

attachment of a cholesterol moiety at its carboxyl terminus and of a palmitic acid group at its N-terminus. The dually lipid-modified HH-N is finally secreted and triggers signal transduction on recipient cells [101]. In absence of HH ligands, the 12-pass transmembrane receptor Patched1 (PTCH1) or its homologous PTCH2, tonically repress the 7-pass transmembrane G protein-coupled receptor Smoothed (SMO) and the signal cascade is kept inactive [108,109]. While PTCH1 is broadly expressed, PTCH2 is mainly restricted to skin and testes [110]. In this OFF-setting, Kinesin-like protein 7 (KIF7) facilitates the sequential phosphorylation of Glioma-associated oncogene homologs transcription factors GLI2 and GLI3 by Protein Kinase A (PKA), Casein Kinase 1 (CK1) and Glycogen Synthase 3 $\beta$  (GSK3- $\beta$ ). GLIs hyperphosphorylation promotes the binding of  $\beta$ -transducin repeat-containing protein ( $\beta$ TrCP), leading to GLI ubiquitination and partial proteasomal processing into truncated repressor forms (GLI2R and GLI3R), thus shutting off target gene expression [111,112]. When HH ligands bind PTCH1, PTCH1 is internalized and degraded so that the repression over SMO is relieved [113]. SMO accumulates within the primary cilium and assumes an active conformation allowing the initiation of the signalling cascade, by antagonizing the inhibitory effect of PKA on GLI transcription factors [114]. Bypassing the PKA-induced proteolytic cleavage, full-length GLI proteins are released from the negative regulator Suppressor of Fused (SUFU) [115], enter the nucleus and activate gene transcription. A schematic representation of canonical HH signalling pathway is shown in Figure 3.

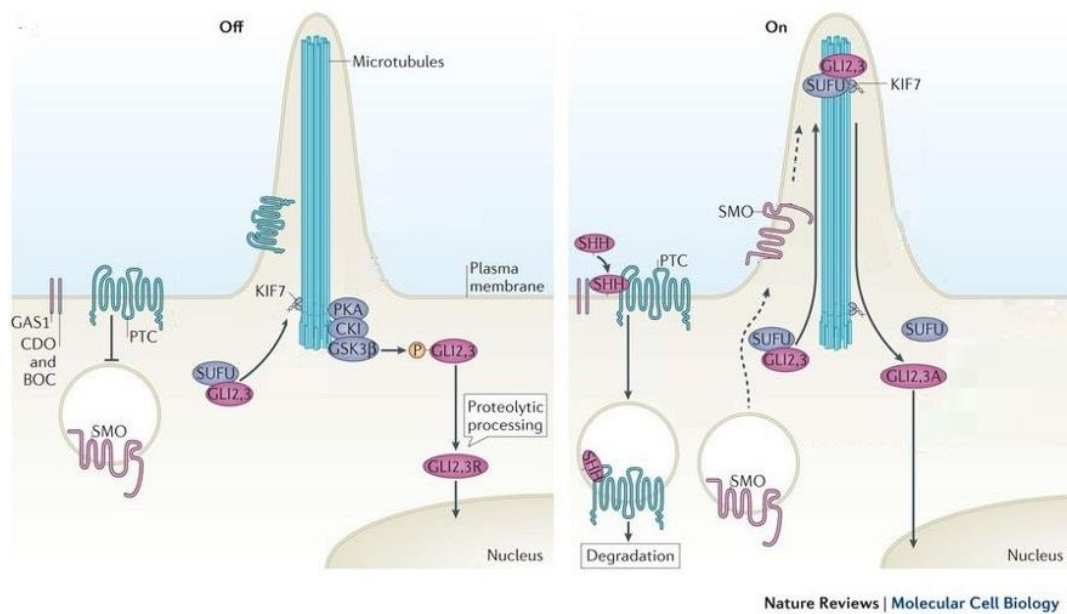


**Figure 3: Overview of the canonical HH signalling pathway**

In absence of HH ligands, PTCH1 inhibits SMO and GLI2/3 proteins are phosphorylated and processed into truncated repressor forms that prevent target gene transcription. Upon ligand binding to the receptor complex formed by PTCH1 and its co-receptors (CDON, BOC, GAS1), SMO accumulates in the plasma membrane of the primary cilium and promotes a signalling cascade that culminates in the nuclear translocation of the full-length active form of GLI1/2 transcription factors. Adapted from Briscoe and Thérond [116].

Mouse genetic studies showed that GLI2 is mostly a transcriptional activator [117,118] and GLI3 is mainly a repressor [119,120], while GLI1 is a HH target gene that exclusively functions as a transcriptional activator to amplify existing HH signalling in a positive feedback loop [121]. Gli1 also triggers the expression of different cell-specific target genes that mediate a plethora of cellular responses, including differentiation and proliferation (*e.g.* Cyclin D1/D2, Cyclin E, N-MYC), cell survival (*e.g.* BCL-2), self-renewal (*e.g.* NANOG, SOX2), epithelial-mesenchymal transition and invasiveness (*e.g.* SNAIL, CXCR4) [122,123]. In addition to PTCH1, a number of co-receptors can modulate HH pathway activation, including positive co-receptors (cell adhesion molecule-related/downregulated by oncogenes CDON, brother of CDO BOC, growth-arrest specific 1 GAS1) and the negative regulator HH interacting protein (HHIP) [124]. Upon pathway activation, the expression of

the negative receptors (PTCH1 and HHIP) is transcriptionally induced by GLI1, while the expression of positive co-receptors (CDON, GAS1, BOC) is repressed, ensuring a negative feedback loop to limit the signalling [122,125]

### 1.2.2 Hedgehog pathway activation and cancer:

The ligand-dependent SMO-mediated activation is by definition the canonical mechanism of activation of HH pathway; however, a number of ligand-dependent and ligand-independent non-canonical mechanisms (Fig. 4) were reported in cancer, leading to an aberrant and persistent activation of HH pathway in up to 25% of human tumors [126]. The role of HH signalling in tumorigenesis is context-dependent and affects tumor cell behavior at different stages, including self-renewal, survival, proliferation and metastasis, as a result of the transcription of diverse target genes [122,123].

#### *Ligand-dependent mechanisms*

Three different ligand-dependent models (*i.e.* autocrine, paracrine, reverse paracrine) have been proposed according to the role of the tumor microenvironment in producing or receiving HH ligands, suggesting that besides targeting the tumor directly, also inhibiting HH pathway in neighboring stromal cells may be effective in the treatment of HH-dependent cancers. Autocrine activation was described in breast, lung, pancreatic and prostate cancer and results in cell autonomous HH signalling due to overexpression of HH ligands [127,128]. In the case of paracrine activation, the tumor cell produces HH ligands that signal to nearby stromal cells, which in turn provide trophic cues to tumor cells [129,130], such as vascular endothelial growth factor (VEGF), IL-6 and IGF. In hematological malignancies like B-

cell lymphoma and multiple myeloma (MM), reverse paracrine activation where stroma-derived HH ligand activates HH signalling within the tumor was also reported [131,132].

### *Ligand-independent mechanisms*

The initial link between HH pathway and cancer came from the observation that patients with Gorlin Syndrome, an autosomal dominant disease characterized by a predisposition to basal cell carcinoma (BCC) and medulloblastoma (MB), harbor loss-of-function mutations in PTCH1[133]. High frequency inactivating mutations in PTCH1 [134-137] and to a lesser extent gain of function mutations in SMO [138,139] were described also in sporadic BCC and MB patients and were proven to drive tumorigenesis in BCC and MB murine models [139-141]. Albeit not sufficient to drive tumorigenesis [142], germline and somatic mutations in the negative regulator SUFU [143] and gene amplifications in GLI1 and GLI2 [144] were also described in MB and glioma respectively.



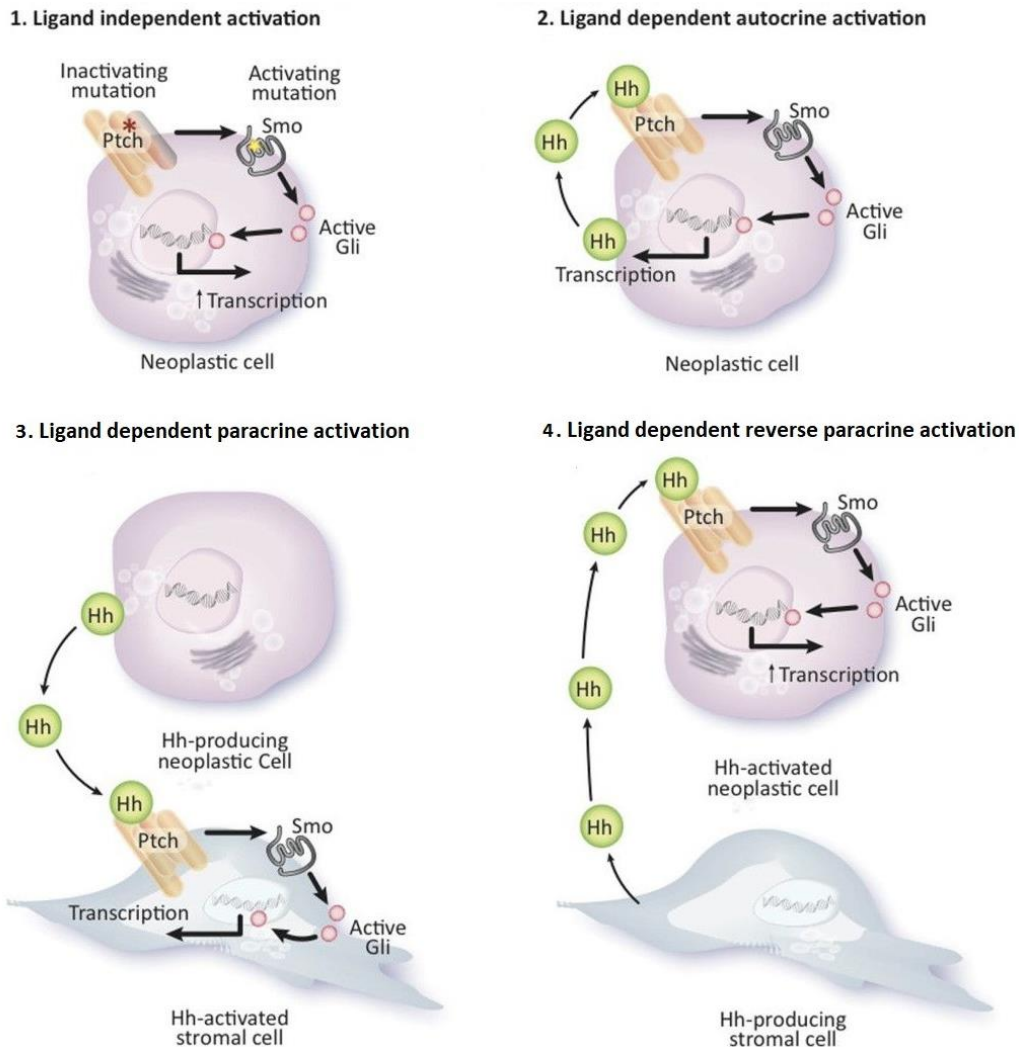


**Figure 4: Mechanisms of HH pathway activation in cancer**

**1. Ligand independent activation:** loss of function mutations in negative regulators (*e.g.* PTCH1, SUFU) and gain of function mutations in positive regulators (*e.g.* SMO) of the pathway lead to constitutively active signalling. **2. Ligand dependent autocrine activation:** augmented expression of HH ligands positively feedbacks onto the tumor cell and perpetuates itself. **3. Ligand dependent paracrine activation:** tumor-derived HH ligands activate HH pathway in stromal cells to induce the production of soluble factors that sustain tumor growth and survival. **4. Ligand dependent reverse paracrine activation:** HH pathway is triggered in tumor cells in response to stroma derived HH ligands. Adapted from Hui *et al.* [145].

## *Non-HH signals and crosstalk with other oncogenic pathways*

In cancer, multiple signalling pathways can be integrated inside the tumor cell and directly or indirectly converge on the regulation of the three GLI proteins in a SMO-independent fashion. SMO-independent transcriptional activation of GLI1 is involved in the maintenance and progression of different neoplastic malignancies, such as melanoma [146], prostate cancer [147], chronic lymphoblastic leukemia (CLL) [148], lymphoma and MM [149]. Moreover, the non-canonical activation of GLIs has also important therapeutic implications for cancer treatment because it limits the efficacy of SMO antagonists. Aberger *et al.* proposed the model of the “GLI code”, as a dynamic, integrated and context-specific modulation of the balance between the repressor and the activator functions of GLI transcription factors [150]. An increase in the oncogenic load of the cell, in terms of loss of tumor suppressors (e.g. p53, Numb), gain of oncogenes (e.g. RAS, c-MYC, EWS/FLI1) or activation of oncogenic pathways (e.g. PI3K/AKT, mTOR/S6K, EGFR, TGF- $\beta$ , WNT, RAS/MAPK) alter the homeostasis of this balance and favor a constitutively ON state of HH pathway [125,151]. The impact on GLI modulation can result either from a transcriptional regulation of GLI genes or from post-translational modifications (e.g. phosphorylation, acetylation, ubiquitination) that alter GLI protein function, affecting its transcriptional activity, protein stability and localization [152]. These diverse mechanisms of non-canonical activation of GLIs are thoroughly summarized in Table 3, extracted from Pietrobono *et al.* [151]:

**Table 3: Mechanisms of non-canonical activation of GLI1**

Upstream Regulator	Mechanism of action	Cancer/Cell type
<b>RAS-RAF-MEK-ERK</b>		
MEK1/2-ERK1/2	Increases expression of Gli target genes; Gli1 required for KRAS-driven transformation Increases GLI1/2 transcriptional activity	KRAS-driven PDAC mouse model NIH3T3 Melanoma PDAC Gastric cancer Colon cancer LAC
	Increases GLI1 nuclear localization Induces GLI1 protein stability Induces GLI2 protein stability	Melanoma PDAC BCC
MEK1/2-RSK2	Promotes GLI2 nuclear localization and stabilization	Multiple myeloma
<b>MAPKKK/MEKK</b>		
MEKK1	Inhibits GLI1 transcriptional activity	MB
MEKK2/3	Inhibits GLI1 transcriptional activity and protein stability through SUFU	MB
<b>PI3K/AKT/mTOR</b>		
AKT	Increases Gli2 transcriptional activity Increases GLI1 transcriptional activity and nuclear translocation Enhances GLI1 protein stability Prevents GLI degradation (GSK3 $\beta$ -dep.)	NIH3T3 Melanoma PDAC, ovarian cancer ALCL
mTOR/S6K1	Enhances GLI1 activation preventing SUFU association	EAC
p70S6K2	Prevents GLI1 degradation (GSK3 $\beta$ -dep.)	NSCLC EAC
<b>TGF<math>\beta</math></b>	Increases GLI2 transcription (SMAD3-dep.) Increases GLI2 expression Stimulates GLI1 transcriptional activity (PCAF-dep.)	PDAC, BC Colon CSC PDAC
<b>PKC signaling</b>		
PKC $\alpha$	Reduces GLI1 transcriptional activity Increases GLI1 transcriptional activity	HEK-293T Hep3B, NIH3T3
PKC $\delta$	Increases GLI1 transcriptional activity Reduces GLI1 transcriptional activity	HEK-293T Hep3B, NIH3T3
aPKC $\zeta/\lambda$	Enhances DNA binding and GLI1 transcriptional activity	BCC
<b>DYRK family</b>		
DYRK1A	Promotes GLI1 nuclear translocation  Induces GLI1 degradation, mediated by F-actin and MKL1	NIH3T3, HEK-293T  Lung carcinoma, rhabdomyosarcoma
DYRK1B	Enhances GLI1 transcriptional activity	PDAC, MB
DYRK2	Induces GLI2 protein degradation	NIH3T3
<b>Oncogenic drivers</b>		
EWS/FLI1	Induces GLI1 transcription	Ewing sarcoma
SOX9	Prevents $\beta$ TrCP-mediated GLI1 degradation	Pancreatic CSC
FOXC1	Enhances GLI2 transcriptional activity	Basal-like BC
c-MYC	Enhances GLI1 transcription	Burkitt lymphoma
IKK $\beta$	Promotes GLI1 stability	DLBCL
SRF-MKL1	Induces GLI transcription and enhances DNA binding	BCC
WIP1	Enhances GLI1 transcriptional activity, nuclear localization and protein stability	Melanoma

# 1. Introduction

Upstream Regulator	Mechanism of action	Cancer/Cell type
<b>Tumor suppressors</b>		
p53	Inhibits GLI1 transcriptional activity, nuclear translocation and protein stability Promotes proteasome-dependent degradation of GLI1 (PCAF-dep.) Interferes with DNA binding ability of GLI1 (TAF9-dep.)	Glioblastoma MB Rhabdomyosarcoma, Osteosarcoma
NUMB	Induces GLI1 ubiquitination and proteasome degradation (ITCH-dep.)	MB
SNF5	Interferes with promoter occupancy of GLI1	Rhabdoid Tumors
<b>miRNAs</b>		
miR-324-5p	Represses GLI1 expression	CGCPs
miR-361	Represses GLI1 expression Represses GLI1 and GLI3 expression	Prostate cancer Retinoblastoma and CSC
miR-326	Represses GLI2 expression	Ptch+/- MB CSC
<b>BET proteins</b>		
BRD4	Increases GLI1/2 transcription	BCC MB
BET	Upregulates Gli1 in murine CAFs	PDAC
BET	Promotes GLI occupancy on target promoters	PDAC
<b>HDAC</b>		
HDAC	Stimulates GLI1 nuclear localization and transcriptional activity	Multiple Myeloma
HDAC class I	Increases DNA binding ability of GLI1 (HDAC1)	MB MB, murine BCC
HDAC class II	Transcriptional control of GLI2 (HDAC6)	MB
<b>HAT</b>		
p300	Prevents GLI2 recruitment to chromatin	HEK-293T, NIH3T3
PCAF	Acts as GLI1 transcriptional cofactor Promotes GLI1 ubiquitination and proteolysis	Glioblastoma, MB MB
<b>PRMTs</b>		
PRMT1	Enhances DNA binding ability of GLI1	PDAC
PRMT5	Enhances GLI1 protein stabilization and nuclear translocation Inhibits GLI1 expression through Menin1	C3H10T1/2, HEK-293T, SCLC Neuroendocrine tumors

*ALCL, anaplastic large cell lymphoma; b-TrCP, b-transducing repeat-containing protein; BC, breast cancer; BCC, basal cell carcinoma; BET, bromo- and extra-terminal domain; CAF, cancer-associated fibroblasts; CSC, cancer stem cells; DLBCL, diffuse large B-cell lymphoma; DYRK, dual-specificity tyrosine phosphorylation-regulated kinase; EAC, esophageal adenocarcinoma; CGCPs, cerebellar granule cell precursors; GSK3b, glycogen synthase kinase 3b; HAT, histone acetyltransferase; HDAC, histone deacetylase; LAC, lung adenocarcinoma; MEF, mouse embryonic fibroblasts; NSCLC, non-small cell lung cancer; PCAF, p300/CREB-binding protein-associated factor; PDAC, pancreatic ductal adenocarcinoma; PKC, protein kinase C; PRMT, protein arginine methyltransferases; SCLC, small cell lung cancer; SUFU, Suppressor of Fused.*

### 1.2.3. SHH signalling in T-cell maturation

Among the numerous functions in organogenesis, SHH was reported to regulate early stages of thymic development [153] and to have a role, though controversial, in primitive and definitive hematopoiesis [154,155]. In the thymus, SHH is expressed in epithelial cells of the medullary and subcapsular regions and the cortico-medullary junction, while SHH-responsive cells can be found both in thymic lymphoid and stromal compartments [156,157]. Consistent with its morphogen function, the strength of SHH signal depends on where cells are located in the thymus: SP cells in the medulla are closer to SHH source, while early thymocyte progenitors, that are located closer to the cortico-medullary junction, receive a weaker SHH stimulus [153]. Expression of SHH pathway components varies during T-cell maturation: SMO expression is highest in DN2, decreases gradually during maturation from DN3 to DN4 subsets to become undetectable in DP populations, but it is upregulated again in a small fraction of CD4 and CD8 SP thymocytes [156,158]. The same pattern of expression is seen also for GLI1 transcription factor, confirming that DN cells and a proportion of SP cells are the actual SHH-responsive cells in the thymus [153]. Studies of embryonic thymic development in SHH- and GLI3- deficient mouse models have shown that SHH signalling is essential for the homeostasis of DN subsets before pre-TCR signalling, providing positive cues for differentiation, expansion and survival at the transition from DN1 to DN2 stage [157,159]. Moreover, SHH signalling shapes the T-cell receptor (TCR) repertoire selection [160], modulating TCR strength and outcome according to the SHH concentration that the developing thymocytes are exposed to while they move across the thymus. As a matter of fact, *Shh*<sup>-/-</sup> mice show a stronger TCR signal and as result, an increased CD4:CD8 SP cell ratio. Consistently, constitutive pathway activation in transgenic mice by the N-terminally truncated form of GLI2

(GLI2 $\Delta$ N<sub>2</sub>) results in decreased TCR signal, thus impairing positive and negative selection and reducing the CD4:CD8 ratio [160].

### 1.2.4. SHH signalling in hematological malignancies

Focusing on hematological malignancies, several works suggested a role for HH pathway in a range of both myeloid and lymphoid disorders. Zhao *et al.* and Dierks *et al.* demonstrated that - adopting two independent approaches of SMO ablation in mice - HH signalling is active in BCR-ABL1<sup>+</sup> CML and essential for disease progression. In both studies, SMO deletion was shown to decrease the number of leukemic stem cells and to reduce the incidence and delay the onset of leukemia [161,162]. Moreover, HH inhibition was shown to be effective against CML *in vitro* and *in vivo*, either alone or in combination with tyrosine kinase inhibitors (TKIs). Such therapeutic combinations of SMO inhibitors and TKIs are now under evaluation in clinical trials [163]. Other evidence of the implication of HH signalling in cancer stem cell maintenance in hematological tumors came from MM, where an inverse paracrine mechanism of pathway activation was proposed, with the bone marrow microenvironment acting as a source of HH ligands for MM progenitors [131,164]. The complex nature of leukemic stem cell populations also suggests that targeting HH pathway alone is unlikely to be successful. Hoffmann *et al.* showed that SMO is completely dispensable in a form of acute myeloid leukemia (AML) model; on the other hand, in 2018 the small molecule SMO inhibitor Glasdegib was FDA-approved in combination with low-dose cytarabine for newly diagnosed AML patients [165]. A contribution of HH signalling is now emerging also in T-ALL, with recent studies showing that pathway components are expressed and signalling is active in T-ALL cell lines and primary samples [155,166,167]. Rare somatic mutations in HH pathway components were found in T-ALL patients,

including truncating mutations in SMO (R726\* and R763\*) and missense mutations in GLI1 (S538F) and GLI3 (G727R) [168]. More recently, Burns *et al.* identified HH pathway mutations in 16% of childhood T-ALL cases, with PTCH1 being the single most commonly mutated gene. These PTCH1 missense mutations did not have a prognostic value, but were associated to resistance to induction chemotherapy and were shown to accelerate the onset of NOTCH1-induced T-ALL in a zebrafish model [167]. HH pathway was also reported to be active in a subset of T-ALL cases through augmented expression of SHH and IHH ligands and of GLI1 transcription factor, suggesting that pathway-intrinsic mutational events are only partially responsible for this activation [166]. Moreover, ectopic expression of HH ligand in JAK3 mutant mouse model of T-ALL induced growth advantage, higher infiltration rates, and thymic epithelial cell activation, indicating a supportive role in leukemia development. However, Gao *et al.* found HH signalling to be dispensable for NOTCH1-induced leukemia induction and progression [155]. The debated effects of SMO deficiency in normal hematopoiesis [154] and leukemogenesis [155], together with the reduced efficacy of SMO inhibitors (cyclopamine and GDC-0449) on cell line growth with respect to GLI1 inhibitors [166,169], underscores the importance of non-canonical SMO-independent modulation of HH signalling and the necessity of dissecting the complex regulatory network upstream of GLI1 in discrete tumor entities [170].





## **2. Aim of the thesis**

Current efforts in T-ALL research are focusing on a deeper genetic and molecular characterization of the disease to identify new therapeutic targets for the development of effective treatment strategies for primary resistant/relapsed patients.

HH signalling pathway was reported to be aberrantly activated in a variety of solid and hematological tumors by ligand-dependent as well as by ligand-independent mechanisms, contributing to tumour development and progression, and cancer stem cell maintenance. Recently, rare somatic mutations of HH signalling components were described in T-ALL and approximately 20% of primary T-ALL samples were shown to express high levels of GLI1 and HH ligands. Interestingly, therapeutic targeting *in vitro* and *in vivo* of HH pathway in T-ALL suggests that the inhibition of the signalling at the level of GLI1 transcription factors, rather than at the level of SMO receptor, might be more effective, emphasizing the importance of the non-canonical activation of GLI1.

Given these premises, the overall purpose of this work was to characterize the role of HH signalling and its therapeutic targeting in the pathogenesis of T-ALL. We first evaluated the expression of pathway components in a panel of T-ALL cell lines, patient-derived xenografts and Notch1-dependent murine models and determined their *in vitro* sensitivity to HH inhibitors with distinct mechanisms of action. In line with the literature, our data suggested a SMO receptor-independent activation of HH pathway, prompting us to investigate the interplay between HH signalling with other therapeutically relevant deregulated pathways in T-ALL which contribute to the non-canonical activation of GLI1. To this end, we further explored the newly observed crosstalk between HH signalling pathway and the glucocorticoid receptor pathway, with particular emphasis on the definition of its therapeutic potential and the molecular mechanisms underlying the crosstalk.



### **3. Materials and Methods**

### 3.1 Cell lines and primary T-ALL xenografts

T-ALL cell lines were grown in RPMI-1640 medium (Euroclone) supplemented with 10% fetal bovine serum (FBS; Gibco) and additives (1% Ultra-Glutamine 200mM, 1% Sodium-Pyruvate 100mM, 1% HEPES 1M, 1% Penicillin-Streptomycin 10000 U/mL; Lonza) at 37°C in a humidified atmosphere under 5% CO<sub>2</sub>. Human Embryonic Kidney-293T cells (HEK-293T) were cultured in Dulbecco's modified Eagle's medium (DMEM; Euroclone), supplemented as described before.

For functional studies -other than cell viability assays- requiring glucocorticoid treatment, DMEM and RPMI-1640 media were supplemented with Charcoal-stripped FBS.

Primary T-ALL xenografts were previously established from our collaborator Dr. Stefano Indraccolo (Istituto Oncologico Veneto - IOV, Padova, Italy) from the bone marrow of newly diagnosed pediatric patients, with informed consent according to the guidelines of the local ethics committee. For xenografts establishment, 6- to 8- week-old Non-obese diabetic/severe combined immunodeficiency interleukin 2 receptor gamma chain null (NOD/SCID IL2R $\gamma$ <sup>null</sup>) immunodeficient mice were intravenously injected with 10x10<sup>6</sup> T-ALL cells. For short-term *in vitro* experiments, primary T-ALL xenograft-derived cells were maintained in MEM- $\alpha$  GlutaMAX™ medium (Gibco) with 10% FBS, 10% human serum (Gibco), hIL-7 (10ng/mL, Peprotech), hSCF (50ng/mL, Peprotech), hFLT3-ligand (20ng/mL, Peprotech) and Insulin (20nM, Sigma-Aldrich).

### 3.2 Drug treatments

For *in vitro* studies, T-ALL cells were plated at a density of 0.25-0.3x10<sup>6</sup>/mL in triplicate for each experimental condition in 24 well-plates. Cells were treated with different doses of Dexamethasone (1nM-1μM), GANT61 (5-40μM) and cyclopamine (1-20μM). For drug combination screening, the following inhibitors were used in combination with 2.5μM GANT61: DBZ (iNOTCH1, 2.5-20nM), BEZ235 (imTOR, 2.5-20nM), MK2206 (iAKT, 5-40nM), PF4708671 (iS6K, 1-10μM), H89 (iPKA, 1-5μM), Vitamin D3 (5-10μM), PD98059 (iMAPK, 1-10μM), GSK650394 (iSGK, 1-5μM). For functional analysis of HH pathway, cells were treated with different concentrations of Dexa (10nM-1μM), RU486 (1-10μM), trichostatin A (TSA, 1μM). Control wells were treated with an equivalent percentage of DMSO (vehicle).

### 3.3 Cell viability assay

Cell viability was assessed by ATPlite Luminescence ATP Detection Assay System (PerkinElmer), an ATP-monitoring system that indirectly determines ATP concentration as an indicator of active cellular metabolism. The system is based on the quantification of light emission from the ATP-dependent oxidative reaction of luciferine substrate by the luciferase enzyme. Briefly, 100μL of cell culture from each condition of a 24-well plate were transferred in duplicate in a dark 96-well plate. Cells were then lysed at room temperature in 50μL of Mammalian cell lysis solution for 5 minutes. Subsequently, 100μL of ATPlite substrate were added to each well and after 5 minutes of dark adaptation, luminescence signal was detected on a VICTOR X5 Multilabel Plate Reader (Perkin Elmer).

### 3.4 Apoptosis and cell cycle analysis

Evaluation of apoptosis was performed by flow cytometry following cell staining with Annexin-V-FLUOS Staining Kit (Roche) and SYTOX™ Red Dead Cell Stain (Thermo Fischer) according to manufacturer instructions.

Cell cycle analysis was performed by flow cytometry following Propidium Iodide (PI) staining (Sigma-Aldrich).

Samples were analyzed on a FACSCalibur flow cytometer (BD Biosciences) supporting Cell Quest software (BD Biosciences). All the analyses were performed in triplicate. Flow cytometry data were analyzed with FlowJo™ Software (BD Biosciences).

### 3.5 Plasmids

To overexpress GLI1, the following plasmids were used: pcDNA3.1-His-hGli1 (Riken), pBABEPuro-HA-GLI1 (Addgene), hGli1-flag3x (Addgene), pcDNA3.1-GLI1-FLAG (a gift from Prof. Gianluca Canettieri, University La Sapienza, Rome, Italy). To overexpress the glucocorticoid receptor NR3C1, the retroviral construct pMSCV-HA-NR3C1 was used (a gift from Prof. Adolfo Ferrando, Columbia University, New York, USA). pBJ5-HDAC1-FLAG, pCMV $\beta$ -p300-myc and pCI-flag-PCAF (Addgene) constructs were used to study GLI1 acetylation. pcDNA 3.1-empty (Addgene) and pMSCV-puro (Addgene) were used as empty control vectors. For constructs used in dual luciferase assays see Paragraph 3.9.

### 3.6 Retrovirus production

Retroviral particles were generated by a transient three-plasmid vector packaging system in HEK 293T cells transfected using JetPEI transfection agent (Polyplus). Briefly, cells were plated in 10cm culture dishes and co-transfected with a combination of the following vectors: (i) retroviral packaging plasmid (2.7µg), encoding *gag*, *pol* and *rev* genes; (ii) the Vesicular stomatitis virus G glycoprotein (VSV-G) envelop plasmid (300ng); (iii) pMSCV-puro control plasmid or pMSCV-HA-NR3C1 overexpression plasmid (3.5µg). 48 hours after transfection, viral supernatants were collected and filtered, and then supplemented with hexadimethrine bromide (Sigma-Aldrich) to a final concentration of 5µg/mL to infect HEK 293T target cells. Infected cells were subjected to puromycin selection (1µg/mL; Sigma-Aldrich) for 5-7 days.

### 3.7 RNA extraction, reverse-transcription and quantitative Real Time PCR

Total RNA was extracted by acid guanidinium thiocyanate-phenol-chloroform extraction method using TRIzol Reagent (Invitrogen) following manufacturer instructions. cDNA was synthesized from 0.5-1µg of total RNA using SensiFAST™ cDNA Synthesis Kit (Bioline). Real time RT-PCR reactions were performed using SensiFAST™ SYBR® Hi-ROX Kit (Bioline) and run on a ABI Prism 7900 Sequence Detection System (Applied Biosystems). Relative gene expression levels were calculated using the  $2^{-\Delta\Delta Ct}$  method [171] and normalized against the expression of  $\beta_2$ -microglobulin and  $\beta$ -Actin housekeeping genes for murine samples or *GAPDH* and *RPL19* housekeeping genes for human samples. Primer sequences used for Real time RT-PCR reactions are listed below.



Table 4: Primer sequences for Real time RT-PCR reactions

	Gene	Sequence (5' - 3')
Human	GLI1 FW	AGATGAATCACCAAAAAGGG
	GLI1 RV	ATATCACCTTCCAAGGGTTC
	GLI2 FW	TACCAGCAGATTCTGAGC
	GLI2 RV	CTCTGCTTGTTCTGGTTG
	GLI3 FW	CTTCTAATGAGGATGAAAGTCC
	GLI3 RV	ACCCATGGATCTCTTTCTTG
	PTCH1 FW	ATCCTGAAATCCTTCTCTGAC
	PTCH1 RV	AGGAAATTCCGATCAATGAG
	PTCH2 FW	TCCAAGTATCACTCTATGGG
	PTCH2 RV	AATCATCCGCTCAATCATT
	SMO FW	GAGAAGATCAACCTGTTTGC
	SMO RV	CATCTTGCTCTTCTTGATCC
	HHIP FW	TTAAGTGATTTACAGGCTC
	HHIP RV	CTTGGTATGGAATAAGGCAC
	SUFU FW	TTCTCCAGAGGAATTCAAAC
	SUFU RV	CAACTGTTACACTGGAAGTC
	SHH FW	GAGCGATTTAAGGAACTCAC
	SHH RV	CCTTACACCTCCTGAGTCATC
	IHH FW	AGTTGATGCTGCTAAATTCC
	IHH RV	GAATGTCATACCTCAGAATGG
GAPDH FW	GAAGGTGAAGGTCTGGAGT	
GAPDH RV	CATGGGTGGAATCATATTGGAA	
RPL19 FW	CAGAAGATACCGTGAATCTAAG	
RPL19 RV	TGTTTTTGAACACATTCCCC	
Mouse	GLI1 FW	TACCATGAGCCCTTCTTTAG
	GLI1 RV	TCATATCCAGCTCTGACTTC
	GLI2 FW	CAACGCCTACTCTCCCAGAC
	GLI2 RV	GAGCCTTGATGTACTGTACCAC
	PTCH1 FW	CAACCAAACCTCTTGATGTG
	PTCH1 RV	CCTGCCAATGCATATACTTC
	PTCH2 FW	CAGATGTTGATTTCAGACTGC
	PTCH2 RV	AATCCCAGGATTTCCCATAG
SMO FW	TAGGCTACAAGAACTATCGG	

<b>SMO RV</b>	TCTTGATGGAGAACAGAGTC
<b>HHIP FW</b>	GAAAGATTGTACGGAAGCTATG
<b>HHIP RV</b>	ACCTCTCCTAATTCATCTTCTC
<b>SHH FW</b>	GGGAAGATCACAAGAAACTC
<b>SHH RV</b>	TTAACTTGTCTTTGCACCTC
<b>IHH FW</b>	ACTACAATCCCGACATCATC
<b>IHH RV</b>	CCCTCATAGTGTAAGACTCC
<b>β2-MICRO FW</b>	GTATGCTATCCAGAAAACCC
<b>β2-MICRO RV</b>	CTGAAGGACATATCTGACATC
<b>β-ACTIN FW</b>	GATGTATGAAGGCTTTGGTC
<b>β-ACTIN RV</b>	TGTGCACTTTTATTGGTCTC

### 3.8 Western blot analysis

Total cell lysates were obtained in RIPA lysis buffer (Cell Signalling) supplemented with phosphatase inhibitors (Protease Inhibitors Cocktail 2 and Cocktail 3, Sigma-Aldrich) and protease inhibitors (cOmplete™ ULTRA Tablets, Roche). Protein concentration was determined by Quantum Protein Assay Kit (Euroclone) according to manufacturer instructions. For Western blot analysis, protein lysates (20-30µg) were separated on 4-12% gradient NuPAGE® Bis-Tris polyacrylamide or 3-8% gradient NuPAGE® Tris-Acetate SDS-PAGE gels (Thermo Fisher) and transferred to nitrocellulose membranes (Protran). Membranes were then blocked in 5% non-fat dry milk in Phosphate Buffer Saline (PBS)-0.1% Tween 20 and incubated overnight with primary antibodies. Primary antibodies were diluted either in 5% milk or in 5% BSA in PBS-0.1% Tween 20 buffer, according to manufacturer instructions. The following primary antibodies were used: rabbit α-GLI1 (Cell Signalling), rabbit α-PTEN (Cell Signalling), rabbit α-SHH (C9C5, Cell Signalling), rabbit α-SHH/IHH (Santa Cruz Biotechnology), rabbit α-SUFU (Cell Signalling), rabbit α-NR3C1 (E20, Santa Cruz Biotechnology), rabbit α-GILZ (Santa Cruz), rabbit α-β-actin (Cell Signalling), mouse α-tubulin α

(Santa Cruz Biotechnology), rabbit  $\alpha$ -Lamin B1 (Cell Signalling), rabbit  $\alpha$ -MAX (C-17, Santa Cruz Biotechnology), rabbit  $\alpha$ -HA (Cell Signalling), rabbit  $\alpha$ -FLAG (Cell Signalling), mouse  $\alpha$ -MYC (9E10, Santa Cruz Biotechnology), rabbit  $\alpha$ -acetylated lysine (Cell Signalling).

The morning after, membranes were washed in PBS-0.1% Tween 20 buffer and incubated 1 hour at room temperature with HRP-conjugated goat anti-rabbit or goat anti-mouse IgG (Perkin Elmer) diluted 1:5000 in 2% milk in PBS-0.1% Tween 20 buffer. For signal detection, equal volumes of Western Lightning® Plus ECL Enhanced Luminol Reagent Plus and Western Lightning® Plus ECL Oxidizing Reagent Plus (Perkin Elmer) were mixed together and added to the membranes. Images were acquired on a ChemiDoc XRS Imager (Biorad) acquisition image system and analyzed with Quantity One® 1-D analysis software and ImageJ software (National Institutes of Health., USA).

#### **3.9 Cellular fractionation, immunoprecipitation analysis and protein half-life determination**

For cell fractioning analysis, nuclear and cytoplasmic fractions were collected using Nuclear Extract Kit (Active Motif).

For Immunoprecipitation (IP) analysis, cells were lysed in Co-IP buffer (50mM Tris pH 7.5, 150mM NaCl, 0.1% NP-40, 10% glycerol, 1mM EDTA). At least 3mg of whole cell lysates per sample were pre-cleared in Protein L-agarose (Santa Cruz Biotechnology) at 4° for 30'. IP was performed overnight with EZview™ Red anti-FLAG or anti-HA M2 Affinity Gel (Sigma-Aldrich) at 4° under gentle rotation. The morning after, immunoprecipitates were extensively washed at 4° in CO-IP buffer and eluted in NuPage LDS sample buffer (Thermo Fisher Scientific) by heating 8' at 95°.

For protein half-life determination, cells were pre-treated for 18h with DMSO or Dexa and cycloheximide (CHX) was added at a final concentration of 50µg/mL to inhibit protein synthesis. Whole cell lysates were then harvested at different time points and Western blot analysis was performed as previously described.

#### **3.10 Dual Luciferase reporter assay**

HEK 293T cells were seeded at a concentration of  $8 \times 10^4$  cells per well in 24-well plates and transfected with 100ng of GLI1-expression plasmid or pcDNA3.1 empty vector (Addgene) using JetPEI transfection agent (Polyplus). 8x3'Gli-BS-delta51-LucII vector (250ng, Riken), a Firefly luciferase reporter plasmid carrying eight copies of the GLI-responsive element, was used as reporter plasmid. For internal normalization of transfection efficiency, cells were co-transfected with pGL4.74 [hRluc/TK] plasmid (100ng, Promega), encoding Renilla luciferase. 24h after transfection, cell culture medium was replaced with fresh complete DMEM medium. When cells reached confluence, cell culture medium was switched to serum-restricted DMEM (<2% FBS) and treatments were started for 24h. Luciferase activity was measured 72h post-transfection by Dual-Luciferase Reporter® assay kit (Promega). Briefly, transfected cells were gently rinsed from culture medium with PBS and lysed for 15 minutes in 100µL of passive lysis buffer. Cleared cell lysates (10µL/sample) were transferred to a 96-well plate and Luciferase Assay Reagent (LAR II, 50µL/well) was added. Firefly luciferase activity was detected on a VICTOR X5 Multilabel Plate Reader (Perkin Elmer). Renilla luciferase activity was then measured adding Stop & Glo® reagent (50µL/well).

### 3.11 Statistical analysis

Unpaired two-tailed Student's T-test was used for statistical comparison between groups (\* $p < 0.05$ , \*\* $p < 0.01$ , \*\*\* $p < 0.001$ ). Statistical analyses were performed with GraphPad Prism software (GraphPad Software).



## **4. Results**

---

## 4.1 Expression of Hedgehog pathway components in T-ALL

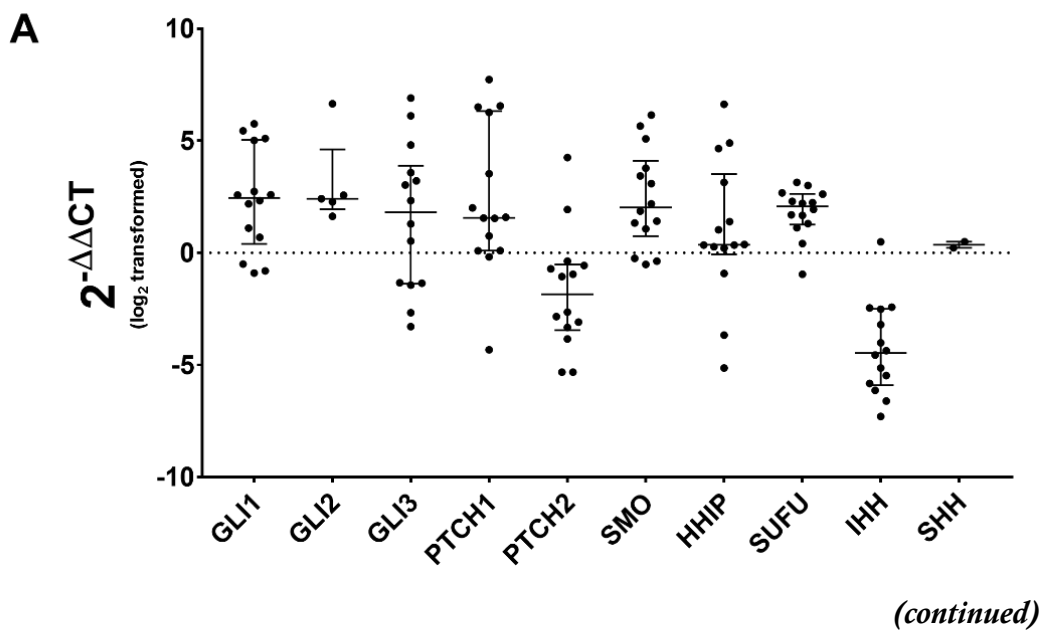
A recent study by Dagklis *et al.* provided evidence of HH pathway activation in T-ALL, revealing ectopic expression of SHH, IHH and GLI1 in a subgroup of T-ALL patients [166]. We therefore sought to confirm and assess the expression of the main HH pathway members by quantitative Real-Time RT-PCR in different T-ALL samples, including cell lines (n=14), PDX samples (n=20) and Notch1-induced mouse models (n=8).

A panel of 14 cell lines (ALL-SIL, CUTLL1, DND41, JURKAT E6, HPB-ALL, KOPTK1, MOLT3, P12 ICHIKAWA, RPMI8402, PF382, HSB2, MOLT4, CCRF-CEM, TALL1) was considered for gene expression analysis.

In our T-ALL cell line panel (Fig. 5A) GLI1, the principal effector of HH pathway outcome and conventionally considered as a mirror for pathway activation, resulted overexpressed with respect to normal thymocytes in 79% (11/14) of T-ALL cell lines. Interestingly, the other transcriptional activator of HH pathway GLI2, which was not expressed by normal thymocytes, was detected at low levels only in a minority of T-ALL cell lines, while the transcriptional repressor GLI3 was expressed in all of them. Despite the heterogeneous patterns of gene expression, a general upregulation in transcript levels was observed also for GLI1 targets PTCH1 and HHIP. Consistently, the expression of GLI1 transcript positively correlated with the expression levels of PTCH1 (Fig. 5B). PTCH1 paralog PTCH2 was the only target of GLI1 to be downregulated in T-ALL cell lines with respect to normal samples. Other major HH pathway components like SUFU and SMO were also overexpressed in T-ALL cell lines. Looking at HH ligands, SHH was universally not expressed, with the only exceptions of CUTLL1 and DND41 cell lines, expressing very low levels of the ligand. On the other hand, IHH



ligand was expressed and generally downregulated in T-ALL cell lines in comparison to normal thymocytes. However, no correlation was found between IHH expression and GLI1 (Fig. 5C) or between IHH and GLI1 main targets PTCH1 and HHIP (Fig. 5D), suggesting that T-ALL cell lines are not subjected to autocrine HH activation.



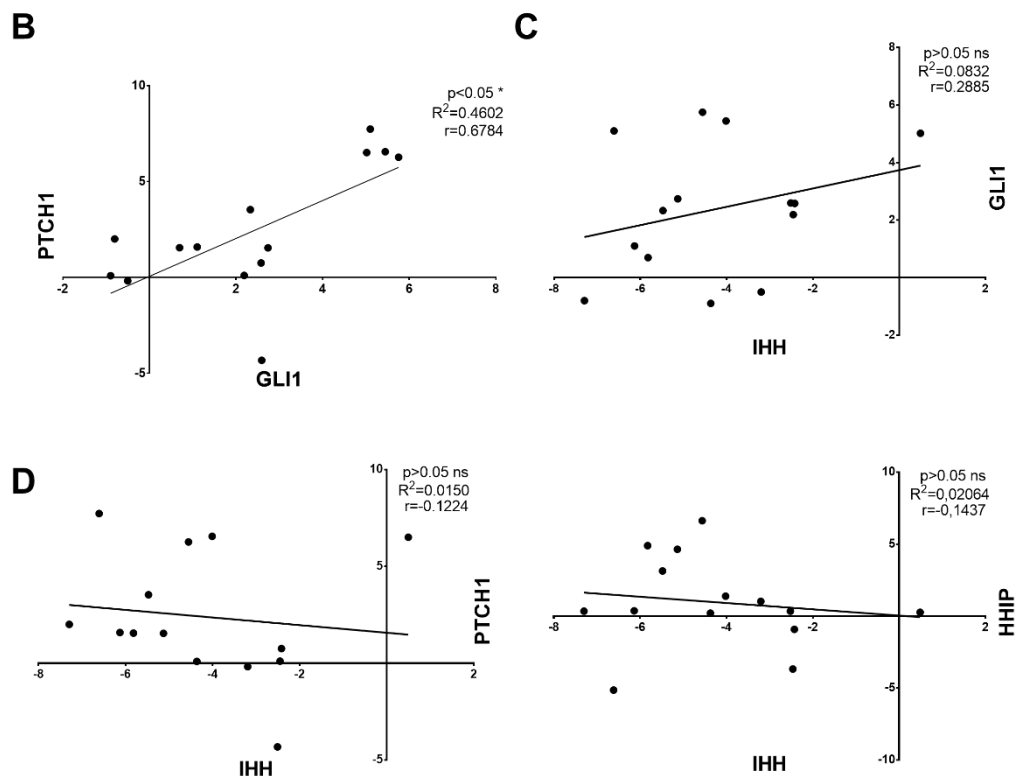
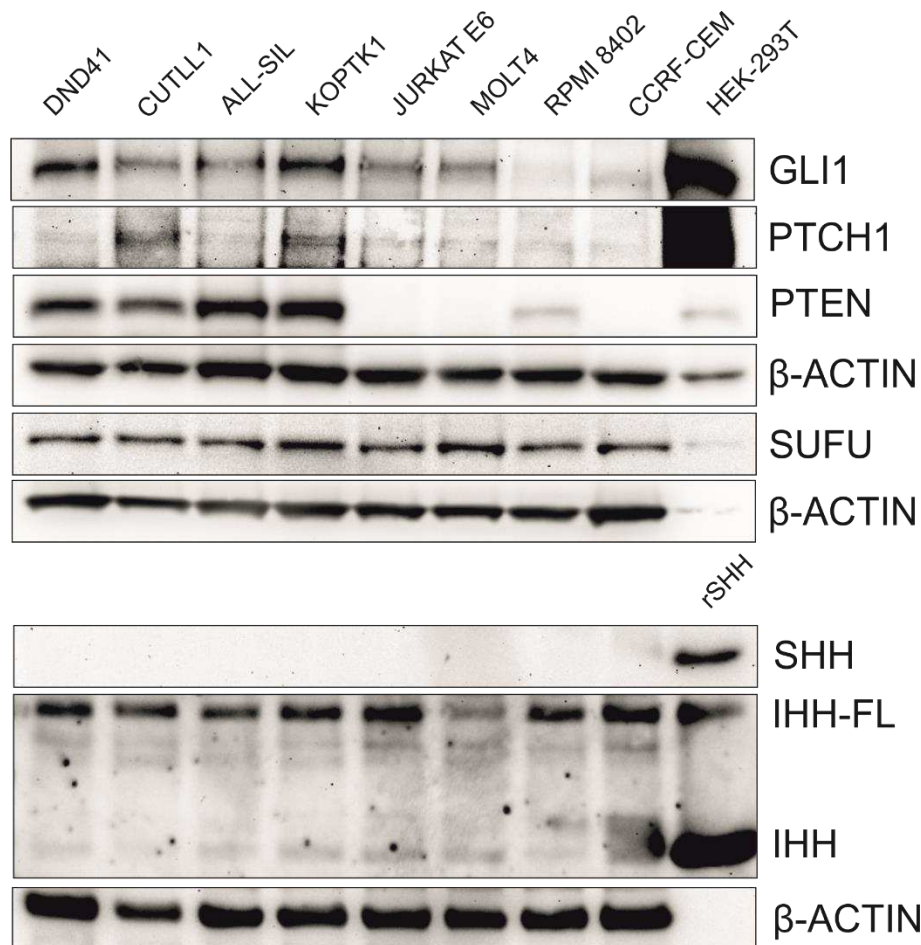


**Figure 5: Transcripts of HH pathway components are aberrantly expressed in T-ALL cell lines**

**A)** Relative expression analysis by Real time RT-PCR of genes encoding HH pathway components in T-ALL cell lines (n=14). Scatter dot plots show mRNA levels as log<sub>2</sub>-transformed fold change ( $2^{-\Delta\Delta CT}$ ) to normal human thymocytes (n=1). Dashed line indicates normal human thymocytes expression levels. Results are presented with horizontal bars indicating the median and error bars indicating interquartile range. RPL19 gene was used as housekeeping gene. **B-D)** Correlation between expression levels of HH genes evaluated by linear regression analysis and Pearson's correlation test. (ns,  $p > 0.05$ , \*  $p < 0.05$ , \*\*  $p < 0.01$ )

Western blot analysis in selected cell lines (ALL-SIL, CUTLL1, DND41, JURKAT E6, KOPTK1, RPMI8402, MOLT4, CCRF-CEM) confirmed the expression of GLI1 protein, with a trend for higher expression in PTEN<sup>+</sup> (DND41, CUTLL1, ALL-SIL, KOPTK1) versus PTEN<sup>-</sup> (JURKAT E6, MOLT4, RPMI8402, CCRF-CEM) cell lines (Fig. 6). Consistently, PTCH1 levels showed a similar trend as GLI1 protein levels, while SUFU protein was homogeneously expressed amongst the tested cell lines. Further, in

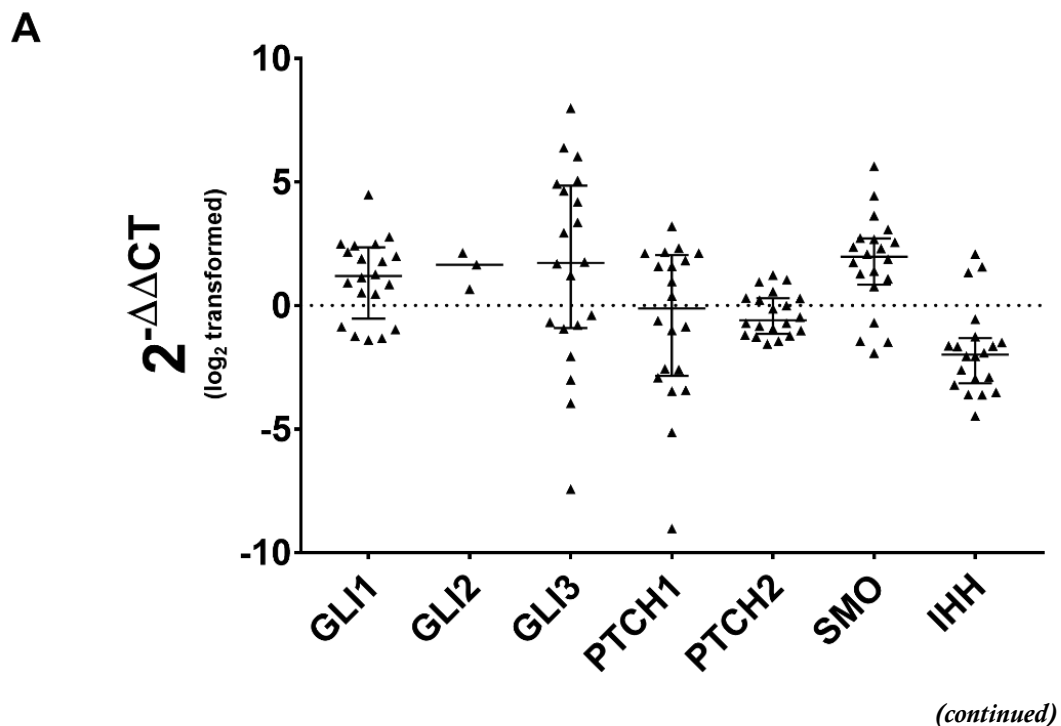
accordance with the transcriptional data, SHH ligand was not expressed in T-ALL cell lines, whereas IHH was clearly detectable in its full-length precursor form (IHH-FL), but much less so in its mature secretable form. Additional HH pathway members were evaluated, but subsequently excluded due to poor technical performance of primary antibodies (data not shown).



**Figure 6: Protein expression levels of HH pathway components in selected T-ALL cell lines**

Western blot analysis of selected HH pathway components in T-ALL cell lines.  $\beta$ -Actin was used as loading control. Lysates from HEK-293T cells and recombinant SHH protein (rSHH) were used as positive controls.

Next, we evaluated the activation of HH pathway in cells derived from a cohort of PDX (Fig. 7A), previously derived in our Institute from primary leukemic patients. A similar trend to T-ALL cells lines was observed, with GLI1 being overexpressed compared to normal thymocytes in most PDX samples and GLI2 being detectable only in sporadic cases. The transcription factor GLI3 and the membrane receptors PTCH1, PTCH2 and SMO were variably expressed in all the tested samples. As for T-ALL lines, SHH was completely absent, whereas IHH was expressed and mostly downregulated compared to normal thymocytes. Among GLI1 targets, PTCH2 was the only one to correlate with GLI1 and IHH (Fig. 7B), while no correlation was found for IHH-GLI1 and IHH-PTCH1 (Fig. 7C), strengthening the hypothesis of a mechanism of HH activation other than autocrine signalling.



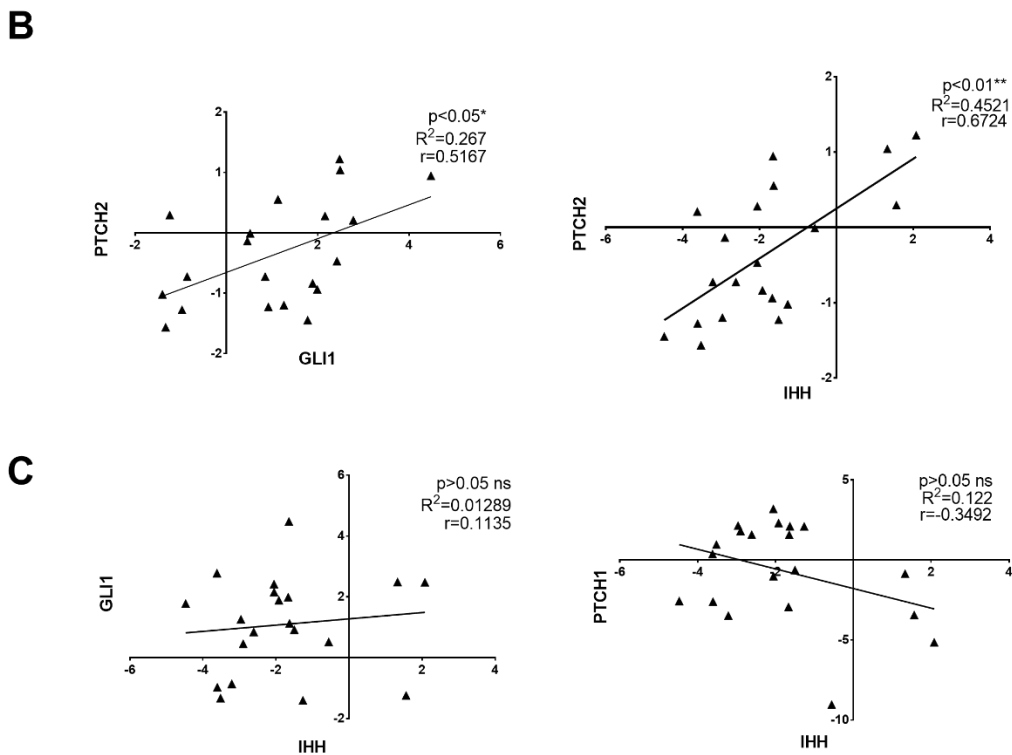


**Figure 7: HH pathway components are aberrantly expressed in T-ALL PDX samples**

**A)** Relative expression analysis by RT-PCR of genes encoding HH pathway components in PDX samples (n=20). Scatter dot plots show mRNA levels as log<sub>2</sub>-transformed fold change ( $2^{-\Delta\Delta CT}$ ) to normal human thymocytes (n=4). Dashed line indicates median expression levels in normal human thymocytes. Results are presented with horizontal bars indicating the median and error bars indicating interquartile range. GAPDH and RPL19 genes were used as housekeeping genes. **B-C)** Correlation between expression levels of HH genes evaluated by linear regression analysis and Pearson's correlation test. (ns,  $p > 0.05$ , \*  $p < 0.05$ )

Finally, we assessed the expression of major mediators and targets of HH signalling in two different Notch1-induced T-ALL murine models, previously generated in our lab. One murine model (HD- $\Delta$ PEST) is induced by an activated form of NOTCH1 that closely resembles human NOTCH1 mutated alleles and carries a L1601P mutation in the heterodimerization domain (HD), together with a deletion in the PEST domain. The other model of murine NOTCH1-induced leukemia ( $\Delta$ E) is based on the over-expression of the  $\Delta$ E allele, presenting a deletion in the EGF-like domain. As shown in

Figure 8, in both models we could detect HH pathway activation, with a frequent upregulation of signalling components with respect to normal murine thymocytes.

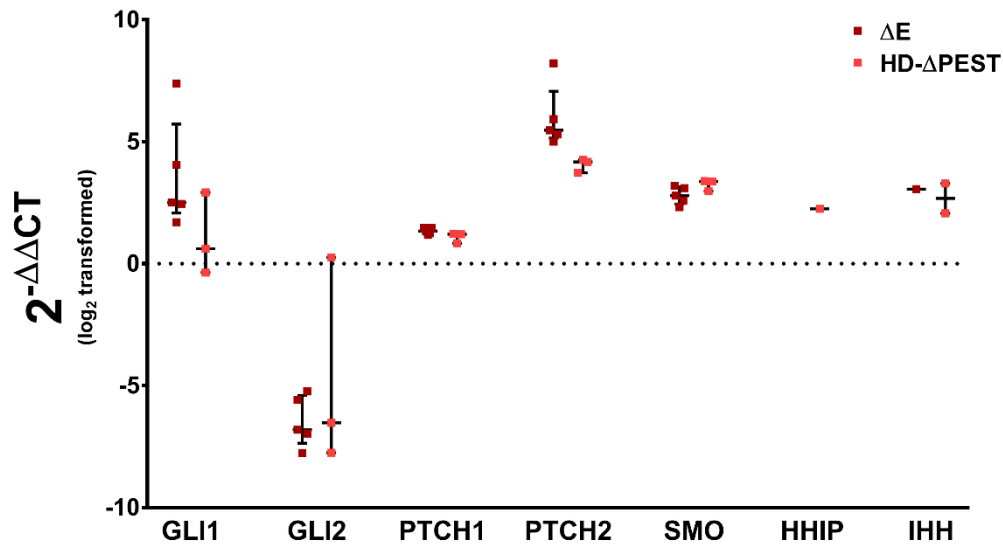


**Figure 8: HH pathway components are aberrantly expressed in Notch1-induced T-ALL murine models**

Relative expression analysis by RT-PCR of genes encoding HH pathway components in  $\Delta E$  (n=5) and HD- $\Delta PEST$  (n=3) T-ALL murine models. Scatter dot plots show mRNA levels as log<sub>2</sub>-transformed fold change ( $2^{-\Delta\Delta CT}$ ) to normal murine thymocytes (n=5). Dashed line indicates median expression levels in normal murine thymocytes. Results are presented with horizontal bars indicating the median and error bars indicating interquartile range.  $\beta$ -Actin and  $\beta$ 2-microglobulin genes were used as housekeeping genes.

Collectively our data suggest that, despite the absence or weak expression of HH ligands, pathway components are expressed in T-ALL cells and most importantly GLI1 transcription factor, the main signalling mediator, is upregulated in T-ALL samples compared to their normal counterpart.

## 4.2 Assessment of the effects of Hedgehog inhibition on T-ALL cells *in vitro*

Since our expression data indicated a frequent upregulation of HH pathway components in T-ALL, we next evaluated the sensitivity of T-ALL samples to HH inhibition *in vitro*. We tested the effects as single agents of two HH inhibitors, cyclopamine and GANT61, which block the signalling cascade at two distinct levels. Cyclopamine is a natural steroidal alkaloid antagonizing SMO receptor [172], while GANT61 is a small molecule acting downstream of SMO which impairs the DNA-binding capacity of GLI1/2 transcription factors [173]. We treated T-ALL cell lines and PDX-derived cells with a range of concentrations of cyclopamine (1-20 $\mu$ M) and GANT61 (5-40 $\mu$ M) and assessed cell viability by ATPlite assay.

After 72h of treatment, IC<sub>50</sub> values of GANT61 ranged from 11 to 45 $\mu$ M (median IC<sub>50</sub>=18.8 $\mu$ M) for T-ALL cell lines (n=14, Fig. 9A) and sensitivity to GANT61 positively correlated with the expression levels of GLI1 transcript (Fig. 9B). The effects of HH inhibition via GANT61 treatment were also evaluated in cells derived from 17 PDX treated *ex vivo*. IC<sub>50</sub> values from Annexin V-FITC/Sytox Red staining experiments (Fig. 9A) after 48h of GANT61 treatment confirmed a reduction in cell viability (median IC<sub>50</sub>=21.1 $\mu$ M). As expected, higher GLI1 expression was associated with higher sensitivity to GANT61 treatment also in PDX-derived cells (Fig. 9C).

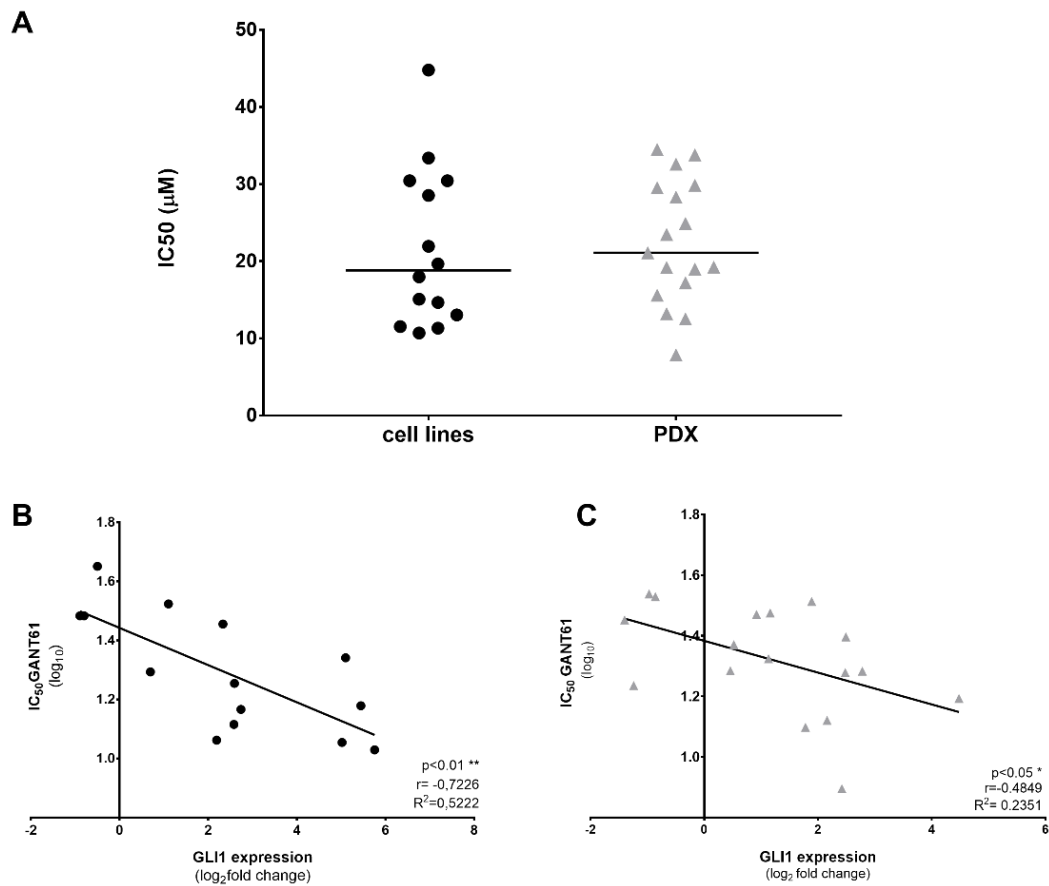


**Figure 9: A subset of T-ALL cell lines and PDX samples are sensitive to HH inhibitor GANT61**

A) Drug sensitivity (represented as individual IC<sub>50</sub> values) evaluated in T-ALL cell lines (n=14) and PDX samples (n=17) treated *in vitro* with a range of concentrations of GLI1 inhibitor GANT61. Horizontal bars are medians for IC<sub>50</sub> distributions. B-C) Correlation between GLI1 gene expression and GANT61 sensitivity (IC<sub>50</sub>) in T-ALL cell lines (B) and PDX (C) evaluated by linear regression analysis and Pearson's correlation test (\* p<0.05, \*\* p<0.01).



T-ALL cell lines (n=12) showed a modest sensitivity to cyclopamine treatment (Fig. 10A), with  $IC_{50}$  concentrations ranging from 12 to 50  $\mu\text{M}$  (median  $IC_{50}$ =18.8 $\mu\text{M}$ ). However, Tomatidine, an inactive structural analogue of cyclopamine, exerted a comparable cytotoxic effect (median  $IC_{50}$ =13.1 $\mu\text{M}$ ) on the tested cell lines, suggesting an off-target action of Cyclopamine other than Smo inhibition (Fig. 10A). Moreover, response to cyclopamine did not correlate with SMO expression levels (Fig. 10B).

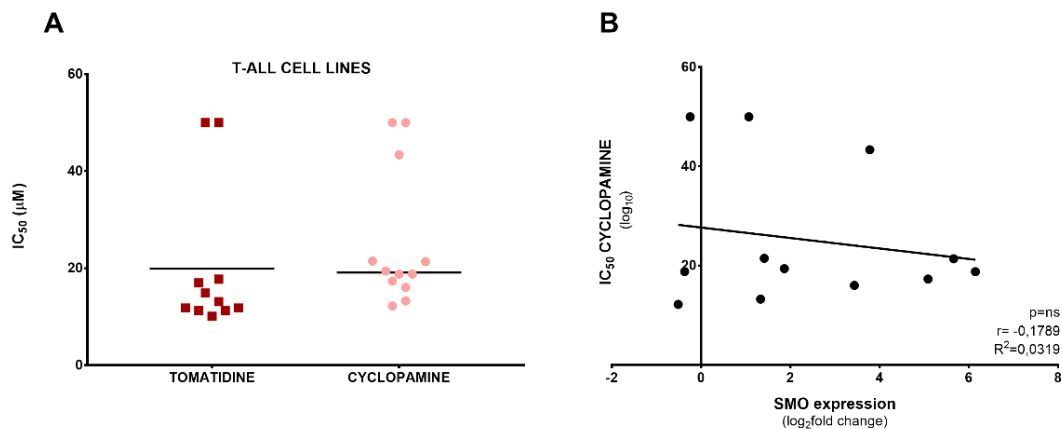


**Figure 10: T-ALL cell lines are not sensitive to HH inhibition by cyclopamine**

**A)** Drug sensitivity (represented as individual  $IC_{50}$  values) evaluated in T-ALL cell lines (n=12) treated in vitro with a range of concentrations of SMO inhibitor cyclopamine or its inactive structural analogue Tomatidine. Horizontal bars are medians for  $IC_{50}$  distributions. **B)** Correlation between SMO gene expression and cyclopamine sensitivity ( $IC_{50}$ ) in T-ALL cell lines evaluated by linear regression analysis and Pearson's correlation test (ns  $p>0.05$ ).

### 4.3 GANT61 and Dexamethasone show a synergistic anti-leukemic effect *in vitro*

Our data indicating relative insensitivity to SMO inhibition, together with the mounting literature highlighting a role for non-canonical SMO-independent HH activation in cancer, prompt us to investigate possible crosstalks between HH signalling pathway and other commonly deregulated oncogenic pathways in T-ALL. For this purpose, HD- $\Delta$ PEST mouse-derived cells were treated *ex vivo* with 2.5 $\mu$ M GANT61 in combination with a panel of inhibitors targeting diverse oncogenic pathways. The exclusive dependence of this T-ALL murine model on Notch1 pathway makes it ideal for this type of analysis, excluding the interference of confounding factors. As shown in Figure 11, the pharmacological combinations under study revealed a strong synergistic action between GANT61 and NOTCH1 pathway inhibitor dibenzazepine (DBZ), as well as between GANT61 and glucocorticoids (GCs).

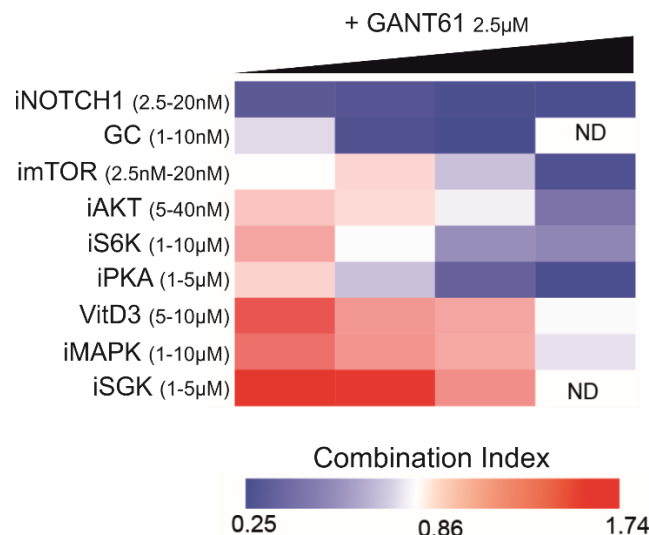


**Figure 11: Signalling pathways modulating sensitivity to HH pathway inhibitor GANT61**  
Heatmap representation of combination indexes (CI) of inhibitors targeting commonly deregulated pathways in T-ALL in combination with 2.5 $\mu$ M GANT61 in HD- $\Delta$ PEST mouse-derived cells. CI>1 indicates antagonism, CI<1 indicates synergism.


Given the prominent function of GCs in the treatment of lymphoid malignancies and the unfavorable prognosis of prednisone poor responders among T-ALL patients [50,174], we further explored the potential crosstalk between the HH pathway and the GC receptor (NR3C1, Nuclear Receptor Subfamily 3 Group C Member 1) pathway.

Five T-ALL cell lines (CCRF-CEM, DND41, MOLT4, HSB2, CUTLL1), differing for their sensitivity to GCs, were cultured *in vitro* with incremental doses of Dexamethasone (Dexa, 1nM-1 $\mu$ M) alone or in combination with 10 $\mu$ M GANT61. Cell viability analysis assessed by ATPlite after 48h (or 72h where indicated) of treatment revealed that all the tested lines showed enhanced cytotoxicity when treated with Dexa in combination with GANT61, with respect to either drugs alone (Fig. 12). Indeed, all the tested lines displayed a combination index value <1 for every drug combination, confirming the synergistic activity of GANT61 plus Dexa, as shown in Table 5.

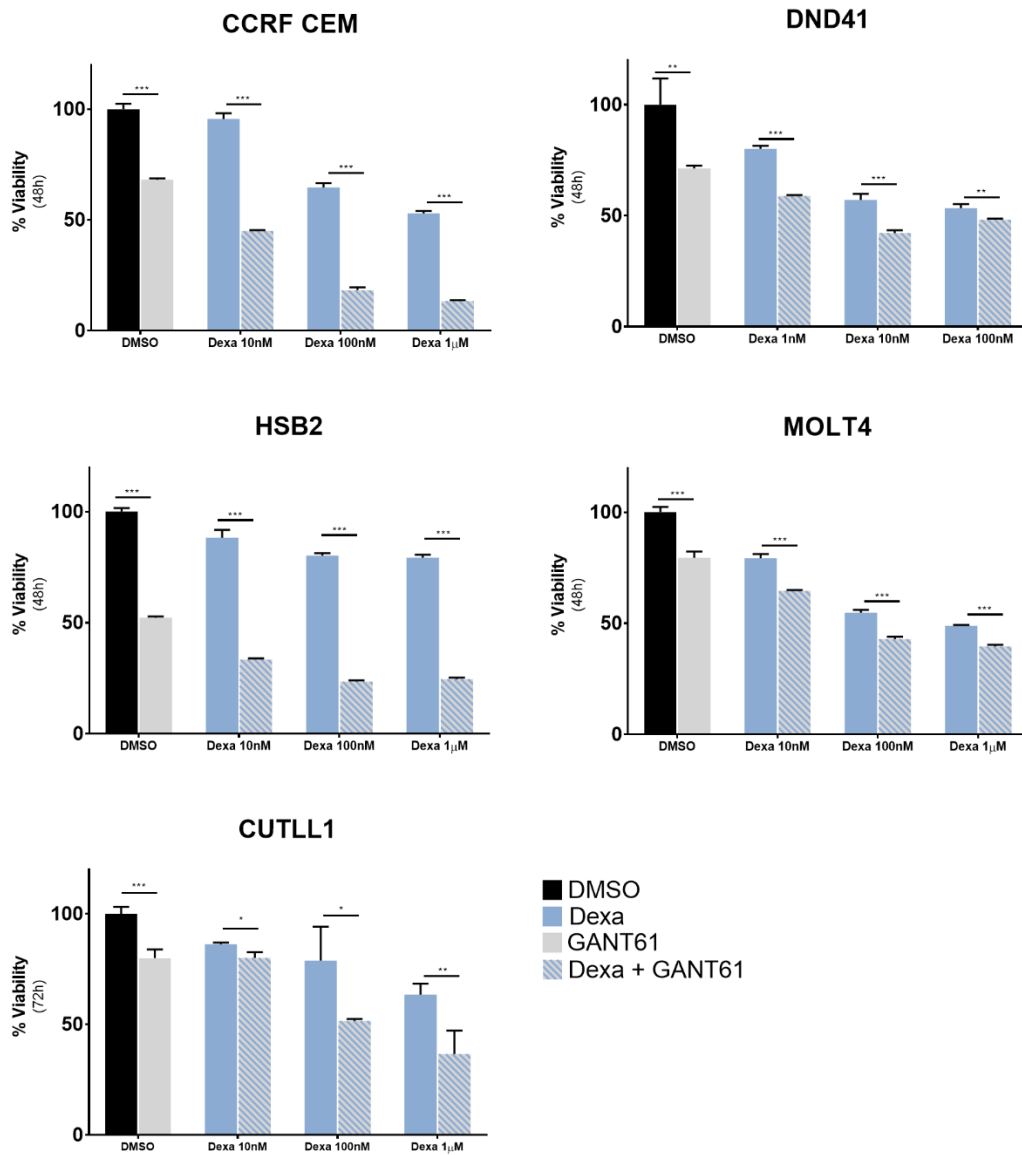


**Figure 12: GANT61 sensitizes T-ALL cell lines to Dexa treatment**

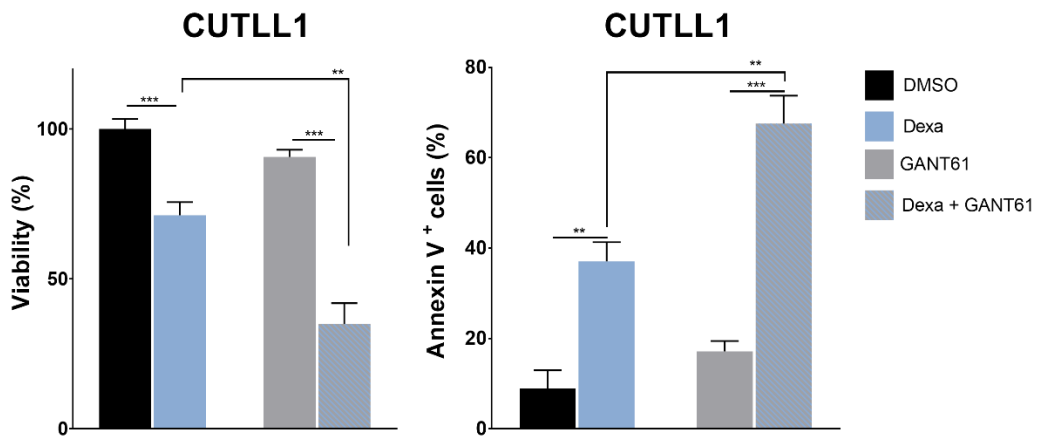
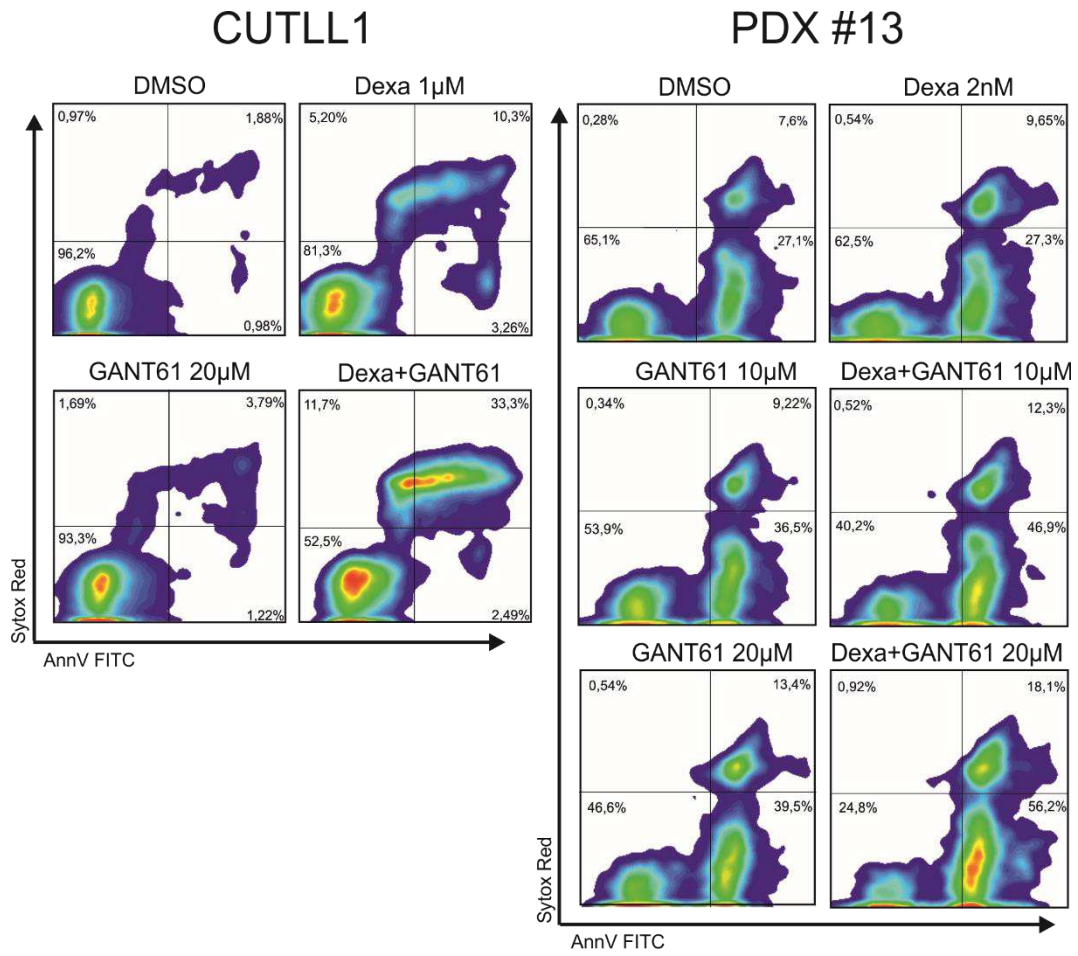
Cell viability analysis in CEM-ATCC, DND41, MOLT4, HSB2 and CUTLL1 T-ALL cell lines treated *in vitro* with DMSO (vehicle), Dexa (1nM-1 $\mu$ M), GANT61 (10 $\mu$ M) or Dexa plus GANT61. Results are shown as the mean $\pm$ SD. (ns,  $p > 0.05$ , \*  $p < 0.05$ , \*\*  $p < 0.01$ , \*\*\*  $p < 0.001$ )

COMBINATION INDEX (CI)			
	DEXA 		
<b>CCRF-CEM</b>	0.19	0.18	0.20
<b>DND 41</b>	0.18	0.07	0.90
<b>MOLT 4</b>	0.23	0.08	0.48
<b>HSB2</b>	0.69	0.52	0.54
<b>CUTLL1</b>	0.20	0.48	0.63

**Table 5: Combination index values (CI) for Dexa and GANT61 combinations in T-ALL cell lines**

CI>1 indicates antagonism, CI<1 indicates synergism.

Increased cytotoxicity of the combination treatment was also confirmed evaluating apoptosis by Annexin V-FITC/Sytox Red experiments. As shown in Figure 13, treatment for 72h with the combination Dexa plus GANT61 induced a more pronounced pro-apoptotic effect in comparison to single drugs, both in CUTLL-1 cells and PDX cells (n=4). CI values for drug combinations in PDX samples are shown in Table 6.



(continued)

## 4. Results

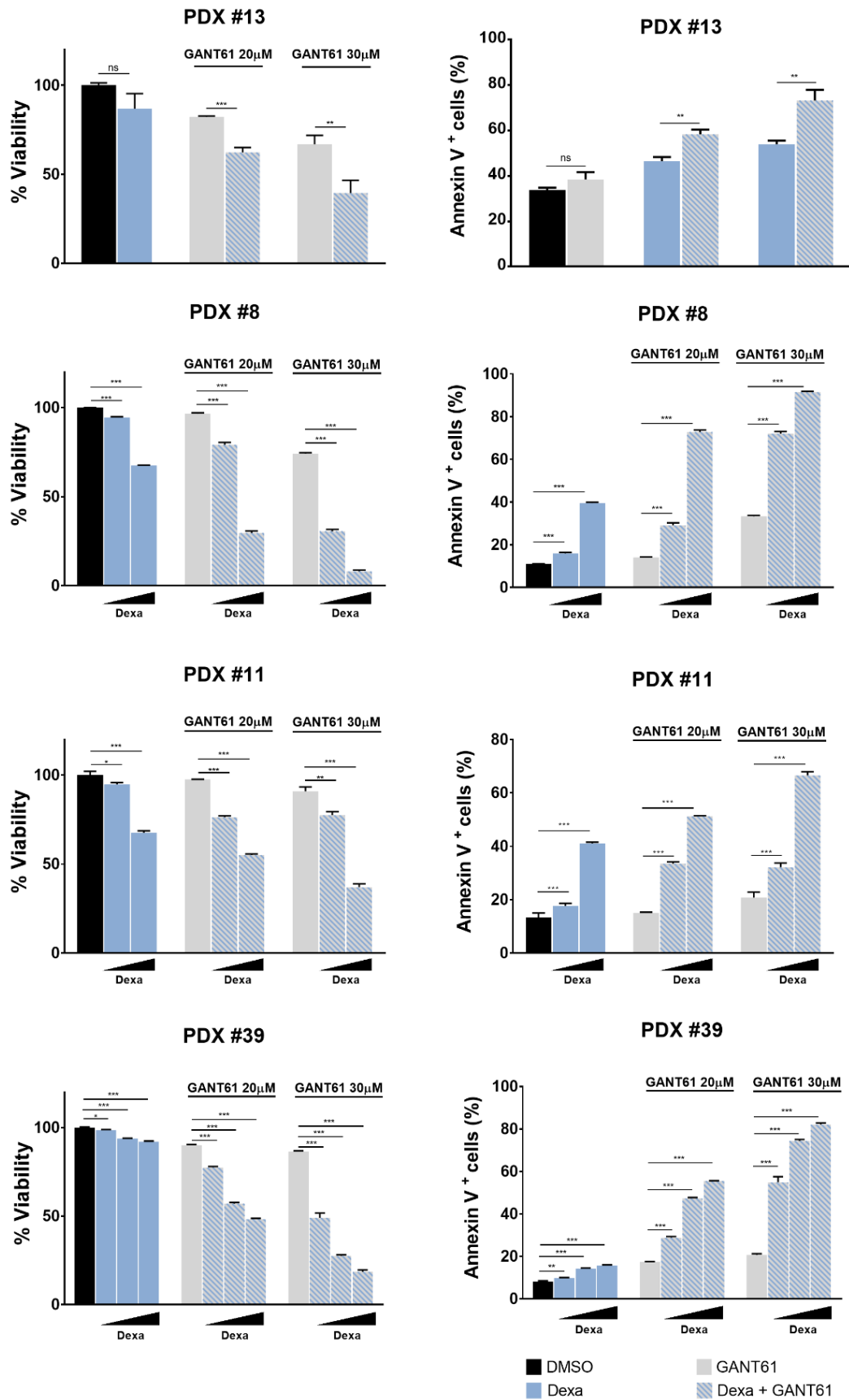


**Figure 13: GANT61 and Dexa induce a synergistic pro-apoptotic effect in cell lines and PDX samples**

Representative plots of Annexin V-FITC/ Sytox Red staining and quantification of cell viability and apoptosis in CUTLL1 cells and PDX samples (#8, #11, #13, #39) treated *in vitro* with DMSO as vehicle, Dexa only (10nM-1 $\mu$ M), GANT61 only (10-30 $\mu$ M) or Dexa+GANT61. (ns  $p > 0.05$ , \*  $p < 0.05$ , \*\*  $p < 0.01$ , \*\*\*  $p < 0.001$ ).

COMBINATION INDEX (CI)

		<table border="1" style="display: inline-table; vertical-align: middle;"> <tr> <td style="border: none;"></td> <td style="border: none;">D</td> </tr> <tr> <td style="border: none;">G</td> <td style="border: none;"></td> </tr> </table>				D	G	
	D							
G								
PDX 8	20 $\mu$ M	0.89	0.65	-				
	30 $\mu$ M	0.74	0.57	-				
PDX 11	20 $\mu$ M	0.64	0.93	-				
	30 $\mu$ M	0.91	0.70	-				
PDX 39	20 $\mu$ M	0.32	0.10	0.07				
	30 $\mu$ M	0.10	0.03	0.02				

**Table 6: Combination index values (CI) for Dexa and GANT61 combinations in PDX-derived cells**

CI > 1 indicates antagonism, CI < 1 indicates synergism. D=Dexa, G=GANT61.

Finally, we evaluated by Propidium Iodide (PI) staining the effects of the combination treatment on cell cycle regulation in PDX-derived cells (n=3). For one of the tested samples (PDX #39), cell cycle analysis after 72h treatment revealed a synergistic action of the combination Dexa plus GANT61 in inducing cell cycle arrest at G1 phase, enhancing the already massive effect of single drugs alone. No such prominent results were observed for PDX #8 and PDX #11, suggesting that in these samples the observed reduced viability was a consequence of apoptosis induction rather cell cycle arrest (Fig. 14).



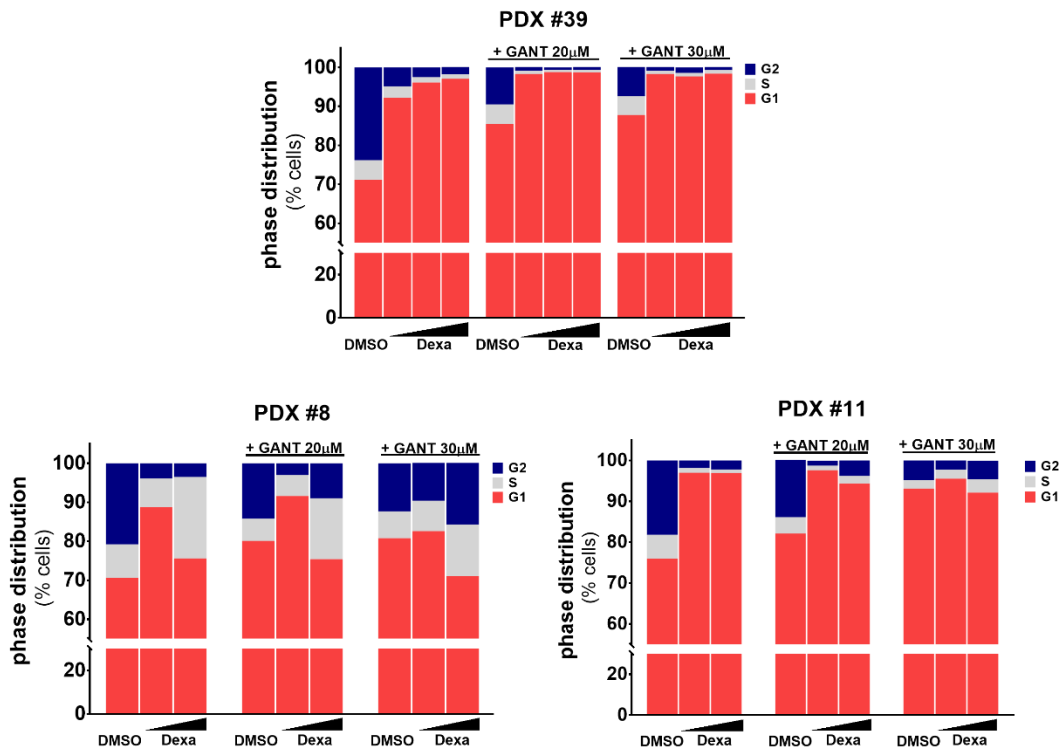


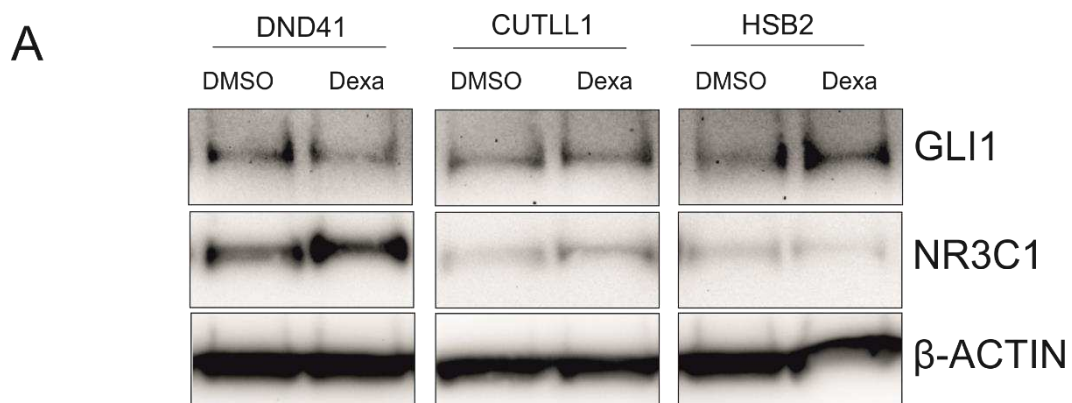
**Figure 14: The combination of Dexa plus GANT61 predominantly exerts a pro-apoptotic effect**

Cell cycle analysis following PI staining in PDX samples (#8, #11, #39) treated *in vitro* with DMSO as vehicle, Dexa only (10nM-1μM), GANT61 only (20-30μM) or Dexa+GANT61. Stacked bars represent cell cycle phase distribution.

#### 4.4 Dexamethasone impairs GLI1 function

In order to gain mechanistic insights on the found synergistic anti-leukemic action of the combination Dexa plus GANT61 -implying a crosstalk between HH pathway and the NR3C1 pathway- we studied the effect of Dexa on the modulation of HH signalling in T-ALL cell lines.

Selected T-ALL cell lines differing for their sensitivity to GCs were treated with 1 $\mu$ M Dexa and the expression of GLI1 and its principal targets PTCH1 and HHIP were assessed by Western blot analysis (Fig. 15A) and Real time RT-PCR (Fig. 15B) after 24h. The GC-sensitive DND41 cell line showed an upregulation in transcript levels of GLI1 and its targets upon Dexa treatment, while GLI1 protein was surprisingly downregulated. In the GC-resistant CUTLL1 cell line, GLI1 transcript was downregulated in response to Dexa, while GLI1 protein levels and GLI1 targets were not consistently modulated. Finally, the highly GC-resistant HSB2 cell line displayed a general upregulation of GLI1 transcript and protein, which was also associated with an induction of its targets.



*(continued)*

B

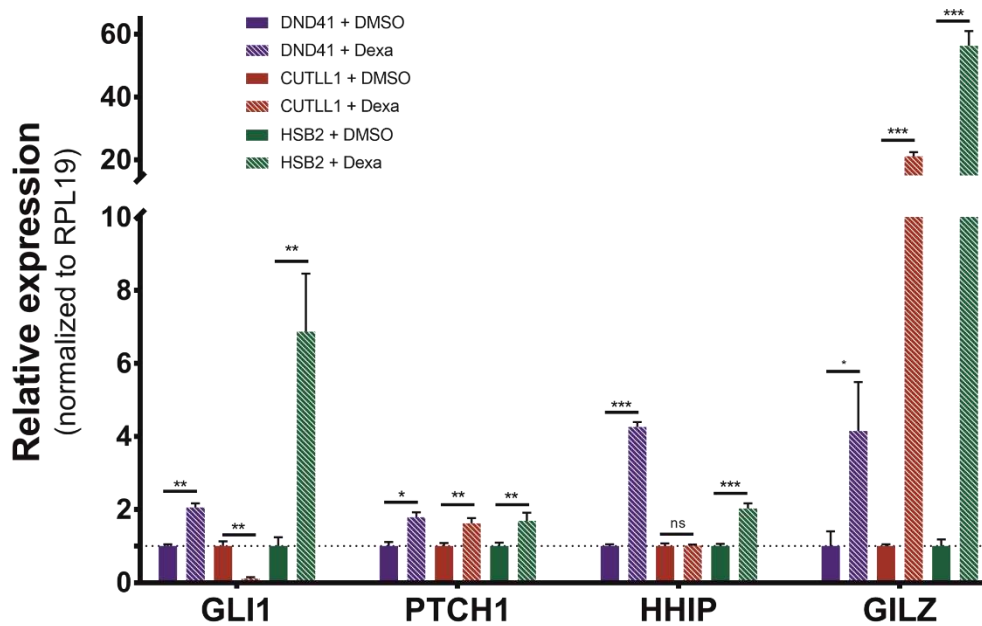


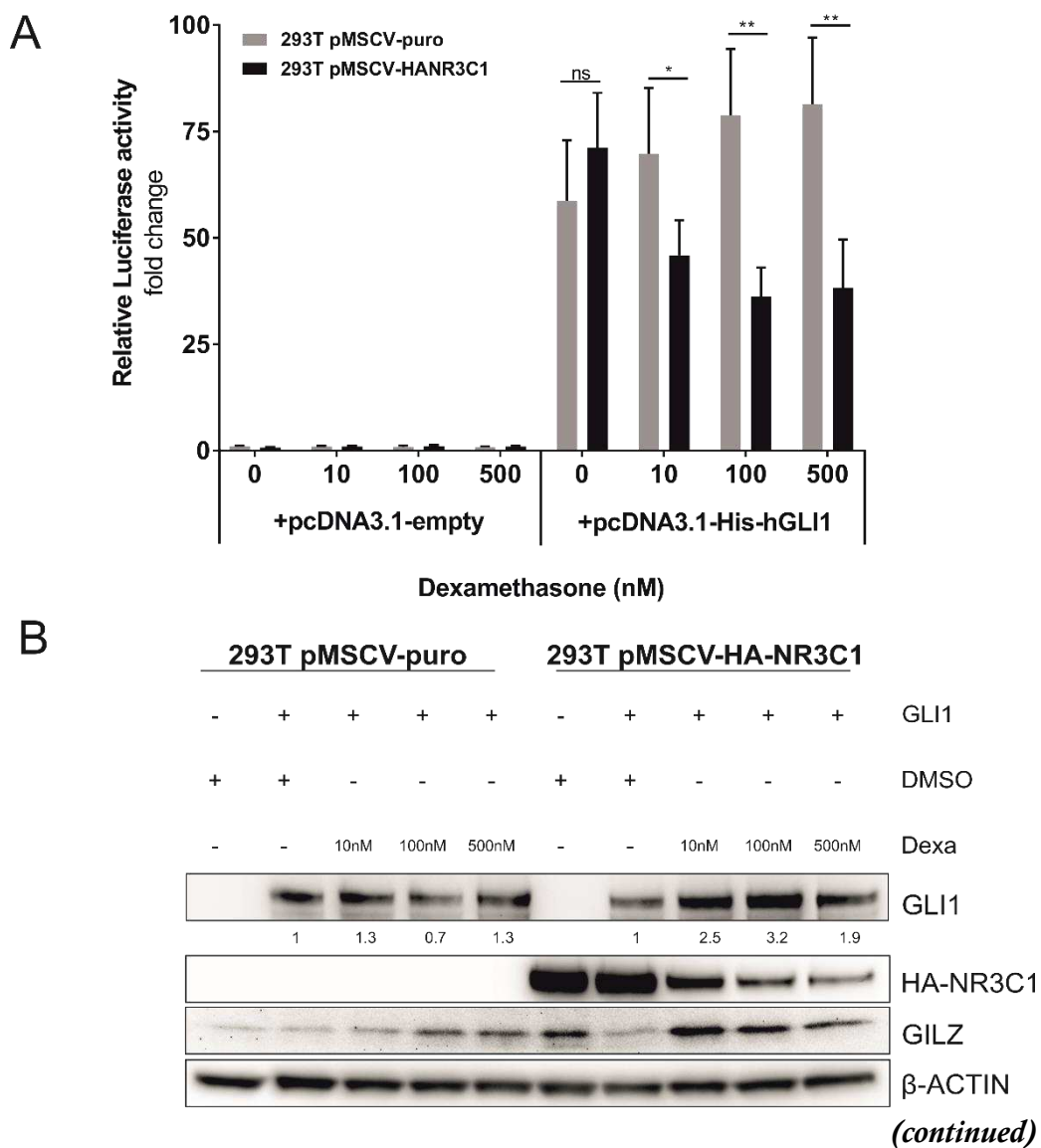
**Figure 15: Dexa induces heterogeneous modulation of HH signalling targets**

Western blot analysis (A) and Real time RT-PCR (B) of selected T-ALL cell lines treated for 24h with 1 $\mu$ M Dexa.  $\beta$ -Actin was used as loading control in A. NR3C1 protein and GILZ transcript were evaluated as controls for GC treatment. Relative expression is represented as fold change ( $2^{-\Delta\Delta CT}$ ) normalized to RPL19 housekeeping gene in panel B. Results are shown as the mean $\pm$ SD. (ns,  $p > 0.05$ , \*  $p < 0.05$ , \*\*  $p < 0.01$ , \*\*\*  $p < 0.001$ )

Altogether, our data did not disclose a clear and coherent transcriptional effect of Dexa-activated GC signalling on HH pathway, suggesting inherent genetic heterogeneity of T-ALL cell lines may hinder further mechanistic studies. To bypass this issue, we turned to a more versatile cellular system, HEK-293T cells. To clarify the functional impact of GCs on GLI1 transcriptional activity, we generated HEK-293T cells stably expressing HA-tagged NR3C1 (hereinafter referred to as 293T HA-NR3C1) and transiently transfected them with a GLI-responsive reporter (8x3'Gli-BS-delta51-LucII) together with exogenous GLI1 or empty vector. After 24h treatment, we found that Dexa (10nM-500nM) could repress promoter activation (Fig. 16A) in a dose-dependent manner in these cells, while no effect was observed in control cells

not expressing NR3C1 (293T pMSCV-puro). Western blot analysis did not reveal a reduction in GLI1 protein levels, but rather an upregulation, as shown in Figure 16B. GC treatment determined the downregulation of NR3C1 protein, with the induction of the NR3C1 target gene GILZ.

Dexa-mediated repression of GLI1 activity was further validated by dual luciferase reporter assay in 293T HA-NR3C1 cells transfected with different plasmids encoding GLI1, confirming a comparable negative effect on GLI1 function for every expression construct evaluated (Fig. 16C).



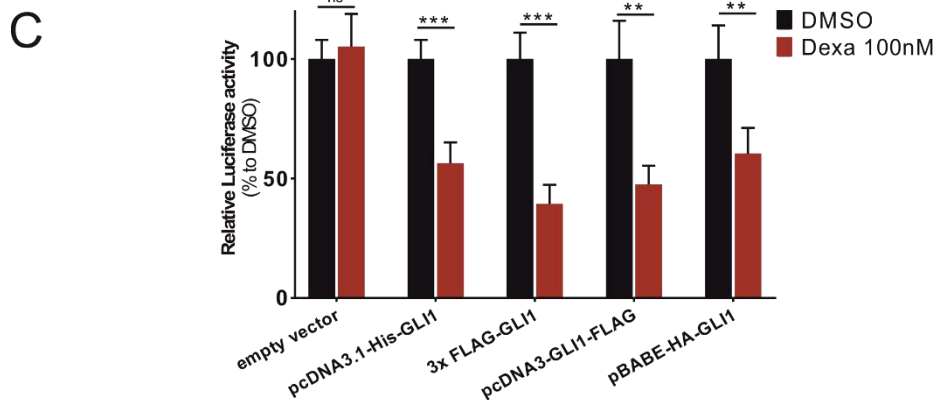
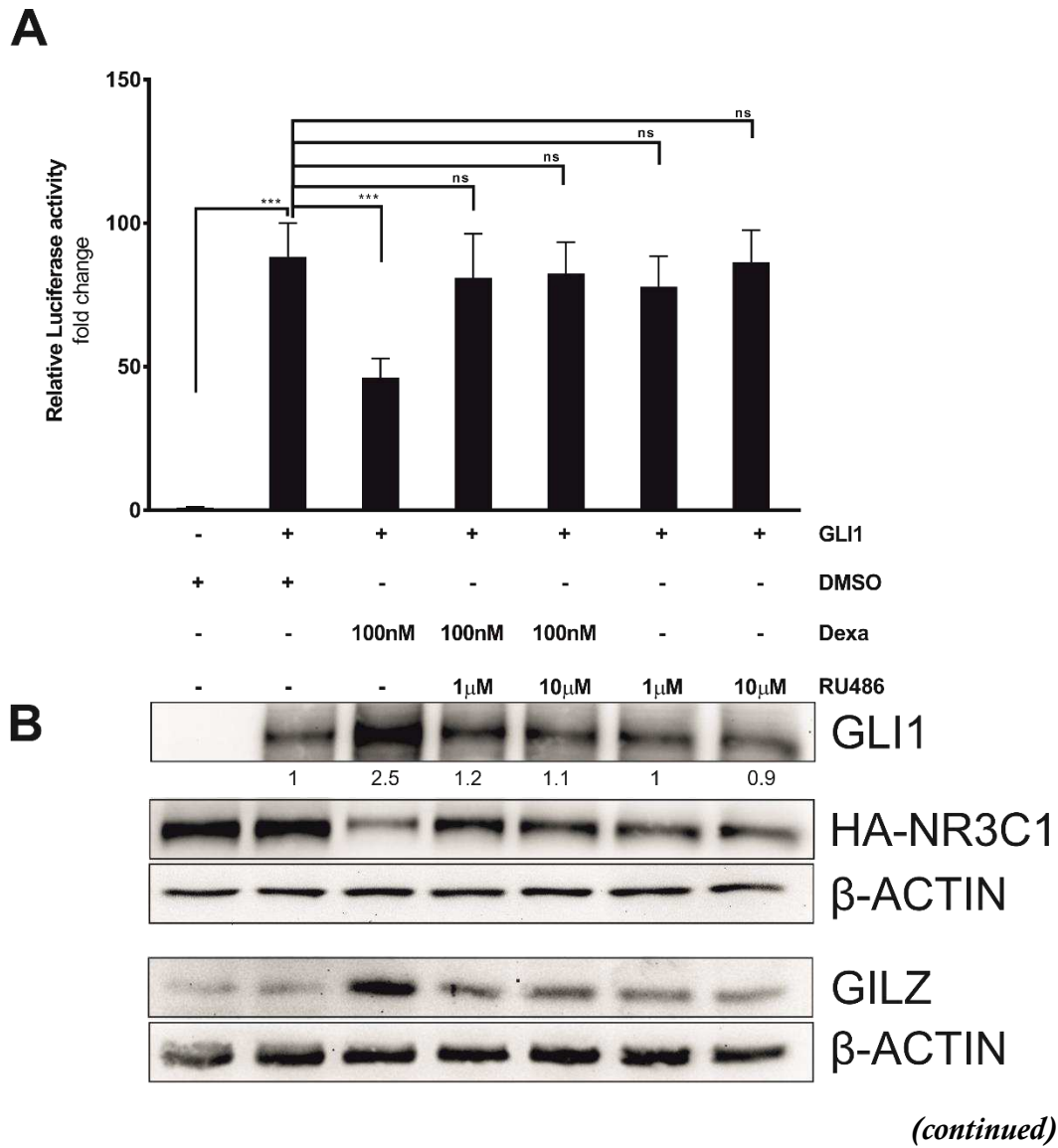


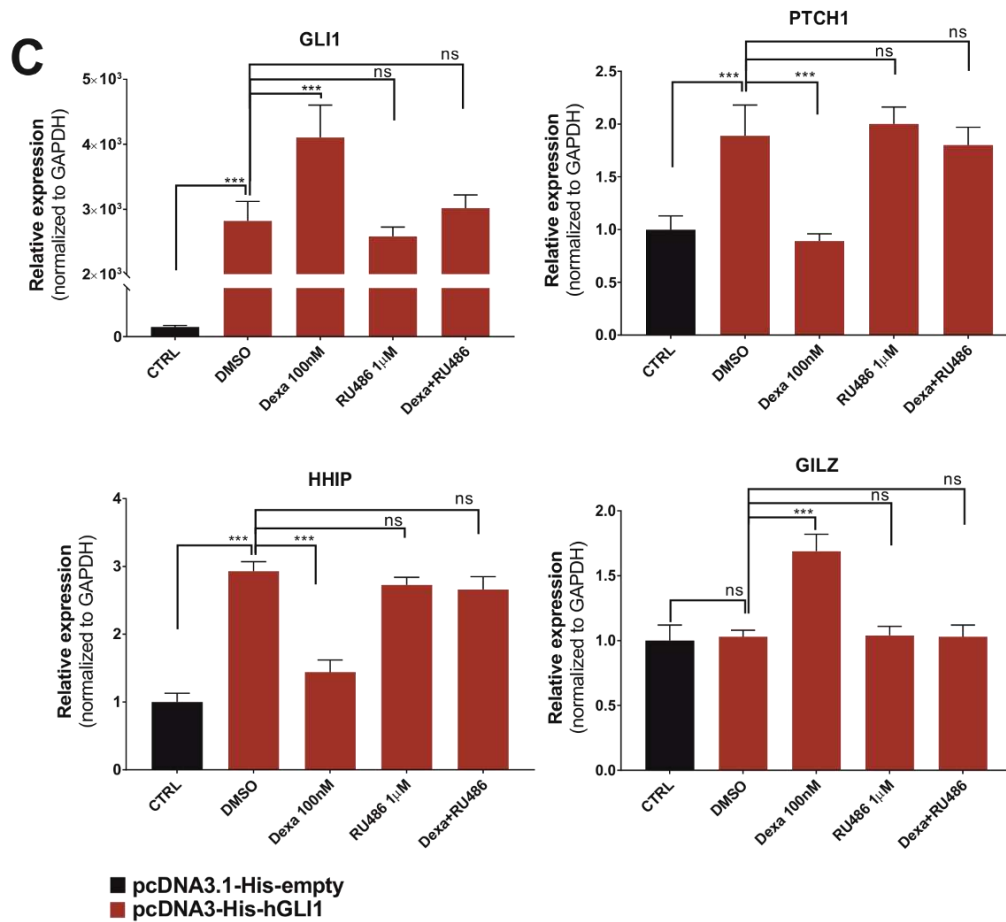
**Figure 16: Dexa negatively affects GLI1 transcriptional activity**

Dual luciferase reporter assay (A) and Western blot analysis (B) of 293T cells expressing HA-tagged NR3C1 or control plasmid (pMSCV-puro), transfected with GLI1 or empty vector and treated with Dexa or DMSO (vehicle). Luciferase activity (calculated as relative Firefly luciferase activity normalized against Renilla luciferase activity) is represented as fold change to empty vector.  $\beta$ -Actin was used as loading control in panel B. Numbers indicate results of densitometric analysis of GLI1 bands normalized to  $\beta$ -Actin. C) Dual luciferase reporter assay of 293T HA-NR3C1 cells, transfected with different GLI1-expressing constructs or empty vector and treated with Dexa or DMSO (vehicle). Relative luciferase activity for each expression plasmid was normalized against DMSO-treated condition, set to 100%. 8x3'Gli-BS-delta51-LucII was used as a reporter plasmid in panels A and C. Results are shown as the mean  $\pm$  SD. (ns,  $p > 0.05$ , \*  $p < 0.05$ , \*\*  $p < 0.01$ , \*\*\*  $p < 0.001$ ).

In order to confirm the specific requirement for NR3C1 in Dexa-mediated repression, we treated 293T HA-NR3C1 cells with GC antagonist mifepristone (RU486, 1-10  $\mu$ M) alone or in combination with 100nM Dexa. As shown in Figure 17, RU486 could reverse the negative effect of Dexa on GLI1 transcriptional activity (Fig. 17A) and abolish the Dexa-induced stabilization of GLI1 protein (Fig. 17B). As expected, RU486 could also revert the induction of NR3C1 target gene GILZ and the downregulation of NR3C1 protein following Dexa treatment (Fig. 17B).

Gene expression analysis by quantitative Real-time RT-PCR confirmed the functional repression of GLI1 by Dexa, showing a downregulation of HH target genes PTCH1 and HHIP, despite higher expression levels of GLI1 (Fig. 17C).

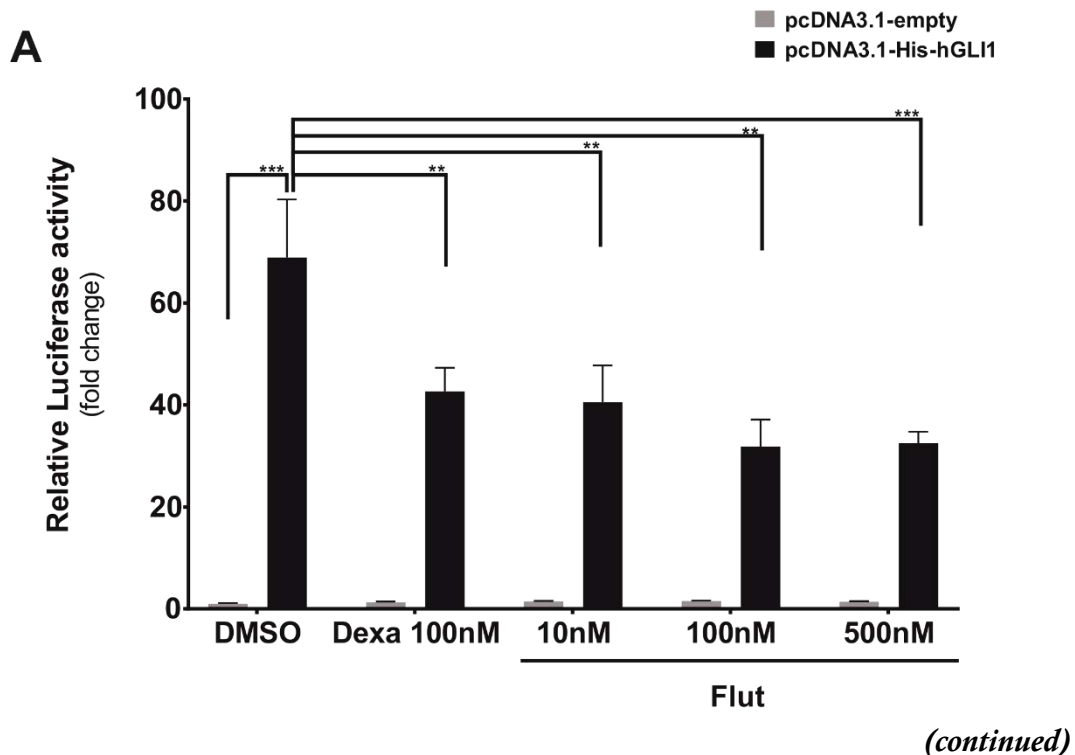




**Figure 17: RU486 reverts the effects of Dexa on GLI1 transcriptional activity**

Luciferase reporter assay (A), Western blot analysis (B) and Real time RT-qPCR (C) of 293T HA-NR3C1 cells transfected with GLI1 or empty vector and treated with Dexa, RU486 or the combination Dexa+RU486.  $8 \times 3'$ Gli-BS-delta51-LucII was used as a reporter plasmid in panel A. Luciferase activity (calculated as relative Firefly luciferase activity normalized against Renilla luciferase activity) is represented as fold change to empty vector.  $\beta$ -Actin was used as loading control in panel B. Numbers indicate results of densitometric analysis of GLI1 bands normalized to  $\beta$ -Actin. GILZ protein and transcript were evaluated as control for GC treatment. Relative expression is represented as fold change ( $2^{-\Delta\Delta CT}$ ) to empty vector, normalized to GAPDH housekeeping gene in panel C. Results are shown as the mean  $\pm$  SD. (ns,  $p > 0.05$ , \*  $p < 0.05$ , \*\*  $p < 0.01$ , \*\*\*  $p < 0.001$ )

We also tested the fluorinated steroid Fluticasone (Flut, 10-500nM), which was previously identified as a SMO agonist at very high doses by Wang *et al.* [175]; however, we detected the same transcriptional inhibitory effect as Dexa treatment (Fig. 18A), which may indicate that Flut can have a dual role in regulating HH signalling, possibly depending on the dose and cell type. Western blot analysis (Fig. 18B) showed an upregulation in GLI1 protein after treatment with Dexa and Flut 10nM, while an upregulation in GLI1 protein levels was not observed for higher concentrations (100-500nM) of Flut, despite the comparable effect on GLI1 transcriptional activity in the functional assay. Interestingly, the induction of NR3C1 target GILZ mirrored the effects seen on GLI1 protein levels. Indeed, there was a significant induction of GILZ only after treatment with 10nM Flut, suggesting possible activation of negative feedback loops at the highest doses used.





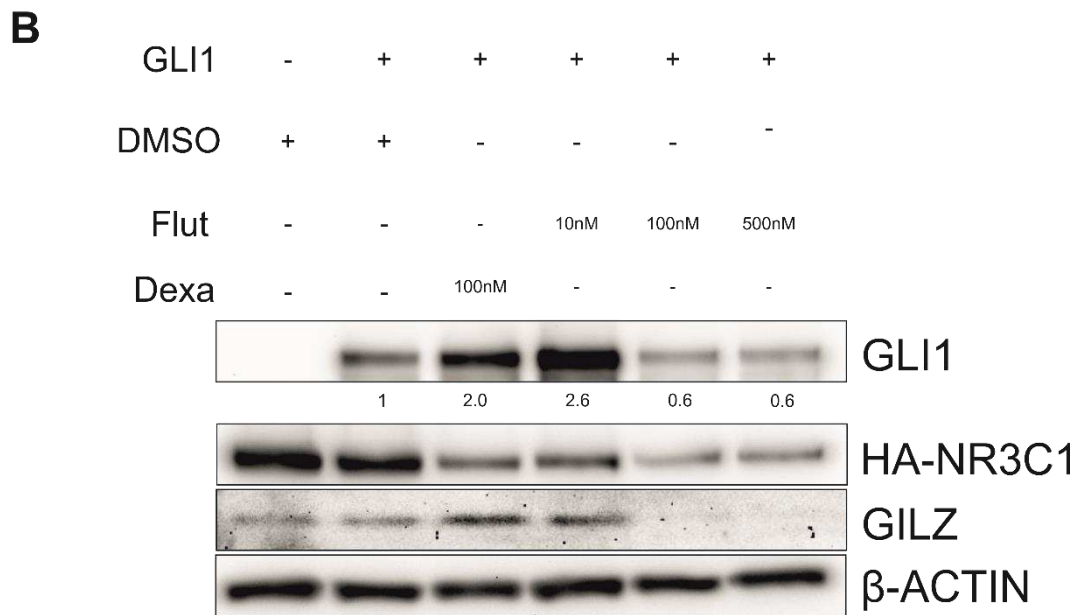


**Figure 18: Additional synthetic glucocorticoids can inhibit GLI1 function**

Dual luciferase reporter assay (A) and Western blot analysis (B) of 293T HA-NR3C1 cells transfected with GLI1 or empty vector and treated with 100nM Dexa, Flut (10-500nM) or DMSO (vehicle). 8x3'Gli-BS-delta51-LucII was used as a reporter plasmid in panel A. Luciferase activity (calculated as relative Firefly luciferase activity normalized against Renilla luciferase activity) is represented as fold change to empty vector. Results are shown as the mean $\pm$ SD.  $\beta$ -Actin was used as loading control in panel B. Numbers indicate results of densitometric analysis of GLI1 bands normalized to  $\beta$ -Actin. (ns,  $p>0.05$ , \*  $p<0.05$ , \*\*  $p<0.01$ , \*\*\*  $p<0.001$ )

Collectively, our data suggest that a post-translational, rather than transcriptional, mechanism might account for the observed Dexa-mediated impairment of GLI1 function. As transcription factors, GLI proteins are in fact subjected to alterations in their stability, subcellular trafficking and DNA binding capacity, with major consequences on their final transcriptional output.

## 4.5 Dexamethasone does not affect GLI1 subcellular localization

HH signalling activation leads to GLI1 translocation and accumulation into the nucleus to regulate target gene transcription. We therefore investigated if GLI1 distribution was altered upon Dexa treatment, as a possible cause of its reduced functionality. Cell fractionation of 293T cells stably expressing HA-tagged NR3C1 and HA-tagged GLI1 followed by immunoblotting (Fig. 19, upper left corner) indicated a preferential nuclear expression of GLI1 protein, but no changes in its distribution were observed in response to 100nM Dexa treatment. Nevertheless, GLI1 protein levels were upregulated in Dexa-treated cells in comparison to control, in agreement with previous results. As expected, Dexa-activated HA-NR3C1 shuttled from the cytoplasm to the nucleus, confirming the efficacy of the treatment. Next, we evaluated GLI1 subcellular localization in DND41, CUTLL1, and HSB2 T-ALL cell lines, expressing endogenous GLI1 and NR3C1. As for 293T HA-NR3C1 cells, GLI1 expression was predominantly nuclear in all tested T-ALL cell lines and no differences in its distribution between the cytoplasm and the nucleus were observed upon 1 $\mu$ M Dexa treatment. (Fig. 19). Though its distribution was not affected, the amount of GLI1 in the soluble nuclear fractions (*i.e.* not chromatin bound) was decreased in DND41 and HSB2 T-ALL cell lines upon Dexa treatment.

Interestingly, NR3C1 expression following Dexa treatment showed a marked difference between 293T cells and T-ALL cell lines. NR3C1 expression was repressed in 293T cells, while its expression was induced in all T-ALL cell lines analyzed.

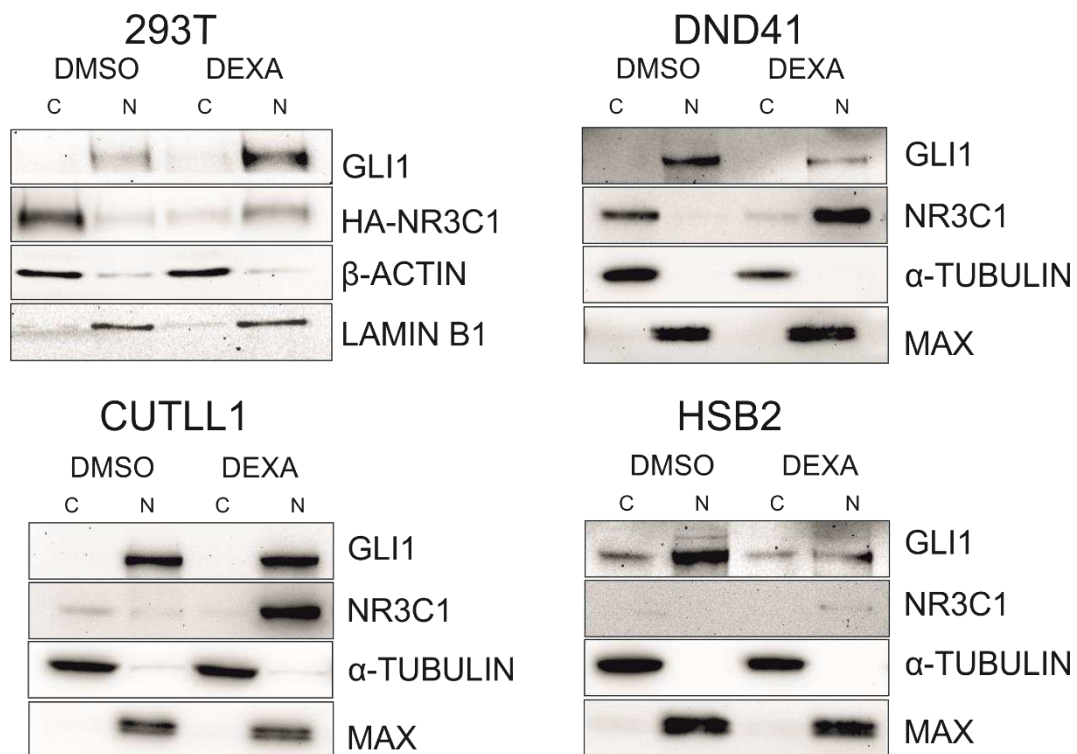


**Figure 19: GLI1 cellular distribution is not affected by Dexa**

Western blot analysis after cell fractionation of 293T cells stably expressing HA-tagged NR3C1 and HA-tagged GLI1 and T-ALL cell lines (DND41, CUTLL1, HSB2) treated with Dexa or DMSO (vehicle).  $\beta$ -Actin and  $\alpha$ -tubulin were used as loading controls for cytoplasmic fractions, lamin B1 and MAX were used as loading controls for nuclear fractions. C, cytoplasmic; N, nuclear.

#### 4.6 Dexamethasone reduces GLI1 protein stability

To determine whether Dexa could interfere with GLI1 function by altering its stability, we evaluated GLI1 protein half-life by cycloheximide (CHX) pulse-chase experiments. 293T cells stably expressing both HA-tagged NR3C1 and HA-tagged GLI1 were pre-treated with Dexa or DMSO (vehicle) and protein expression was assessed by Western blot analysis after protein synthesis inhibition with 50 $\mu$ g/mL CHX for the indicated time points. A

general up-regulation in GLI1 protein levels in the presence of Dexa was observed, however GLI1 protein degradation rate was higher in treated versus untreated cells (Fig. 20). A similar accelerated turnover of GLI1 protein - despite its higher expression levels - was also observed in Dexa-treated HSB2 T-ALL cell line with respect to vehicle-treated control cells.

Unlike GC-resistant 293T and HSB2 cells, the GC-sensitive DND41 T-ALL cell line showed a downregulation in GLI1 protein levels in response to Dexa; however, GLI1 stability was similarly affected.

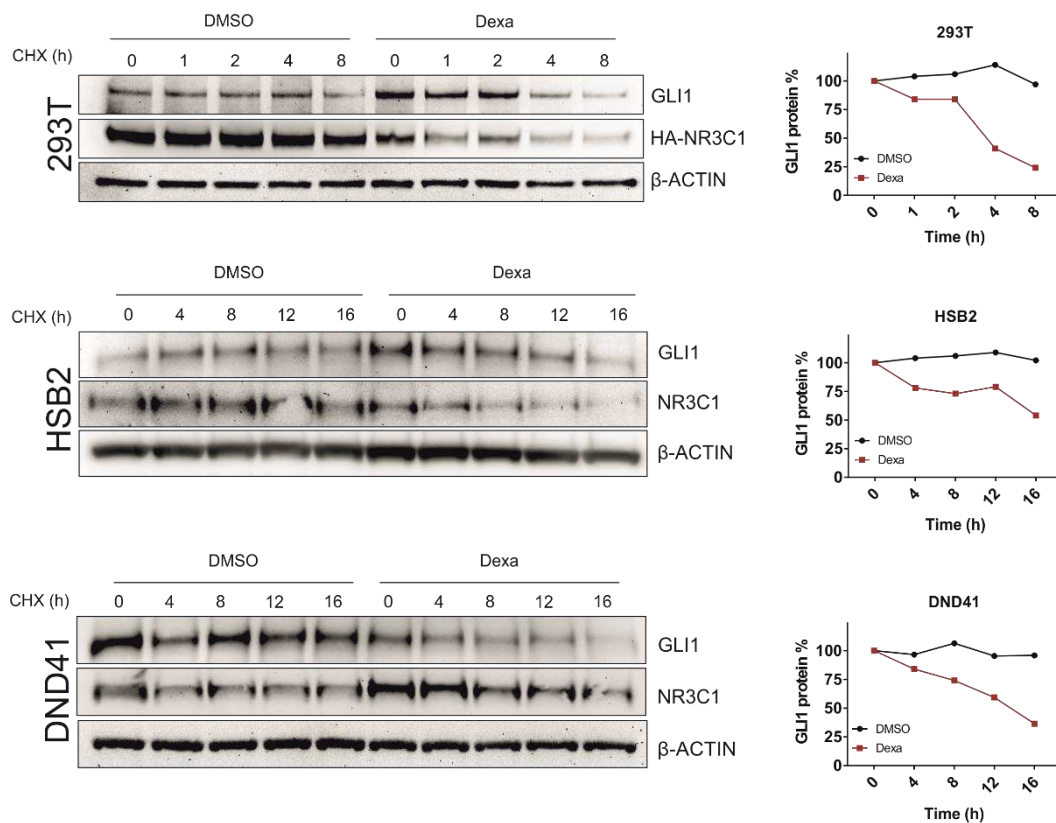


**Figure 20: Dexa promotes GLI1 protein turnover**

CHX pulse-chase experiment in 293T cells stably expressing HA-tagged NR3C1 and HA-tagged GLI1 (upper panel) and in selected T-ALL cell lines (HSB2, mid panel; DND41, lower panel), in the presence of Dexa or DMSO (vehicle). Lysates were harvested at indicated time points and analyzed by Western blot analysis. NR3C1 protein was evaluated as control for Dexa treatment.  $\beta$ -Actin was used as loading control. GLI1 protein levels (represented as % to t=0) were quantified by densitometry analysis and normalized to  $\beta$ -Actin.

### **4.7 NR3C1 interacts with GLI1 and promotes its acetylation**

As previously mentioned, post-translational modifications -namely phosphorylation, acetylation, ubiquitination- play a key role in GLI1 regulation and often are the result of the convergence of different signalling pathways on GLI1, leading to its non-canonical activation.

First, we evaluated whether GLI1 and NR3C1 interacted in 293T HA-NR3C1 cells and DND-41 T-ALL cell line by immunoprecipitation (IP). 293T HA-NR3C1 cells were transfected with FLAG-tagged GLI1 and IP was performed using an anti-FLAG antibody. Western blot analysis following IP revealed the presence of HA-NR3C1 protein in FLAG-GLI1 immunoprecipitates, suggesting a physical interaction between GLI1 and NR3C1 (Fig. 21A). Moreover, IP of GLI1 protein complexes from DND41 T-ALL cell line confirmed the interaction between endogenous GLI1 and NR3C1 (Fig. 21B).

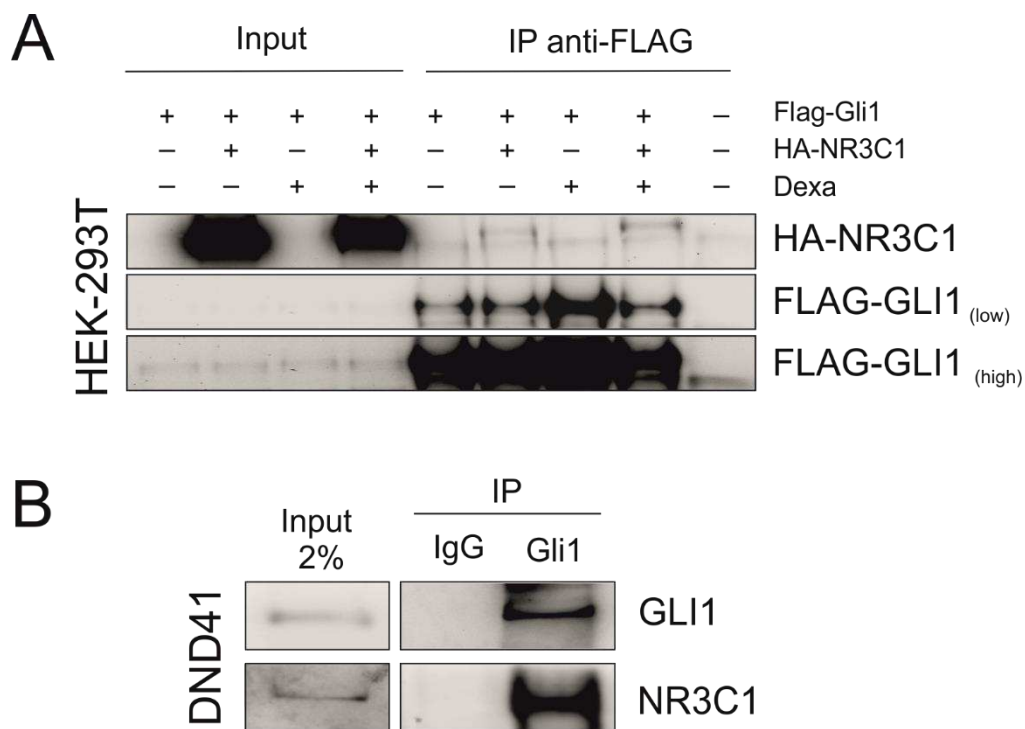


**Figure 21: GLI1 interacts with NR3C1**

Western blot analysis for NR3C1 after GLI1 IP in 293T cells expressing HA-tagged NR3C1 and Flag-tagged GLI1 (**A**) and in DND41 T-ALL cell line (**B**). *Low* and *high* indicate shorter or longer exposures of the same membrane.

Next, we sought to evaluate the acetylation status of GLI1 upon Dexa treatment as acetylation was described to inhibit the transcriptional activity of both GLI1 and GLI2 preventing their target promoter occupancy [176-178]. Moreover, activated NR3C1 is reported to recruit histone acetyltransferases (HATs) and histone deacetylases (HDACs) as transcriptional co-activators/co-repressors to promoter sites [179,180].

IP of transfected GLI1 followed by probing with anti-acetylated lysine antibody confirmed acetylation of GLI1 in 293T HA-NR3C1 cells, indicating that GLI1 is acetylated under basal conditions and its acetylation is further enhanced by Dexa treatment (Fig. 22).

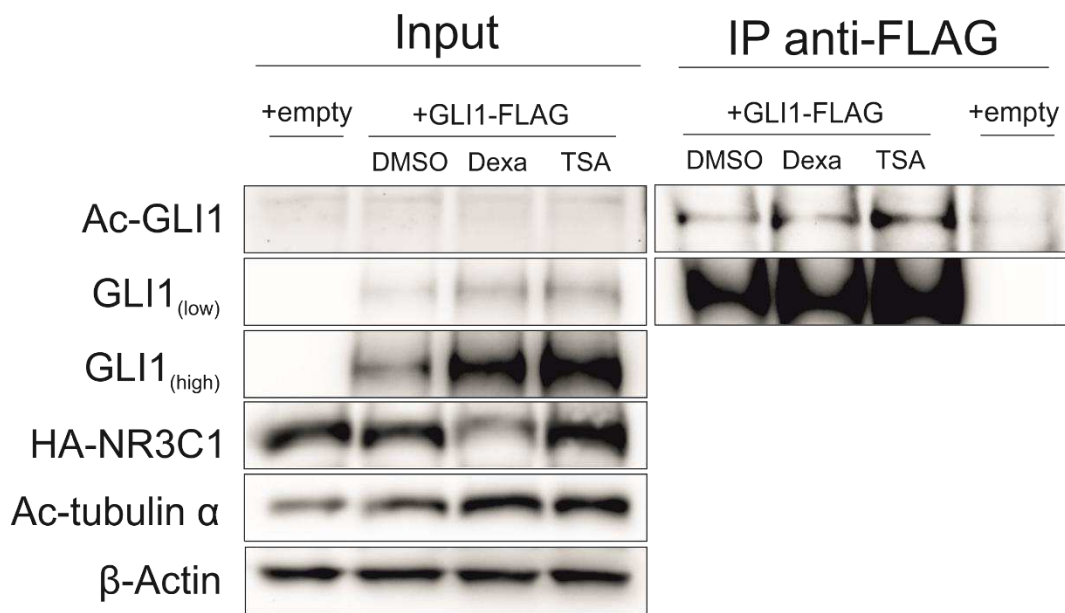


**Figure 22: Dexa treatment enhances GLI1 basal acetylation**

Western blot analysis of acetylated GLI1 (Ac-GLI1) after anti-FLAG IP in 293T HA-NR3C1 cells transfected with FLAG-tagged GLI1 (or empty vector), treated with DMSO, Dexa or HDAC pan-inhibitor Trichostatin A (TSA) as positive control for acetylation. Acetylation of  $\alpha$ -tubulin (Ac-tubulin  $\alpha$ ) was evaluated as positive control for TSA treatment.  $\beta$ -Actin was used as loading control. *Low* and *high* indicate shorter or longer exposures of the same membrane.

In order to assess the functional consequences of acetylation/deacetylation on HH signalling, we tested the effects of known modulators of GLI1 acetylation - including the HATs p300 and p300/CBP-associated factor (PCAF), and the histone deacetylase HDAC1- on GLI1-driven reporter activity. Interestingly, dual luciferase reporter assays in 293T HA-NR3C1 cells transiently transfected with GLI1 showed that overexpression of P300 and PCAF determined the same inhibitory effect on GLI1 transcriptional activity as Dexa treatment. By contrast, HDAC1 alone enhanced GLI1 transcriptional activity, with Dexa reverting this effect, suggesting therefore a role for acetylation behind the mechanism of Dexa-mediated impairment of GLI1 transcriptional function. As expected, HDAC1 in the presence of p300 or

PCAF almost completely reverted the repressive actions of p300 or PCAF (Fig. 23A).

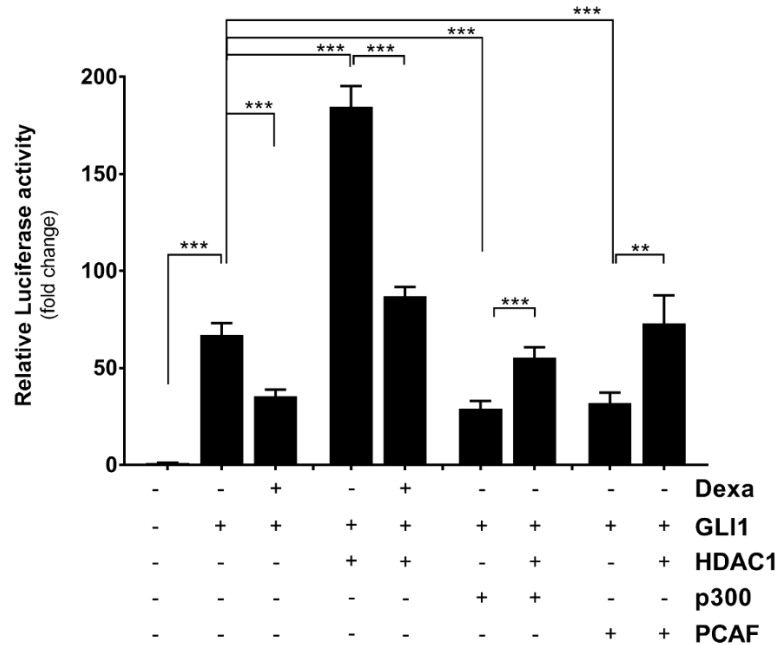


**Figure 23: HDAC1 activates, while p300 and PCAF repress, GLI1 transcriptional activity**  
 Dual luciferase reporter assay of GLI1-transfected 293T HA-NR3C1 and co-transfected with histone deacetylase HDAC1 or histone acetyltransferases p300 and PCAF. *8x3' Gli-BS-delta51-LucII* was used as Firefly reporter plasmid. Relative luciferase activity was calculated as Firefly luciferase activity normalized against Renilla luciferase activity and is represented as fold change to empty vector. Results are shown as the mean $\pm$ SD. (ns,  $p > 0.05$ , \*  $p < 0.05$ , \*\*  $p < 0.01$ , \*\*\*  $p < 0.001$ )

Next, to determine whether Dexa could alter the recruitment of acetylation modulators to GLI1, we performed IP following 24h treatment with 100nM Dexa in 293T HA-NR3C1 transiently co-transfected with GLI1 plus FLAG-tagged HDAC1, FLAG-tagged PCAF or myc-tagged p300. In agreement with previous studies [176,178,181], we could detect both FLAG-tagged HDAC1 and FLAG-tagged PCAF in anti-HA immunoprecipitates, indicating their basal physical association with HA-GLI1 (or HA-NR3C1) (Fig. 24A,B). Upon Dexa treatment, a reduction in immunoprecipitated HDAC1 as well as an



enrichment in immunoprecipitated PCAF were observed, consistent with our hypothesis of activated NR3C1 as a promoter of GLI1 hyperacetylation. Surprisingly p300, a well-described mediator of GLI1 acetylation, was not detected as a GLI1 partner after IP under basal conditions and was not recruited after Dexa treatment (Fig. 24C).

Interestingly, regardless of the opposite action on GLI1 function, both HDAC1 and p300 upregulated GLI1 protein levels, with Dexa further enhancing its expression.

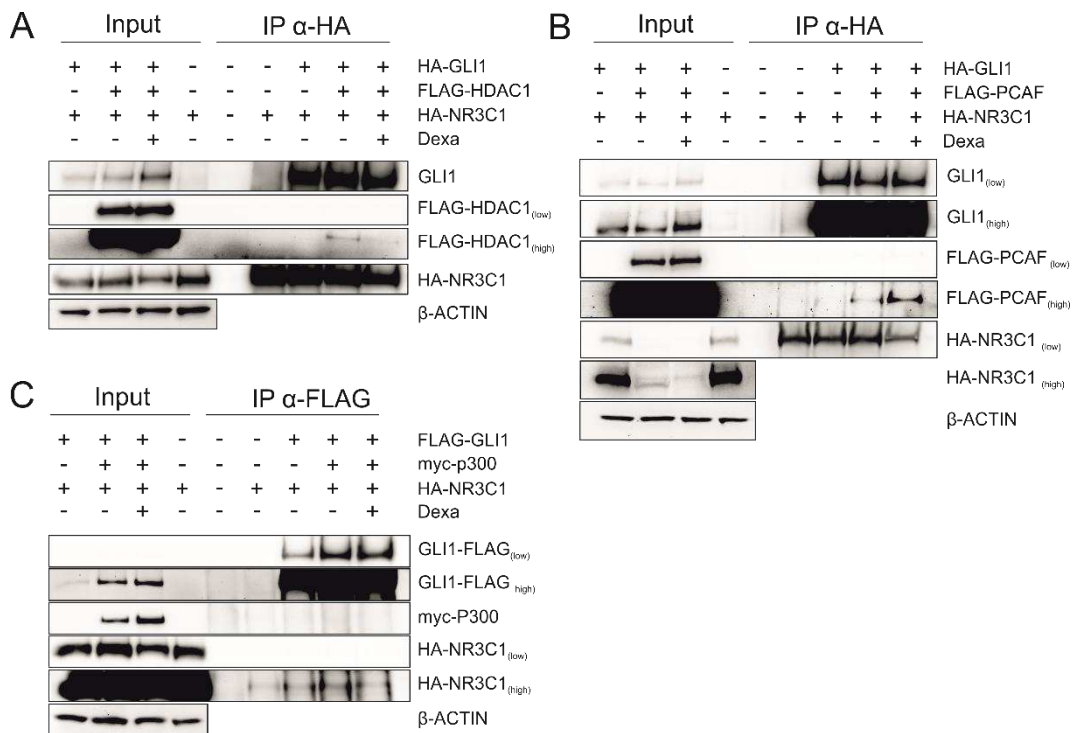


**Figure 24: Dexa dynamically regulates the interaction between HDAC1 and PCAF with GLI1**

Western blot analysis of FLAG-tagged HDAC1 (A) and FLAG-tagged PCAF (B) after anti-HA IP in 293T HA-NR3C1 cells transfected with HA-tagged GLI1. C) Western blot analysis of myc-tagged p300 after anti-FLAG IP in 293T HA-NR3C1 cells transfected with FLAG-tagged GLI1. β-Actin was used as loading control. *Low* and *high* indicate shorter or longer exposures of the same membrane.



## **5. Discussion**

HH signalling pathway is required for primitive hematopoiesis and plays a key role at different stages of intrathymic T-cell development, regulating thymocytes proliferation and differentiation. As other major developmental pathways, HH signalling is found to be disrupted in several hematological tumors. Indeed, despite the inability of HH pathway to initiate leukemogenesis, it has been shown to contribute to tumor cell proliferation and survival, as well as to cancer stem cell maintenance and chemoresistance. Thus, HH inhibition might be an interesting therapeutic option not merely restricted to a limited number of HH-dependent tumors, but also for a wider range of hematological malignancies, including T-ALL. Despite the substantial improvements over the years in T-ALL patients outcome, the significant fraction of primary resistant and relapsed patients demands a deeper characterization of the disease to identify novel therapeutic targets.

To address the hypothesis of HH pathway activation in T-ALL, we first analyzed a panel of T-ALL cell lines, PDX samples and Notch1-dependent T-ALL murine models for the expression of critical components of HH signalling cascade.

We could detect a frequent overexpression of GLI1 transcription factor, the main effector of HH pathway and conventional marker of signalling activation, in the majority of examined T-ALL samples, in comparison to normal thymocytes. Moreover, GLI1 expression positively correlated with its transcriptional targets PTCH1 and PTCH2, confirming pathway activation. Interestingly, while IHH ligand was expressed, though to a lesser extent with respect to normal thymocytes, SHH ligand was almost universally absent in our sample cohort. Also, no correlation was found between IHH expression and GLI1 or between IHH and HH targets. Unfortunately, our observations could not be confirmed in primary T-ALL samples from the largest publicly available RNA-seq dataset [182], as the arbitrary threshold set by the authors to discriminate GLI1 expression from background noise virtually excluded all

samples from analysis. Also, the absent or weak expression of HH ligands that we observed seems to disagree with the autocrine activation loop proposed by Dagklis *et al.* [166], which reported ectopic expression of SHH, IHH and GLI1 to account for HH activation in an independent group of T-ALL patients. The high expression of the HH transduction machinery in our samples, including membrane receptors PTCH1/2 and SMO, might rather suggest an inverse paracrine activation of the pathway, with stromal cells secreting HH ligands and T-ALL cells responding to the signal. However, *in vitro* inhibition of HH pathway at distinct steps of the signalling cascade highlighted a differential sensitivity of T-ALL cells to HH inhibitors cyclopamine and GANT61, hinting to a SMO-independent mechanism of HH activation. Indeed, the SMO antagonist cyclopamine exerted a comparable cytotoxic effect as its structural inactive analogue tomatidine, while GLI1/2 inhibitor GANT61 was shown to efficiently affect cell viability in both T-ALL cell lines and PDX-derived cells, with GANT61 sensitivity positively correlating with GLI1 expression.

The relative insensitivity to SMO inhibition and the lack of evidence in the literature of the presence of primary cilia - cellular organelles required for SMO-mediated signal transduction- on T-ALL blasts, indicate that HH pathway is likely activated at the level of downstream effector GLI1, bypassing SMO receptor in a ligand-independent fashion. This non-canonical activation of GLI1 is frequently reported in cancer and hematological tumors are no exception. The transcriptional deregulation characterizing the genetic landscape of T-ALL, as well as the aberrant activation of oncogenic signalling pathways, might converge on the regulation of GLI proteins, making the HH cascade far more complex than the canonical axis linking HH ligands to GLI proteins activation. These findings also have some attracting clinical implications suggesting that GLI1 represents a preferential therapeutic target in comparison to SMO. With this purpose, we performed pharmacological

combination studies *in vitro* in murine T-ALL-derived cells, screening commonly altered signalling pathways. The joint targeting of HH pathway by GANT61 and the glucocorticoid receptor pathway by Dexa revealed a strong synergism, which was further explored for its significant therapeutic potential, as GCs are administered throughout T-ALL therapeutic regimen and GC-responsiveness is a strong prognostic marker for T-ALL patients.

Intriguingly, Dexa and GANT61 were further shown to synergize *in vitro* in human T-ALL cell lines and PDX-derived cells, with the combination of the two drugs enhancing the cytotoxicity and pro-apoptotic effect of single drugs. Dexa treatment on T-ALL cell lines did not reveal a clear transcriptional effect on GLI1, inducing heterogeneous modulation of HH signalling, which might reflect the genetic diversity of the tested cell lines and their different degrees of sensitivity to Dexa treatment.

Mechanistically, we showed that synthetic GCs like Dexa and Fluticasone could impair GLI1 transcriptional activity in 293T cells, and this repressive effect required the GC receptor NR3C1. Considering the action of GANT61 on inhibiting GLI1 DNA binding, the capacity of Dexa to impair GLI1 transcriptional function seems plausible in light of the synergistic therapeutic effect of two drugs. These findings also agree with previous works showing that Dexa impairs the proliferation of cerebellar neuronal precursors by inhibiting SHH mitogenic effect [175,183,184], even if the mechanism was not elucidated. The link between HH and GCs is gaining interest, with selected GC compounds identified as SMO agonists promoting its accumulation in the primary cilium (though not sufficient to trigger HH pathway by itself); while some others (*e.g.* Budesonide and Ciclesonide) reported to impair ciliary localization and to inhibit HH pathway [175,185]. In cell-based assays, Dexa failed to compete for known SMO binding sites, but still was able to inhibit HH pathway [186], in agreement with our findings. It is important to note that in these works HH pathway modulation is presented as an off-target effect of

GCs on SMO receptor, occurring at much higher concentrations than those required for NR3C1 activation. This could explain the discrepancy observed in the repressive effect of Fluticasone in our reporter assays with respect to its putative role as SMO agonist reported by Wang *et al.* [175].

Gene and protein expression data in 293T HA-NR3C1 cells after treatment with Dexa indicated an increase in GLI1 transcript and protein levels notwithstanding its reduced function, therefore suggesting a post-translational mechanism of action. Indeed, the non-canonical activation of GLI1 may result not only from transcriptional upregulation of GLI genes, but also from various post-translational mechanisms altering GLI1 protein function at multiple levels, including subcellular trafficking and stability [151].

Looking at cellular localization, we detected a marked nuclear accumulation of GLI1 protein, which is line with active pathway, but we could not observe any re-distribution upon Dexa treatment in none of the tested cell lines. Further immunofluorescence analyses need to be performed to validate these observations and confirm a lack of GLI1 cytoplasmic relocation following Dexa treatment. Next, we showed that Dexa could affect GLI1 stability by promoting an accelerated turnover of the protein, which interestingly suggested a shared mechanism for both GC-sensitive and GC-resistant cell lines. Further studies are required to confirm ubiquitination-mediated degradation of GLI1 upon Dexa treatment and to potentially unveil if known E3 ubiquitin ligases (*e.g.* ITCH,  $\beta$ TrCP, Cul3/SPOP [187-189]) or others are responsible for this effect.

Subsequently, we focused our attention on GLI1 acetylation, as acetylation was reported to be a key post-translational modification negatively affecting GLI1 transcriptional activity [176-178]. Moreover, a proposed model for NR3C1-mediated transrepression suggests that NR3C1 and targeted transcription factors participate in an interacting complex, thereby affecting the transcription factor DNA-binding or altering the recruitment of co-

activators/repressors, including HATs and HDACs, to the transcriptional machinery [179,180].

We first demonstrated that GLI1 and NR3C1 physically interact both in transfected 293T cells and endogenously in T-ALL cells. If the nature of the interaction is direct or is indirectly mediated by a third adaptor, is yet to be elucidated.

Next, we showed that Dexa could enhance GLI1 acetylation, and that GLI1 transcriptional activity was likewise impaired by Dexa treatment and by overexpression of the HATs p300 and PCAF, with HDAC1 overexpression reverting the observed repressive effects.

GLI1 and GLI2 are known to be acetylated at lysine 518 and 527 respectively, with a major impact on their transcriptional output [176,177]. Moreover, acetylation was recently suggested to be a nuclear event that enhances GLI1 retention in the nucleus by a chaperoning system that sequesters it to the inner nuclear membrane [190]. On the other hand, HDAC1-mediated deacetylation represents the transcriptional switch that promotes GLI transcriptional activity [176]. Our IP experiments seem to suggest a model of action where PCAF recruitment to GLI1 is enhanced upon Dexa treatment, while HDAC1 is released, thereby promoting a hyperacetylated and less active status of GLI1 (Fig. 25). Interestingly, PCAF was previously reported to also possess a E3 ubiquitin ligase domain that promotes GLI1 degradation [191], so it would be tempting to speculate a role for PCAF in Dexa-induced instability of GLI1. Surprisingly, we could not detect p300 as a GLI1 partner, which might reflect a technical limitation due to inadequate overexpression of p300.

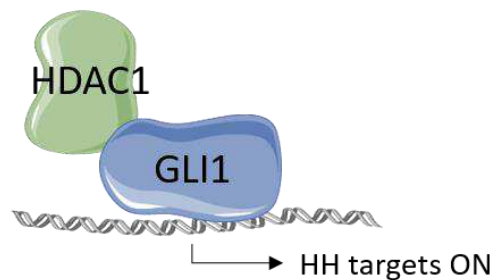
We acknowledge that our analysis was restricted to well-described mediators of GLI1 acetylation, therefore we cannot exclude a role for other HATs being recruited by NR3C1. These findings are currently being translated to T-ALL cells and will require shRNA-mediated knock down approaches to confirm a



role for these regulators on GLI1 acetylation/de-acetylation interplay in the repressive action of GCs on GLI1.

In conclusion, we demonstrated that HH pathway is active in a subset of T-ALLs putatively through a ligand-independent non-canonical mechanism of activation. We also collected evidence of a crosstalk between the GC signalling and HH pathway, highlighting a before undescribed role for NR3C1 as negative regulator of GLI1 transcription factor, setting the therapeutic rationale for combining GLI1 inhibitors and GCs.

### Basal condition:



### GC treatment:

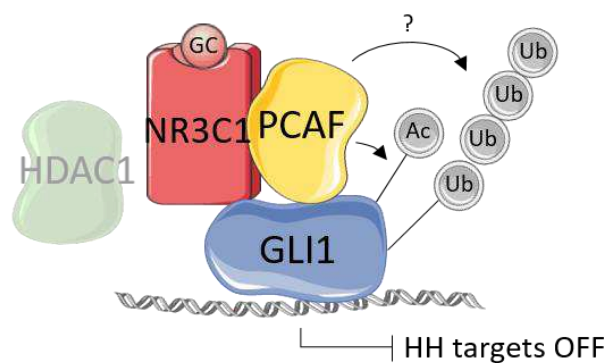


**Figure 25: Proposed mechanism for the crosstalk between HH signalling pathway and the glucocorticoid receptor pathway**

In absence of GC ligand, HDAC1 deacetylase promotes a deacetylated and transcriptionally active status of GLI1. Upon GC treatment, ligand-bound activated NR3C1 translocates to the nucleus and favors the recruitment of PCAF acetyltransferase as well as the dissociation of HDAC1 deacetylase. Acetylation impairs GLI1 transcriptional activity and possibly its protein stability. Ac, acetylation; Ub, ubiquitination.



## **6. References**

1. Hunger, S.P.; Mullighan, C.G. Acute Lymphoblastic Leukemia in Children. *N Engl J Med* **2015**, *373*, 1541-1552, doi:10.1056/NEJMra1400972.
2. Greaves, M.F.; Janossy, G.; Peto, J.; Kay, H. Immunologically defined subclasses of acute lymphoblastic leukaemia in children: their relationship to presentation features and prognosis. *Br J Haematol* **1981**, *48*, 179-197.
3. Roberts, K.G.; Mullighan, C.G. Genomics in acute lymphoblastic leukaemia: insights and treatment implications. *Nat Rev Clin Oncol* **2015**, *12*, 344-357, doi:10.1038/nrclinonc.2015.38.
4. Belver, L.; Ferrando, A. The genetics and mechanisms of T cell acute lymphoblastic leukaemia. *Nature Reviews Cancer* **2016**, *16*, 494-507, doi:10.1038/nrc.2016.63.
5. Hebert, J.; Cayuela, J.M.; Berkeley, J.; Sigaux, F. Candidate tumor-suppressor genes MTS1 (p16INK4A) and MTS2 (p15INK4B) display frequent homozygous deletions in primary cells from T- but not from B-cell lineage acute lymphoblastic leukemias. *Blood* **1994**, *84*, 4038-4044.
6. Begley, C.G.; Aplan, P.D.; Davey, M.P.; Nakahara, K.; Tchorz, K.; Kurtzberg, J.; Hershfield, M.S.; Haynes, B.F.; Cohen, D.I.; Waldmann, T.A., et al. Chromosomal translocation in a human leukemic stem-cell line disrupts the T-cell antigen receptor delta-chain diversity region and results in a previously unreported fusion transcript. *Proc Natl Acad Sci U S A* **1989**, *86*, 2031-2035, doi:10.1073/pnas.86.6.2031.
7. Xia, Y.; Brown, L.; Yang, C.Y.; Tsan, J.T.; Siciliano, M.J.; Espinosa, R., 3rd; Le Beau, M.M.; Baer, R.J. TAL2, a helix-loop-helix gene activated by the (7;9)(q34;q32) translocation in human T-cell leukemia. *Proc Natl Acad Sci U S A* **1991**, *88*, 11416-11420, doi:10.1073/pnas.88.24.11416.
8. Mellentin, J.D.; Smith, S.D.; Cleary, M.L. lyl-1, a novel gene altered by chromosomal translocation in T cell leukemia, codes for a protein with a helix-loop-helix DNA binding motif. *Cell* **1989**, *58*, 77-83, doi:10.1016/0092-8674(89)90404-2.
9. Wang, J.; Jani-Sait, S.N.; Escalon, E.A.; Carroll, A.J.; de Jong, P.J.; Kirsch, I.R.; Aplan, P.D. The t(14;21)(q11.2;q22) chromosomal translocation associated with T-cell acute lymphoblastic leukemia activates the BHLHB1 gene. *Proc Natl Acad Sci U S A* **2000**, *97*, 3497-3502, doi:10.1073/pnas.97.7.3497.
10. Royer-Pokora, B.; Loos, U.; Ludwig, W.D. TTG-2, a new gene encoding a cysteine-rich protein with the LIM motif, is overexpressed in acute T-cell leukaemia with the t(11;14)(p13;q11). *Oncogene* **1991**, *6*, 1887-1893.
11. McGuire, E.A.; Hockett, R.D.; Pollock, K.M.; Bartholdi, M.F.; O'Brien, S.J.; Korsmeyer, S.J. The t(11;14)(p15;q11) in a T-cell acute lymphoblastic leukemia cell line activates multiple transcripts, including

- Ttg-1, a gene encoding a potential zinc finger protein. *Mol Cell Biol* **1989**, *9*, 2124-2132, doi:10.1128/mcb.9.5.2124.
12. Hatano, M.; Roberts, C.W.; Minden, M.; Crist, W.M.; Korsmeyer, S.J. Dereglulation of a homeobox gene, HOX11, by the t(10;14) in T cell leukemia. *Science* **1991**, *253*, 79-82, doi:10.1126/science.1676542.
  13. Bernard, O.A.; Busson-LeConiat, M.; Ballerini, P.; Mauchauffe, M.; Della Valle, V.; Monni, R.; Nguyen Khac, F.; Mercher, T.; Penard-Lacronique, V.; Pasturaud, P., et al. A new recurrent and specific cryptic translocation, t(5;14)(q35;q32), is associated with expression of the Hox11L2 gene in T acute lymphoblastic leukemia. *Leukemia* **2001**, *15*, 1495-1504.
  14. Homminga, I.; Pieters, R.; Langerak, A.W.; de Rooi, J.J.; Stubbs, A.; Verstegen, M.; Vuerhard, M.; Buijs-Gladdines, J.; Kooi, C.; Klous, P., et al. Integrated transcript and genome analyses reveal NKX2-1 and MEF2C as potential oncogenes in T cell acute lymphoblastic leukemia. *Cancer Cell* **2011**, *19*, 484-497, doi:10.1016/j.ccr.2011.02.008.
  15. Nagel, S.; Ehrentraut, S.; Tomasch, J.; Lienenklaus, S.; Schneider, B.; Geffers, R.; Meyer, C.; Kaufmann, M.; Drexler, H.G.; MacLeod, R.A. Transcriptional activation of prostate specific homeobox gene NKX3-1 in subsets of T-cell lymphoblastic leukemia (T-ALL). *PLoS One* **2012**, *7*, e40747, doi:10.1371/journal.pone.0040747.
  16. Soulier, J.; Clappier, E.; Cayuela, J.M.; Regnault, A.; Garcia-Peydro, M.; Dombret, H.; Baruchel, A.; Toribio, M.L.; Sigaux, F. HOXA genes are included in genetic and biologic networks defining human acute T-cell leukemia (T-ALL). *Blood* **2005**, *106*, 274-286, doi:10.1182/blood-2004-10-3900.
  17. Erikson, J.; Finger, L.; Sun, L.; ar-Rushdi, A.; Nishikura, K.; Minowada, J.; Finan, J.; Emanuel, B.S.; Nowell, P.C.; Croce, C.M. Dereglulation of c-myc by translocation of the alpha-locus of the T-cell receptor in T-cell leukemias. *Science* **1986**, *232*, 884-886, doi:10.1126/science.3486470.
  18. Clappier, E.; Cuccuini, W.; Kalota, A.; Crinquette, A.; Cayuela, J.M.; Dik, W.A.; Langerak, A.W.; Montpellier, B.; Nadel, B.; Walrafen, P., et al. The C-MYB locus is involved in chromosomal translocation and genomic duplications in human T-cell acute leukemia (T-ALL), the translocation defining a new T-ALL subtype in very young children. *Blood* **2007**, *110*, 1251-1261, doi:10.1182/blood-2006-12-064683.
  19. Gutierrez, A.; Sanda, T.; Ma, W.; Zhang, J.; Grebliunaite, R.; Dahlberg, S.; Neuberg, D.; Protopopov, A.; Winter, S.S.; Larson, R.S., et al. Inactivation of LEF1 in T-cell acute lymphoblastic leukemia. *Blood* **2010**, *115*, 2845-2851, doi:10.1182/blood-2009-07-234377.
  20. Gutierrez, A.; Kentsis, A.; Sanda, T.; Holmfeldt, L.; Chen, S.C.; Zhang, J.; Protopopov, A.; Chin, L.; Dahlberg, S.E.; Neuberg, D.S., et al.

- The BCL11B tumor suppressor is mutated across the major molecular subtypes of T-cell acute lymphoblastic leukemia. *Blood* **2011**, *118*, 4169-4173, doi:10.1182/blood-2010-11-318873.
21. Zhang, J.; Ding, L.; Holmfeldt, L.; Wu, G.; Heatley, S.L.; Payne-Turner, D.; Easton, J.; Chen, X.; Wang, J.; Rusch, M., et al. The genetic basis of early T-cell precursor acute lymphoblastic leukaemia. *Nature* **2012**, *481*, 157-163, doi:10.1038/nature10725.
  22. Tosello, V.; Mansour, M.R.; Barnes, K.; Paganin, M.; Sulis, M.L.; Jenkinson, S.; Allen, C.G.; Gale, R.E.; Linch, D.C.; Palomero, T., et al. WT1 mutations in T-ALL. *Blood* **2009**, *114*, 1038-1045, doi:10.1182/blood-2008-12-192039.
  23. Van Vlierberghe, P.; Ambesi-Impiombato, A.; Perez-Garcia, A.; Haydu, J.E.; Rigo, I.; Hadler, M.; Tosello, V.; Della Gatta, G.; Paietta, E.; Racevskis, J., et al. ETV6 mutations in early immature human T cell leukemias. *J Exp Med* **2011**, *208*, 2571-2579, doi:10.1084/jem.20112239.
  24. Van der Meulen, J.; Van Roy, N.; Van Vlierberghe, P.; Speleman, F. The epigenetic landscape of T-cell acute lymphoblastic leukemia. *Int J Biochem Cell Biol* **2014**, *53*, 547-557, doi:10.1016/j.biocel.2014.04.015.
  25. Bongiovanni, D.; Saccomani, V.; Piovan, E. Aberrant Signaling Pathways in T-Cell Acute Lymphoblastic Leukemia. *Int J Mol Sci* **2017**, *18*, doi:10.3390/ijms18091904.
  26. Weng, A.P.; Ferrando, A.A.; Lee, W.; Morris, J.P.; Silverman, L.B.; Sanchez-Irizarry, C.; Blacklow, S.C.; Look, A.T.; Aster, J.C. Activating mutations of NOTCH1 in human T cell acute lymphoblastic leukemia. *Science (New York, N.Y.)* **2004**, *306*, 269-271, doi:10.1126/science.1102160.
  27. Radtke, F.; Wilson, A.; Stark, G.; Bauer, M.; van Meerwijk, J.; MacDonald, H.R.; Aguet, M. Deficient T cell fate specification in mice with an induced inactivation of Notch1. *Immunity* **1999**, *10*, 547-558.
  28. Aster, J.C.; Blacklow, S.C.; Pear, W.S. Notch signalling in T-cell lymphoblastic leukaemia/lymphoma and other haematological malignancies. *J Pathol* **2011**, *223*, 262-273, doi:10.1002/path.2789.
  29. Gonzalez-Garcia, S.; Garcia-Peydro, M.; Martin-Gayo, E.; Ballestar, E.; Esteller, M.; Bornstein, R.; de la Pompa, J.L.; Ferrando, A.A.; Toribio, M.L. CSL-MAML-dependent Notch1 signaling controls T lineage-specific IL-7R $\alpha$  gene expression in early human thymopoiesis and leukemia. *J Exp Med* **2009**, *206*, 779-791, doi:10.1084/jem.20081922.
  30. Medyouf, H.; Gusscott, S.; Wang, H.; Tseng, J.C.; Wai, C.; Nemirovsky, O.; Trumpp, A.; Pflumio, F.; Carboni, J.; Gottardis, M., et al. High-level IGF1R expression is required for leukemia-initiating cell activity in T-ALL and is supported by Notch signaling. In *J Exp Med*, 2011; Vol. 208, pp. 1809-1822.
  31. Silva, A.; Yunes, J.A.; Cardoso, B.A.; Martins, L.R.; Jotta, P.Y.; Abecasis, M.; Nowill, A.E.; Leslie, N.R.; Cardoso, A.A.; Barata, J.T.

- PTEN posttranslational inactivation and hyperactivation of the PI3K/Akt pathway sustain primary T cell leukemia viability. *Journal of Clinical Investigation* **2008**, *118*, 3762-3774, doi:10.1172/JCI34616.
32. Palomero, T.; Sulis, M.L.; Cortina, M.; Real, P.J.; Barnes, K.; Ciofani, M.; Caparros, E.; Buteau, J.; Brown, K.; Perkins, S.L., et al. Mutational loss of PTEN induces resistance to NOTCH1 inhibition in T-cell leukemia. *Nature Medicine* **2007**, *13*, 1203-1210, doi:10.1038/nm1636.
  33. Barata, J.T.; Silva, A.; Brandao, J.G.; Nadler, L.M.; Cardoso, A.A.; Boussiotis, V.A. Activation of PI3K is indispensable for interleukin 7-mediated viability, proliferation, glucose use, and growth of T cell acute lymphoblastic leukemia cells. *The Journal of experimental medicine* **2004**, *200*, 659-669, doi:10.1084/jem.20040789.
  34. Dibirdik, I.; Langlie, M.C.; Ledbetter, J.A.; Tuel-Ahlgren, L.; Obuz, V.; Waddick, K.G.; Gajl-Peczalska, K.; Schieven, G.L.; Uckun, F.M. Engagement of interleukin-7 receptor stimulates tyrosine phosphorylation, phosphoinositide turnover, and clonal proliferation of human T-lineage acute lymphoblastic leukemia cells. *Blood* **1991**, *78*, 564-570.
  35. Touw, I.; Pouwels, K.; van Agthoven, T.; van Gorp, R.; Budel, L.; Hoogerbrugge, H.; Delwel, R.; Goodwin, R.; Namen, A.; Löwenberg, B. Interleukin-7 is a growth factor of precursor B and T acute lymphoblastic leukemia. *Blood* **1990**, *75*, 2097-2101.
  36. Zenatti, P.P.; Ribeiro, D.; Li, W.; Zuurbier, L.; Silva, M.C.; Paganin, M.; Tritapoe, J.; Hixon, J.a.; Silveira, A.B.; Cardoso, B.a., et al. Oncogenic IL7R gain-of-function mutations in childhood T-cell acute lymphoblastic leukemia. *Nature genetics* **2011**, *43*, 932-939, doi:10.1038/ng.924.
  37. Flex, E.; Petrangeli, V.; Stella, L.; Chiaretti, S.; Hornakova, T.; Knoop, L.; Ariola, C.; Fodale, V.; Clappier, E.; Paoloni, F., et al. Somatically acquired JAK1 mutations in adult acute lymphoblastic leukemia. *The Journal of experimental medicine* **2008**, *205*, 751-758, doi:10.1084/jem.20072182.
  38. Bains, T.; Heinrich, M.C.; Loriaux, M.M.; Beadling, C.; Nelson, D.; Warrick, a.; Neff, T.L.; Tyner, J.W.; Dunlap, J.; Corless, C.L., et al. Newly described activating JAK3 mutations in T-cell acute lymphoblastic leukemia. *Leukemia* **2012**, *26*, 2144-2146, doi:10.1038/leu.2012.74.
  39. Kontro, M.; Kuusanmaki, H.; Eldfors, S.; Pemovska, T.; Rajala, H.L.M.; Edgren, H.; Ellonen, P.; Lagstrom, S.; Lundan, T.; Kallioniemi, O., et al. Novel Activating STAT5B Mutations As Drivers Of T-ALL. *Blood* **2013**, *122*, 3863--3863-.
  40. Balgobind, B.V.; Van Vlierberghe, P.; Van Den Ouweland, A.M.W.; Beverloo, H.B.; Terlouw-Kromosoeto, J.N.R.; Van Wering, E.R.; Reinhardt, D.; Horstmann, M.; Kaspers, G.J.L.; Pieters, R., et al. Leukemia-associated NF1 inactivation in patients with pediatric T-ALL

- and AML lacking evidence for neurofibromatosis. *Blood* **2008**, *111*, 4322-4328, doi:10.1182/blood-2007-06-095075.
41. Hagemeyer, A.; Graux, C. ABL1 rearrangements in T-cell acute lymphoblastic leukemia. *Genes Chromosomes Cancer* **2010**, *49*, 299-308, doi:10.1002/gcc.20743.
  42. Raanani, P.; Trakhtenbrot, L.; Rechavi, G.; Rosenthal, E.; Avigdor, A.; Brok-Simoni, F.; Leiba, M.; Amariglio, N.; Nagler, A.; Ben-Bassat, I. Philadelphia-Chromosome-Positive T-Lymphoblastic Leukemia: Acute Leukemia or Chronic Myelogenous Leukemia Blastic Crisis. *Acta Haematologica* **2005**, *113*, 181-189.
  43. Graux, C.; Stevens-Kroef, M.; Lafage, M.; Dastugue, N.; Harrison, C.J.; Mugneret, F.; Bahloula, K.; Struski, S.; Grégoire, M.J.; Nadal, N., et al. Heterogeneous patterns of amplification of the NUP214-ABL1 fusion gene in T-cell acute lymphoblastic leukemia. *Leukemia* **2009**, *23*, 125-133, doi:10.1038/leu.2008.278.
  44. Burmeister, T.; Gökbuget, N.; Reinhardt, R.; Rieder, H.; Hoelzer, D.; Schwartz, S. NUP214-ABL1 in adult T-ALL: The GMALL study group experience. *Blood* **2006**, *108*, 3556-3559, doi:10.1182/blood-2006-04-014514.
  45. De Keersmaecker, K.; Atak, Z.K.; Li, N.; Vicente, C.; Patchett, S.; Girardi, T.; Gianfelici, V.; Geerdens, E.; Clappier, E.; Porcu, M., et al. Exome sequencing identifies mutation in CNOT3 and ribosomal genes RPL5 and RPL10 in T-cell acute lymphoblastic leukemia. *Nat Genet* **2013**, *45*, 186-190, doi:10.1038/ng.2508.
  46. Girardi, T.; Vicente, C.; Cools, J.; De Keersmaecker, K. The genetics and molecular biology of T-ALL. 2017; Vol. 129, pp 1113-1123.
  47. Chiaretti, S.; Zini, G.; Bassan, R. Diagnosis and subclassification of acute lymphoblastic leukemia. *Mediterr J Hematol Infect Dis* **2014**, *6*, e2014073, doi:10.4084/mjhid.2014.073.
  48. Graux, C.; Cools, J.; Michaux, L.; Vandenberghe, P.; Hagemeyer, A. Cytogenetics and molecular genetics of T-cell acute lymphoblastic leukemia: from thymocyte to lymphoblast. *Leukemia* **2006**, *20*, 1496-1510, doi:10.1038/sj.leu.2404302.
  49. Bene, M.C.; Castoldi, G.; Knapp, W.; Ludwig, W.D.; Matutes, E.; Orfao, A.; van't Veer, M.B. Proposals for the immunological classification of acute leukemias. European Group for the Immunological Characterization of Leukemias (EGIL). *Leukemia* **1995**, *9*, 1783-1786.
  50. Schrappe, M.; Valsecchi, M.G.; Bartram, C.R.; Schrauder, A.; Panzer-Grumayer, R.; Moricke, A.; Parasole, R.; Zimmermann, M.; Dworzak, M.; Buldini, B., et al. Late MRD response determines relapse risk overall and in subsets of childhood T-cell ALL: results of the AIEOP-BFM-ALL 2000 study. *Blood* **2011**, *118*, 2077-2084, doi:10.1182/blood-2011-03-338707.



51. Van Vlierberghe, P.; Ferrando, A. The molecular basis of T cell acute lymphoblastic leukemia. *J Clin Invest* **2012**, *122*, 3398-3406, doi:10.1172/jci61269.
52. Coustan-Smith, E.; Mullighan, C.G.; Onciu, M.; Behm, F.G.; Raimondi, S.C.; Pei, D.; Cheng, C.; Su, X.; Rubnitz, J.E.; Basso, G., et al. Early T-cell precursor leukaemia: a subtype of very high-risk acute lymphoblastic leukaemia. *Lancet Oncol* **2009**, *10*, 147-156, doi:10.1016/s1470-2045(08)70314-0.
53. Patrick, K.; Wade, R.; Goulden, N.; Mitchell, C.; Moorman, A.V.; Rowntree, C.; Jenkinson, S.; Hough, R.; Vora, A. Outcome for children and young people with Early T-cell precursor acute lymphoblastic leukaemia treated on a contemporary protocol, UKALL 2003. *Br J Haematol* **2014**, *166*, 421-424, doi:10.1111/bjh.12882.
54. Van Vlierberghe, P.; Ambesi-Impombato, A.; De Keersmaecker, K.; Hadler, M.; Paietta, E.; Tallman, M.S.; Rowe, J.M.; Forne, C.; Rue, M.; Ferrando, A.A. Prognostic relevance of integrated genetic profiling in adult T-cell acute lymphoblastic leukemia. *Blood* **2013**, *122*, 74-82, doi:10.1182/blood-2013-03-491092.
55. Haydu, J.E.; Ferrando, A.A. Early T-cell precursor acute lymphoblastic leukaemia. *Curr Opin Hematol* **2013**, *20*, 369-373, doi:10.1097/MOH.0b013e3283623c61.
56. Ferrando, A.A.; Neuberg, D.S.; Staunton, J.; Loh, M.L.; Huard, C.; Raimondi, S.C.; Behm, F.G.; Pui, C.H.; Downing, J.R.; Gilliland, D.G., et al. Gene expression signatures define novel oncogenic pathways in T cell acute lymphoblastic leukemia. *Cancer Cell* **2002**, *1*, 75-87.
57. De Smedt, R.; Morscio, J.; Goossens, S.; Van Vlierberghe, P. Targeting steroid resistance in T-cell acute lymphoblastic leukemia. *Blood Rev* **2019**, 100591, doi:10.1016/j.blre.2019.100591.
58. Dordelmann, M.; Reiter, A.; Borkhardt, A.; Ludwig, W.D.; Gotz, N.; Viehmann, S.; Gadner, H.; Riehm, H.; Schrappe, M. Prednisone response is the strongest predictor of treatment outcome in infant acute lymphoblastic leukemia. *Blood* **1999**, *94*, 1209-1217.
59. AIEOP-BFM ALL 2017. International collaborative treatment protocol for children and adolescents with acute lymphoblastic leukemia. Protocol version 1.5. Available online: (accessed on
60. Marks, D.I.; Rowntree, C. Management of adults with T-cell lymphoblastic leukemia. *Blood* **2017**, *129*, 1134-1142, doi:10.1182/blood-2016-07-692608.
61. Pui, C.-H.; Robison, L.L.; Look, A.T. Acute lymphoblastic leukaemia. *Lancet* **2008**, *371*, 1030-1043, doi:10.1016/S0140-6736(08)60457-2.
62. Typical Treatment of Acute Lymphocytic Leukemia (ALL). Available online: <https://www.cancer.org/cancer/acute-lymphocytic-leukemia/treating/typical-treatment.html> (accessed on

63. den Hoed, M.A.; Klap, B.C.; te Winkel, M.L.; Pieters, R.; van Waas, M.; Neggers, S.J.; Boot, A.M.; Blijdorp, K.; van Dorp, W.; Pluijm, S.M., et al. Bone mineral density after childhood cancer in 346 long-term adult survivors of childhood cancer. *Osteoporos Int* **2015**, *26*, 521-529, doi:10.1007/s00198-014-2878-z.
64. Raetz, E.A.; Teachey, D.T. T-cell acute lymphoblastic leukemia. *Hematology Am Soc Hematol Educ Program* **2016**, *2016*, 580-588, doi:10.1182/asheducation-2016.1.580.
65. Follini, E.; Marchesini, M.; Roti, G. Strategies to Overcome Resistance Mechanisms in T-Cell Acute Lymphoblastic Leukemia. *Int J Mol Sci* **2019**, *20*, doi:10.3390/ijms20123021.
66. Kantarjian, H.; Stein, A.; Gokbuget, N.; Fielding, A.K.; Schuh, A.C.; Ribera, J.M.; Wei, A.; Dombret, H.; Foa, R.; Bassan, R., et al. Blinatumomab versus Chemotherapy for Advanced Acute Lymphoblastic Leukemia. *N Engl J Med* **2017**, *376*, 836-847, doi:10.1056/NEJMoa1609783.
67. Lamb, Y.N. Inotuzumab Ozogamicin: First Global Approval. *Drugs* **2017**, *77*, 1603-1610, doi:10.1007/s40265-017-0802-5.
68. Sheridan, C. First approval in sight for Novartis' CAR-T therapy after panel vote. *Nature Biotechnology* **2017**, *35*, 691-693, doi:doi:10.1038/nbt0817-691.
69. Cohen, M.H.; Johnson, J.R.; Massie, T.; Sridhara, R.; McGuinn, W.D., Jr.; Abraham, S.; Booth, B.P.; Goheer, M.A.; Morse, D.; Chen, X.H., et al. Approval summary: nelarabine for the treatment of T-cell lymphoblastic leukemia/lymphoma. *Clin Cancer Res* **2006**, *12*, 5329-5335, doi:10.1158/1078-0432.ccr-06-0606.
70. Cooper, T.M. Role of nelarabine in the treatment of T-cell acute lymphoblastic leukemia and T-cell lymphoblastic lymphoma. *Ther Clin Risk Manag* **2007**, *3*, 1135-1141.
71. Sanchez-Martin, M.; Ferrando, A. The NOTCH1-MYC highway toward T-cell acute lymphoblastic leukemia. *Blood* **2017**, *129*, 1124-1133, doi:10.1182/blood-2016-09-692582.
72. Milano, J.; McKay, J.; Dagenais, C.; Foster-Brown, L.; Pognan, F.; Gadiant, R.; Jacobs, R.T.; Zacco, A.; Greenberg, B.; Ciaccio, P.J. Modulation of notch processing by gamma-secretase inhibitors causes intestinal goblet cell metaplasia and induction of genes known to specify gut secretory lineage differentiation. *Toxicol Sci* **2004**, *82*, 341-358, doi:10.1093/toxsci/kfh254.
73. Real, P.J.; Ferrando, A.A. NOTCH inhibition and glucocorticoid therapy in T-cell acute lymphoblastic leukemia. *Leukemia* **2009**, *23*, 1374-1377, doi:10.1038/leu.2009.75.
74. Wu, Y.; Cain-Hom, C.; Choy, L.; Hagenbeek, T.J.; de Leon, G.P.; Chen, Y.; Finkle, D.; Venook, R.; Wu, X.; Ridgway, J., et al. Therapeutic

- antibody targeting of individual Notch receptors. *Nature* **2010**, *464*, 1052-1057, doi:10.1038/nature08878.
75. Agnusdei, V.; Minuzzo, S.; Frasson, C.; Grassi, A.; Axelrod, F.; Satyal, S.; Gurney, A.; Hoey, T.; Seganfredo, E.; Basso, G., et al. Therapeutic antibody targeting of Notch1 in T-acute lymphoblastic leukemia xenografts. *Leukemia* **2014**, *28*, 278-288, doi:10.1038/leu.2013.183.
76. Moellering, R.E.; Cornejo, M.; Davis, T.N.; Del Bianco, C.; Aster, J.C.; Blacklow, S.C.; Kung, A.L.; Gilliland, D.G.; Verdine, G.L.; Bradner, J.E. Direct inhibition of the NOTCH transcription factor complex. *Nature* **2009**, *462*, 182-188, doi:10.1038/nature08543.
77. Schnell, S.A.; Ambesi-Impiombato, A.; Sanchez-Martin, M.; Belver, L.; Xu, L.; Qin, Y.; Kageyama, R.; Ferrando, A.A. Therapeutic targeting of HES1 transcriptional programs in T-ALL. *Blood* **2015**, *125*, 2806-2814, doi:10.1182/blood-2014-10-608448.
78. Loosveld, M.; Castellano, R.; Gon, S.; Goubard, A.; Crouzet, T.; Pouyet, L.; Prebet, T.; Vey, N.; Nadel, B.; Collette, Y., et al. Therapeutic targeting of c-Myc in T-cell acute lymphoblastic leukemia, T-ALL. *Oncotarget* **2014**, *5*, 3168-3172, doi:10.18632/oncotarget.1873.
79. Roti, G.; Carlton, A.; Ross, K.N.; Markstein, M.; Pajcini, K.; Su, A.H.; Perrimon, N.; Pear, W.S.; Kung, A.L.; Blacklow, S.C., et al. Complementary genomic screens identify SERCA as a therapeutic target in NOTCH1 mutated cancer. *Cancer Cell* **2013**, *23*, 390-405, doi:10.1016/j.ccr.2013.01.015.
80. Pikman, Y.; Alexe, G.; Roti, G.; Conway, A.S.; Furman, A.; Lee, E.S.; Place, A.E.; Kim, S.; Saran, C.; Modiste, R., et al. Synergistic Drug Combinations with a CDK4/6 Inhibitor in T-cell Acute Lymphoblastic Leukemia. *Clin Cancer Res* **2017**, *23*, 1012-1024, doi:10.1158/1078-0432.ccr-15-2869.
81. Sawai, C.M.; Freund, J.; Oh, P.; Ndiaye-Lobry, D.; Bretz, J.C.; Strikoudis, A.; Genesca, L.; Trimarchi, T.; Kelliher, M.A.; Clark, M., et al. Therapeutic targeting of the cyclin D3:CDK4/6 complex in T cell leukemia. *Cancer Cell* **2012**, *22*, 452-465, doi:10.1016/j.ccr.2012.09.016.
82. Lonetti, A.; Antunes, I.L.; Chiarini, F.; Orsini, E.; Buontempo, F.; Ricci, F.; Tazzari, P.L.; Pagliaro, P.; Melchionda, F.; Pession, A., et al. Activity of the pan-class I phosphoinositide 3-kinase inhibitor NVP-BKM120 in T-cell acute lymphoblastic leukemia. *Leukemia* **2014**, *28*, 1196-1206, doi:10.1038/leu.2013.369.
83. Silveira, A.B.; Laranjeira, A.B.; Rodrigues, G.O.; Leal, P.C.; Cardoso, B.A.; Barata, J.T.; Yunes, R.A.; Zanchin, N.I.; Brandalise, S.R.; Yunes, J.A. PI3K inhibition synergizes with glucocorticoids but antagonizes with methotrexate in T-cell acute lymphoblastic leukemia. *Oncotarget* **2015**, *6*, 13105-13118, doi:10.18632/oncotarget.3524.

84. Piován, E.; Yu, J.; Tosello, V.; Herranz, D.; Ambesi-Impiombato, A.; Da Silva, A.C.; Sanchez-Martin, M.; Perez-Garcia, A.; Rigo, I.; Castillo, M., et al. Direct reversal of glucocorticoid resistance by AKT inhibition in acute lymphoblastic leukemia. *Cancer Cell* **2013**, *24*, 766-776, doi:10.1016/j.ccr.2013.10.022.
85. De Keersmaecker, K.; Lahortiga, I.; Mentens, N.; Folens, C.; Van Neste, L.; Bekaert, S.; Vandenberghe, P.; Odero, M.D.; Marynen, P.; Cools, J. In vitro validation of gamma-secretase inhibitors alone or in combination with other anti-cancer drugs for the treatment of T-cell acute lymphoblastic leukemia. *Haematologica* **2008**, *93*, 533-542, doi:10.3324/haematol.11894.
86. Chiarini, F.; Grimaldi, C.; Ricci, F.; Tazzari, P.L.; Evangelisti, C.; Ognibene, A.; Battistelli, M.; Falcieri, E.; Melchionda, F.; Pession, A., et al. Activity of the novel dual phosphatidylinositol 3-kinase/mammalian target of rapamycin inhibitor NVP-BEZ235 against T-cell acute lymphoblastic leukemia. *Cancer Res* **2010**, *70*, 8097-8107, doi:10.1158/0008-5472.can-10-1814.
87. Hall, C.P.; Reynolds, C.P.; Kang, M.H. Modulation of Glucocorticoid Resistance in Pediatric T-cell Acute Lymphoblastic Leukemia by Increasing BIM Expression with the PI3K/mTOR Inhibitor BEZ235. *Clin Cancer Res* **2016**, *22*, 621-632, doi:10.1158/1078-0432.ccr-15-0114.
88. Fransecky, L.; Mochmann, L.H.; Baldus, C.D. Outlook on PI3K/AKT/mTOR inhibition in acute leukemia. *Mol Cell Ther* **2015**, *3*, 2, doi:10.1186/s40591-015-0040-8.
89. Li, Y.; Buijs-Gladdines, J.G.; Cante-Barrett, K.; Stubbs, A.P.; Vroegindewey, E.M.; Smits, W.K.; van Marion, R.; Dinjens, W.N.; Horstmann, M.; Kuiper, R.P., et al. IL-7 Receptor Mutations and Steroid Resistance in Pediatric T cell Acute Lymphoblastic Leukemia: A Genome Sequencing Study. *PLoS Med* **2016**, *13*, e1002200, doi:10.1371/journal.pmed.1002200.
90. Delgado-Martin, C.; Meyer, L.K.; Huang, B.J.; Shimano, K.A.; Zinter, M.S.; Nguyen, J.V.; Smith, G.A.; Taunton, J.; Winter, S.S.; Roderick, J.R., et al. JAK/STAT pathway inhibition overcomes IL7-induced glucocorticoid resistance in a subset of human T-cell acute lymphoblastic leukemias. *Leukemia* **2017**, *31*, 2568-2576, doi:10.1038/leu.2017.136.
91. Wuchter, C.; Ruppert, V.; Schrappe, M.; Dorken, B.; Ludwig, W.D.; Karawajew, L. In vitro susceptibility to dexamethasone- and doxorubicin-induced apoptotic cell death in context of maturation stage, responsiveness to interleukin 7, and early cyto-reduction in vivo in childhood T-cell acute lymphoblastic leukemia. *Blood* **2002**, *99*, 4109-4115, doi:10.1182/blood.v99.11.4109.
92. Maude, S.L.; Dolai, S.; Delgado-Martin, C.; Vincent, T.; Robbins, A.; Selvanathan, A.; Ryan, T.; Hall, J.; Wood, A.C.; Tasian, S.K., et al.

- Efficacy of JAK/STAT pathway inhibition in murine xenograft models of early T-cell precursor (ETP) acute lymphoblastic leukemia. *Blood* **2015**, *125*, 1759-1767, doi:10.1182/blood-2014-06-580480.
93. Mamonkin, M.; Rouce, R.H.; Tashiro, H.; Brenner, M.K. A T-cell-directed chimeric antigen receptor for the selective treatment of T-cell malignancies. *Blood* **2015**, *126*, 983-992, doi:10.1182/blood-2015-02-629527.
94. Gomes-Silva, D.; Srinivasan, M.; Sharma, S.; Lee, C.M.; Wagner, D.L.; Davis, T.H.; Rouce, R.H.; Bao, G.; Brenner, M.K.; Mamonkin, M. CD7-edited T cells expressing a CD7-specific CAR for the therapy of T-cell malignancies. *Blood* **2017**, *130*, 285-296, doi:10.1182/blood-2017-01-761320.
95. Bride, K.L.; Vincent, T.L.; Im, S.Y.; Aplenc, R.; Barrett, D.M.; Carroll, W.L.; Carson, R.; Dai, Y.; Devidas, M.; Dunsmore, K.P., et al. Preclinical efficacy of daratumumab in T-cell acute lymphoblastic leukemia. *Blood* **2018**, *131*, 995-999, doi:10.1182/blood-2017-07-794214.
96. Passaro, D.; Irigoyen, M.; Catherinet, C.; et al. CXCR4 Is required for leukemia-initiating cell activity in T cell acute lymphoblastic leukemia. *Cancer Cell* **2015**, *27*, 769-779, doi:10.1016/j.ccell.2015.05.003.
97. McMahon, C.M.; Luger, S.M. Relapsed T Cell ALL: Current Approaches and New Directions. *Curr Hematol Malig Rep* **2019**, *14*, 83-93, doi:10.1007/s11899-019-00501-3.
98. Nusslein-Volhard, C.; Wieschaus, E. Mutations affecting segment number and polarity in *Drosophila*. *Nature* **1980**, *287*, 795-801, doi:10.1038/287795a0.
99. Bangs, F.; Anderson, K.V. Primary Cilia and Mammalian Hedgehog Signaling. *Cold Spring Harb Perspect Biol* **2017**, *9*, doi:10.1101/cshperspect.a028175.
100. Gallet, A. Hedgehog morphogen: from secretion to reception. *Trends Cell Biol* **2011**, *21*, 238-246, doi:10.1016/j.tcb.2010.12.005.
101. Ramsbottom, S.A.; Pownall, M.E. Regulation of Hedgehog Signalling Inside and Outside the Cell. *J Dev Biol* **2016**, *4*, 23.
102. Riddle, R.D.; Johnson, R.L.; Laufer, E.; Tabin, C. Sonic hedgehog mediates the polarizing activity of the ZPA. *Cell* **1993**, *75*, 1401-1416, doi:10.1016/0092-8674(93)90626-2.
103. Nieuwenhuis, E.; Hui, C.C. Hedgehog signaling and congenital malformations. *Clin Genet* **2005**, *67*, 193-208, doi:10.1111/j.1399-0004.2004.00360.x.
104. Beachy, P.A.; Karhadkar, S.S.; Berman, D.M. Tissue repair and stem cell renewal in carcinogenesis. *Nature* **2004**, *432*, 324-331, doi:10.1038/nature03100.

- 
105. Fuccillo, M.; Joyner, A.L.; Fishell, G. Morphogen to mitogen: the multiple roles of hedgehog signalling in vertebrate neural development. *Nat Rev Neurosci* **2006**, *7*, 772-783, doi:10.1038/nrn1990.
  106. Petrova, R.; Joyner, A.L. Roles for Hedgehog signaling in adult organ homeostasis and repair. *Development* **2014**, *141*, 3445-3457, doi:10.1242/dev.083691.
  107. Wu, F.; Zhang, Y.; Sun, B.; McMahon, A.P.; Wang, Y. Hedgehog Signaling: From Basic Biology to Cancer Therapy. *Cell Chem Biol* **2017**, *24*, 252-280, doi:10.1016/j.chembiol.2017.02.010.
  108. Rohatgi, R.; Milenkovic, L.; Scott, M.P. Patched1 regulates hedgehog signaling at the primary cilium. *Science* **2007**, *317*, 372-376, doi:10.1126/science.1139740.
  109. Chen, Y.; Struhl, G. Dual roles for patched in sequestering and transducing Hedgehog. *Cell* **1996**, *87*, 553-563, doi:10.1016/s0092-8674(00)81374-4.
  110. Rahnama, F.; Toftgard, R.; Zaphiropoulos, P.G. Distinct roles of PTCH2 splice variants in Hedgehog signalling. *Biochem J* **2004**, *378*, 325-334, doi:10.1042/bj20031200.
  111. Niewiadomski, P.; Kong, J.H.; Ahrends, R.; Ma, Y.; Humke, E.W.; Khan, S.; Teruel, M.N.; Novitsch, B.G.; Rohatgi, R. Gli protein activity is controlled by multisite phosphorylation in vertebrate Hedgehog signaling. *Cell Rep* **2014**, *6*, 168-181, doi:10.1016/j.celrep.2013.12.003.
  112. Yongbin, C.; Jin, J. Decoding the phosphorylation code in Hedgehog signal transduction. *Cell Research* **2013**, *23*, 186-200, doi:doi:10.1038/cr.2013.10.
  113. Incardona, J.P.; Gruenberg, J.; Roelink, H. Sonic hedgehog induces the segregation of patched and smoothed in endosomes. *Curr Biol* **2002**, *12*, 983-995, doi:10.1016/s0960-9822(02)00895-3.
  114. Wilson, C.W.; Chen, M.H.; Chuang, P.T. Smoothed adopts multiple active and inactive conformations capable of trafficking to the primary cilium. *PLoS One* **2009**, *4*, e5182, doi:10.1371/journal.pone.0005182.
  115. Pearse, R.V., 2nd; Collier, L.S.; Scott, M.P.; Tabin, C.J. Vertebrate homologs of Drosophila suppressor of fused interact with the gli family of transcriptional regulators. *Dev Biol* **1999**, *212*, 323-336, doi:10.1006/dbio.1999.9335.
  116. Briscoe, J.; Therond, P.P. The mechanisms of Hedgehog signalling and its roles in development and disease. *Nat Rev Mol Cell Biol* **2013**, *14*, 416-429, doi:10.1038/nrm3598.
  117. Ding, Q.; Motoyama, J.; Gasca, S.; Mo, R.; Sasaki, H.; Rossant, J.; Hui, C.C. Diminished Sonic hedgehog signaling and lack of floor plate differentiation in Gli2 mutant mice. *Development* **1998**, *125*, 2533-2543.

118. Matisse, M.P.; Epstein, D.J.; Park, H.L.; Platt, K.A.; Joyner, A.L. Gli2 is required for induction of floor plate and adjacent cells, but not most ventral neurons in the mouse central nervous system. *Development* **1998**, *125*, 2759-2770.
119. Litingtung, Y.; Chiang, C. Specification of ventral neuron types is mediated by an antagonistic interaction between Shh and Gli3. *Nat Neurosci* **2000**, *3*, 979-985, doi:10.1038/79916.
120. Persson, M.; Stamatakis, D.; te Welscher, P.; Andersson, E.; Bose, J.; Ruther, U.; Ericson, J.; Briscoe, J. Dorsal-ventral patterning of the spinal cord requires Gli3 transcriptional repressor activity. *Genes Dev* **2002**, *16*, 2865-2878, doi:10.1101/gad.243402.
121. Dai, P.; Akimaru, H.; Tanaka, Y.; Maekawa, T.; Nakafuku, M.; Ishii, S. Sonic Hedgehog-induced activation of the Gli1 promoter is mediated by GLI3. *J Biol Chem* **1999**, *274*, 8143-8152, doi:10.1074/jbc.274.12.8143.
122. Katoh, Y.; Katoh, M. Hedgehog target genes: mechanisms of carcinogenesis induced by aberrant hedgehog signaling activation. *Curr Mol Med* **2009**, *9*, 873-886.
123. Sabol, M.; Trnski, D.; Musani, V.; Ozretic, P.; Levanat, S. Role of GLI Transcription Factors in Pathogenesis and Their Potential as New Therapeutic Targets. *Int J Mol Sci* **2018**, *19*, doi:10.3390/ijms19092562.
124. Pak, E.; Segal, R.A. Hedgehog Signal Transduction: Key Players, Oncogenic Drivers, and Cancer Therapy. *Dev Cell* **2016**, *38*, 333-344, doi:10.1016/j.devcel.2016.07.026.
125. Pandolfi, S.; Stecca, B. Cooperative integration between HEDGEHOG-GLI signalling and other oncogenic pathways: implications for cancer therapy. *Expert Rev Mol Med* **2015**, *17*, e5, doi:10.1017/erm.2015.3.
126. Teglund, S.; Toftgard, R. Hedgehog beyond medulloblastoma and basal cell carcinoma. *Biochim Biophys Acta* **2010**, *1805*, 181-208, doi:10.1016/j.bbcan.2010.01.003.
127. Amakye, D.; Jagani, Z.; Dorsch, M. Unraveling the therapeutic potential of the Hedgehog pathway in cancer. *Nature Medicine* **2013**, *19*, 1410-1422, doi:10.1038/nm.3389.
128. Rubin, L.L.; de Sauvage, F.J. Targeting the Hedgehog pathway in cancer. *Nat Rev Drug Discov* **2006**, *5*, 1026-1033, doi:10.1038/nrd2086.
129. Yauch, R.L.; Gould, S.E.; Scales, S.J.; Tang, T.; Tian, H.; Ahn, C.P.; Marshall, D.; Fu, L.; Januario, T.; Kallop, D., et al. A paracrine requirement for hedgehog signalling in cancer. *Nature* **2008**, *455*, 406-410, doi:10.1038/nature07275.
130. Mills, L.D.; Zhang, Y.; Marler, R.J.; Herreros-Villanueva, M.; Zhang, L.; Almada, L.L.; Couch, F.; Wetmore, C.; Pasca di Magliano, M.; Fernandez-Zapico, M.E. Loss of the transcription factor GLI1 identifies a signaling network in the tumor microenvironment mediating KRAS

- oncogene-induced transformation. *J Biol Chem* **2013**, *288*, 11786-11794, doi:10.1074/jbc.M112.438846.
131. Dierks, C.; Grbic, J.; Zirluk, K.; Beigi, R.; Englund, N.P.; Guo, G.R.; Veelken, H.; Engelhardt, M.; Mertelsmann, R.; Kelleher, J.F., et al. Essential role of stromally induced hedgehog signaling in B-cell malignancies. *Nat Med* **2007**, *13*, 944-951, doi:10.1038/nm1614.
132. Hegde, G.V.; Peterson, K.J.; Emanuel, K.; Mittal, A.K.; Joshi, A.D.; Dickinson, J.D.; Kollessery, G.J.; Bociek, R.G.; Bierman, P.; Vose, J.M., et al. Hedgehog-induced survival of B-cell chronic lymphocytic leukemia cells in a stromal cell microenvironment: a potential new therapeutic target. *Mol Cancer Res* **2008**, *6*, 1928-1936, doi:10.1158/1541-7786.mcr-08-0142.
133. Hahn, H.; Wicking, C.; Zaphiropoulos, P.G.; Gailani, M.R.; Shanley, S.; Chidambaram, A.; Vorechovsky, I.; Holmberg, E.; Unden, A.B.; Gillies, S., et al. Mutations of the human homolog of *Drosophila* patched in the nevoid basal cell carcinoma syndrome. *Cell* **1996**, *85*, 841-851, doi:10.1016/s0092-8674(00)81268-4.
134. Gailani, M.R.; Bale, A.E. Acquired and inherited basal cell carcinomas and the patched gene. *Adv Dermatol* **1999**, *14*, 261-283; discussion 284.
135. Vorechovsky, I.; Tingby, O.; Hartman, M.; Stromberg, B.; Nister, M.; Collins, V.P.; Toftgard, R. Somatic mutations in the human homologue of *Drosophila* patched in primitive neuroectodermal tumours. *Oncogene* **1997**, *15*, 361-366, doi:10.1038/sj.onc.1201340.
136. Raffel, C.; Jenkins, R.B.; Frederick, L.; Hebrink, D.; Alderete, B.; Fults, D.W.; James, C.D. Sporadic medulloblastomas contain PTCH mutations. *Cancer Res* **1997**, *57*, 842-845.
137. Wolter, M.; Reifenberger, J.; Sommer, C.; Ruzicka, T.; Reifenberger, G. Mutations in the human homologue of the *Drosophila* segment polarity gene patched (PTCH) in sporadic basal cell carcinomas of the skin and primitive neuroectodermal tumors of the central nervous system. *Cancer Res* **1997**, *57*, 2581-2585.
138. Reifenberger, J.; Wolter, M.; Weber, R.G.; Megahed, M.; Ruzicka, T.; Lichter, P.; Reifenberger, G. Missense mutations in SMOH in sporadic basal cell carcinomas of the skin and primitive neuroectodermal tumors of the central nervous system. *Cancer Res* **1998**, *58*, 1798-1803.
139. Xie, J.; Murone, M.; Luoh, S.M.; Ryan, A.; Gu, Q.; Zhang, C.; Bonifas, J.M.; Lam, C.W.; Hynes, M.; Goddard, A., et al. Activating Smoothed mutations in sporadic basal-cell carcinoma. *Nature* **1998**, *391*, 90-92, doi:10.1038/34201.
140. Mao, J.; Ligon, K.L.; Rakhlin, E.Y.; Thayer, S.P.; Bronson, R.T.; Rowitch, D.; McMahon, A.P. A novel somatic mouse model to survey tumorigenic potential applied to the Hedgehog pathway. *Cancer Res* **2006**, *66*, 10171-10178, doi:10.1158/0008-5472.can-06-0657.



141. Goodrich, L.V.; Milenkovic, L.; Higgins, K.M.; Scott, M.P. Altered neural cell fates and medulloblastoma in mouse patched mutants. *Science* **1997**, *277*, 1109-1113, doi:10.1126/science.277.5329.1109.
142. Lee, Y.; Kawagoe, R.; Sasai, K.; Li, Y.; Russell, H.R.; Curran, T.; McKinnon, P.J. Loss of suppressor-of-fused function promotes tumorigenesis. *Oncogene* **2007**, *26*, 6442-6447, doi:10.1038/sj.onc.1210467.
143. Taylor, M.D.; Liu, L.; Raffel, C.; Hui, C.C.; Mainprize, T.G.; Zhang, X.; Agatep, R.; Chiappa, S.; Gao, L.; Lowrance, A., et al. Mutations in SUFU predispose to medulloblastoma. *Nat Genet* **2002**, *31*, 306-310, doi:10.1038/ng916.
144. Kinzler, K.W.; Bigner, S.H.; Bigner, D.D.; Trent, J.M.; Law, M.L.; O'Brien, S.J.; Wong, A.J.; Vogelstein, B. Identification of an amplified, highly expressed gene in a human glioma. *Science* **1987**, *236*, 70-73, doi:10.1126/science.3563490.
145. Hui, M.; Cazet, A.; Nair, R.; Watkins, D.N.; O'Toole, S.A.; Swarbrick, A. The Hedgehog signalling pathway in breast development, carcinogenesis and cancer therapy. *Breast Cancer Res* **2013**, *15*, 203, doi:10.1186/bcr3401.
146. Stecca, B.; Ruiz, I.A.A. Context-dependent regulation of the GLI code in cancer by HEDGEHOG and non-HEDGEHOG signals. *J Mol Cell Biol* **2010**, *2*, 84-95, doi:10.1093/jmcb/mjp052.
147. Karhadkar, S.S.; Bova, G.S.; Abdallah, N.; Dhara, S.; Gardner, D.; Maitra, A.; Isaacs, J.T.; Berman, D.M.; Beachy, P.A. Hedgehog signalling in prostate regeneration, neoplasia and metastasis. *Nature* **2004**, *431*, 707-712, doi:10.1038/nature02962.
148. Kern, D.; Regl, G.; Hofbauer, S.W.; Altenhofer, P.; Achatz, G.; Dlugosz, A.; Schnidar, H.; Greil, R.; Hartmann, T.N.; Aberger, F. Hedgehog/GLI and PI3K signaling in the initiation and maintenance of chronic lymphocytic leukemia. *Oncogene* **2015**, *34*, 5341-5351, doi:10.1038/onc.2014.450.
149. Blotta, S.; Jakubikova, J.; Calimeri, T.; Roccaro, A.M.; Amodio, N.; Azab, A.K.; Foresta, U.; Mitsiades, C.S.; Rossi, M.; Todoerti, K., et al. Canonical and noncanonical hedgehog pathway in the pathogenesis of multiple myeloma. *Blood* **2012**, *120*, 5002-5013, doi:10.1182/blood-2011-07-368142.
150. Aberger, F.; Ruiz I Altaba, A. Context-dependent signal integration by the GLI code: the oncogenic load, pathways, modifiers and implications for cancer therapy. *Semin Cell Dev Biol* **2014**, *33*, 93-104, doi:10.1016/j.semcdb.2014.05.003.
151. Pietrobono, S.; Gagliardi, S.; Stecca, B. Non-canonical Hedgehog Signaling Pathway in Cancer: Activation of GLI Transcription Factors Beyond Smoothed. *Front Genet* **2019**, *10*, 556, doi:10.3389/fgene.2019.00556.

152. Niewiadomski, P.; Niedziolka, S.M.; Markiewicz, L.; Uspienski, T.; Baran, B.; Chojnowska, K. Gli Proteins: Regulation in Development and Cancer. *Cells* **2019**, *8*, doi:10.3390/cells8020147.
153. Crompton, T.; Outram, S.V.; Hager-Theodorides, A.L. Sonic hedgehog signalling in T-cell development and activation. *Nature Reviews Immunology* **2007**, *7*, 726-735, doi:10.1038/nri2151.
154. Merchant, A.A.; Matsui, W. Smoothing the controversial role of hedgehog in hematopoiesis. *Cell stem cell* **2009**, *4*, 470-471, doi:10.1016/j.stem.2009.05.006.
155. Gao, J.; Graves, S.; Koch, U.; Liu, S.; Jankovic, V.; Buonamici, S.; El Andaloussi, A.; Nimer, S.D.; Kee, B.L.; Taichman, R., et al. Hedgehog signaling is dispensable for adult hematopoietic stem cell function. *Cell Stem Cell* **2009**, *4*, 548-558, doi:10.1016/j.stem.2009.03.015.
156. Outram, S.V.; Varas, A.; Pepicelli, C.V.; Crompton, T. Hedgehog Signaling Regulates Differentiation from Double-Negative to Double-Positive Thymocyte. *Immunity* **2000**, *13*, 187-197, doi:10.1016/S1074-7613(00)00019-4.
157. Shah, D.; Hager-Theodorides, A.; Outram, S.; Ross, S.; Varas, A.; Crompton, T. Reduced thymocyte development in sonic hedgehog knockout embryos. *Journal of immunology (Baltimore, Md : 1950)* **2004**, *172*, 2296-2306, doi:10.4049/jimmunol.172.4.2296.
158. El Andaloussi, A.; Graves, S.; Meng, F.; Mandal, M.; Mashayekhi, M.; Aifantis, I. Hedgehog signaling controls thymocyte progenitor homeostasis and differentiation in the thymus. *Nat Immunol* **2006**, *7*, 418-426, doi:10.1038/ni1313.
159. Hager-Theodorides, A.L.; Dessens, J.T.; Outram, S.V.; Crompton, T. The transcription factor Gli3 regulates differentiation of fetal CD4- CD8-double-negative thymocytes. *Blood* **2005**, *106*, 1296-1304, doi:10.1182/blood-2005-03-0998.
160. Rowbotham, N.J.; Hager-Theodorides, A.L.; Cebecauer, M.; Shah, D.K.; Drakopoulou, E.; Dyson, J.; Outram, S.V.; Crompton, T. Activation of the Hedgehog signaling pathway in T-lineage cells inhibits TCR repertoire selection in the thymus and peripheral T-cell activation. *Blood* **2007**, *109*, 3757-3766, doi:10.1182/blood-2006-07-037655.
161. Zhao, C.; Chen, A.; Jamieson, C.H.; Fereshteh, M.; Abrahamsson, A.; Blum, J.; Kwon, H.Y.; Kim, J.; Chute, J.P.; Rizzieri, D., et al. Hedgehog signalling is essential for maintenance of cancer stem cells in myeloid leukaemia. *Nature* **2009**, *458*, 776-779, doi:10.1038/nature07737.
162. Dierks, C.; Beigi, R.; Guo, G.R.; Zirluk, K.; Stegert, M.R.; Manley, P.; Trussell, C.; Schmitt-Graeff, A.; Landwerlin, K.; Veelken, H., et al. Expansion of Bcr-Abl-positive leukemic stem cells is dependent on Hedgehog pathway activation. *Cancer Cell* **2008**, *14*, 238-249, doi:10.1016/j.ccr.2008.08.003.

163. Al Baghdadi, T.; Abonour, R.; Boswell, H.S. Novel combination treatments targeting chronic myeloid leukemia stem cells. *Clin Lymphoma Myeloma Leuk* **2012**, *12*, 94-105, doi:10.1016/j.clml.2011.10.003.
164. Peacock, C.D.; Wang, Q.; Gesell, G.S.; Corcoran-Schwartz, I.M.; Jones, E.; Kim, J.; Devereux, W.L.; Rhodes, J.T.; Huff, C.A.; Beachy, P.A., et al. Hedgehog signaling maintains a tumor stem cell compartment in multiple myeloma. *Proc Natl Acad Sci U S A* **2007**, *104*, 4048-4053, doi:10.1073/pnas.0611682104.
165. Norsworthy, K.J.; By, K.; Subramaniam, S.; Zhuang, L.; Del Valle, P.L.; Przepiorka, D.; Shen, Y.L.; Sheth, C.M.; Liu, C.; Leong, R., et al. FDA Approval Summary: Glasdegib for Newly Diagnosed Acute Myeloid Leukemia. *Clin Cancer Res* **2019**, doi:10.1158/1078-0432.ccr-19-0365.
166. Dagklis, A.; Demeyer, S.; De Bie, J.; Radaelli, E.; Pauwels, D.; Degryse, S.; Gielen, O.; Vicente, C.; Vandepoel, R.; Geerdens, E., et al. Hedgehog pathway activation in T-cell acute lymphoblastic leukemia predicts response to SMO and GLI1 inhibitors. *Blood* **2016**, *128*, 2642-2654, doi:10.1182/blood-2016-03-703454.
167. Burns, M.A.; Liao, Z.W.; Yamagata, N.; Pouliot, G.P.; Stevenson, K.E.; Neuberg, D.S.; Thorner, A.R.; Ducar, M.; Silverman, E.A.; Hunger, S.P., et al. Hedgehog pathway mutations drive oncogenic transformation in high-risk T-cell acute lymphoblastic leukemia. *Leukemia* **2018**, *32*, 2126-2137, doi:10.1038/s41375-018-0097-x.
168. Dagklis, A.; Pauwels, D.; Lahortiga, I.; Geerdens, E.; Bittoun, E.; Cauwelier, B.; Tousseyn, T.; Uyttebroeck, A.; Maertens, J.; Verhoef, G., et al. Hedgehog pathway mutations in T-cell acute lymphoblastic leukemia. In *Haematologica*, Italy, 2015; Vol. 100, pp. e102-105.
169. Hou, X.; Chen, X.; Zhang, P.; Fan, Y.; Ma, A.; Pang, T.; Song, Z.; Jin, Y.; Hao, W.; Liu, F., et al. Inhibition of hedgehog signaling by GANT58 induces apoptosis and shows synergistic antitumor activity with AKT inhibitor in acute T cell leukemia cells. *Biochimie* **2014**, *101*, 50-59, doi:10.1016/j.biochi.2013.12.019.
170. Katoh, Y.; Katoh, M. Integrative genomic analyses on GLI1: positive regulation of GLI1 by Hedgehog-GLI, TGFbeta-Smads, and RTK-PI3K-AKT signals, and negative regulation of GLI1 by Notch-CSL-HES/HEY, and GPCR-Gs-PKA signals. *Int J Oncol* **2009**, *35*, 187-192.
171. Livak, K.J.; Schmittgen, T.D. Analysis of relative gene expression data using real-time quantitative PCR and the 2(-Delta Delta C(T)) Method. *Methods* **2001**, *25*, 402-408, doi:10.1006/meth.2001.1262.
172. Chen, J.K.; Taipale, J.; Cooper, M.K.; Beachy, P.A. Inhibition of Hedgehog signaling by direct binding of cyclopamine to Smoothed. *Genes Dev* **2002**, *16*, 2743-2748, doi:10.1101/gad.1025302.
173. Agyeman, A.; Jha, B.K.; Mazumdar, T.; Houghton, J.A. Mode and specificity of binding of the small molecule GANT61 to GLI determines

- inhibition of GLI-DNA binding. *Oncotarget* **2014**, *5*, 4492-4503, doi:10.18632/oncotarget.2046.
174. Inaba, H.; Pui, C.-H. Glucocorticoid use in acute lymphoblastic leukemia: comparison of prednisone and dexamethasone. *The Lancet Oncology* **2010**, *11*, 1096-1106, doi:10.1016/S1470-2045(10)70114-5.
175. Wang, J.; Lu, J.; Bond, M.C.; Chen, M.; Ren, X.-R.; Lyerly, H.K.; Barak, L.S.; Chen, W. Identification of select glucocorticoids as Smoothed agonists: Potential utility for regenerative medicine. *Proceedings of the National Academy of Sciences* **2010**, *107*, 9323.
176. Canettieri, G.; Di Marcotullio, L.; Greco, A.; Coni, S.; Antonucci, L.; Infante, P.; Pietrosanti, L.; De Smaele, E.; Ferretti, E.; Miele, E., et al. Histone deacetylase and Cullin3-REN(KCTD11) ubiquitin ligase interplay regulates Hedgehog signalling through Gli acetylation. *Nat Cell Biol* **2010**, *12*, 132-142, doi:10.1038/ncb2013.
177. Coni, S.; Antonucci, L.; D'Amico, D.; Di Magno, L.; Infante, P.; De Smaele, E.; Giannini, G.; Di Marcotullio, L.; Screpanti, I.; Gulino, A., et al. Gli2 acetylation at lysine 757 regulates hedgehog-dependent transcriptional output by preventing its promoter occupancy. *PLoS One* **2013**, *8*, e65718, doi:10.1371/journal.pone.0065718.
178. Coni, S.; Mancuso, A.B.; Di Magno, L.; Sdruscia, G.; Manni, S.; Serrao, S.M.; Rotili, D.; Spiombi, E.; Bufalieri, F.; Petroni, M., et al. Selective targeting of HDAC1/2 elicits anticancer effects through Gli1 acetylation in preclinical models of SHH Medulloblastoma. *Sci Rep* **2017**, *7*, 44079, doi:10.1038/srep44079.
179. Kassel, O.; Herrlich, P. Crosstalk between the glucocorticoid receptor and other transcription factors: molecular aspects. *Mol Cell Endocrinol* **2007**, *275*, 13-29, doi:10.1016/j.mce.2007.07.003.
180. Newton, R.; Holden, N.S. Separating transrepression and transactivation: a distressing divorce for the glucocorticoid receptor? *Mol Pharmacol* **2007**, *72*, 799-809, doi:10.1124/mol.107.038794.
181. Malatesta, M.; Steinhauer, C.; Mohammad, F.; Pandey, D.P.; Squatrito, M.; Helin, K. Histone acetyltransferase PCAF is required for Hedgehog-Gli-dependent transcription and cancer cell proliferation. *Cancer Res* **2013**, *73*, 6323-6333, doi:10.1158/0008-5472.CAN-12-4660.
182. Liu, Y.; Easton, J.; Shao, Y.; Maciaszek, J.; Wang, Z.; Wilkinson, M.R.; McCastlain, K.; Edmonson, M.; Pounds, S.B.; Shi, L., et al. The genomic landscape of pediatric and young adult T-lineage acute lymphoblastic leukemia. *Nature Genetics* **2017**, *49*, 1211-1218, doi:10.1038/ng.3909.
183. Heine, V.M.; Rowitch, D.H. Hedgehog signaling has a protective effect in glucocorticoid-induced mouse neonatal brain injury through an 11betaHSD2-dependent mechanism. *J Clin Invest* **2009**, *119*, 267-277, doi:10.1172/jci36376.

184. Heine, V.M.; Griveau, A.; Chapin, C.; Ballard, P.L.; Chen, J.K.; Rowitch, D.H. A small-molecule smoothed agonist prevents glucocorticoid-induced neonatal cerebellar injury. *Sci Transl Med* **2011**, *3*, 105ra104, doi:10.1126/scitranslmed.3002731.
185. Wang, Y.; Davidow, L.; Arvanites, A.C.; Blanchard, J.; Lam, K.; Xu, K.; Oza, V.; Yoo, J.W.; Ng, J.M.; Curran, T., et al. Glucocorticoid compounds modify smoothed localization and hedgehog pathway activity. *Chem Biol* **2012**, *19*, 972-982, doi:10.1016/j.chembiol.2012.06.012.
186. Chahal, K.K.; Parle, M.; Abagyan, R. Dexamethasone and Fludrocortisone Inhibit Hedgehog Signaling in Embryonic Cells. *ACS Omega* **2018**, *3*, 12019-12025, doi:10.1021/acsomega.8b01864.
187. Di Marcotullio, L.; Greco, A.; Mazza, D.; Canettieri, G.; Pietrosanti, L.; Infante, P.; Coni, S.; Moretti, M.; De Smaele, E.; Ferretti, E., et al. Numb activates the E3 ligase Itch to control Gli1 function through a novel degradation signal. *Oncogene* **2011**, *30*, 65-76, doi:10.1038/onc.2010.394.
188. Zhang, Q.; Shi, Q.; Chen, Y.; Yue, T.; Li, S.; Wang, B.; Jiang, J. Multiple Ser/Thr-rich degrons mediate the degradation of Ci/Gli by the Cul3-HIB/SPOP E3 ubiquitin ligase. *Proc Natl Acad Sci U S A* **2009**, *106*, 21191-21196, doi:10.1073/pnas.0912008106.
189. Zhang, R.; Huang, S.Y.; Ka-Wai Li, K.; Li, Y.H.; Hsu, W.H.; Zhang, G.J.; Chang, C.J.; Yang, J.Y. Dual degradation signals destruct GLI1: AMPK inhibits GLI1 through beta-TrCP-mediated proteasome degradation. *Oncotarget* **2017**, *8*, 49869-49881, doi:10.18632/oncotarget.17769.
190. Mirza, A.N.; McKellar, S.A.; Urman, N.M.; Brown, A.S.; Hollmig, T.; Aasi, S.Z.; Oro, A.E. LAP2 Proteins Chaperone GLI1 Movement between the Lamina and Chromatin to Regulate Transcription. *Cell* **2019**, *176*, 198-212.e115, doi:10.1016/j.cell.2018.10.054.
191. Mazza, D.; Infante, P.; Colicchia, V.; Greco, A.; Alfonsi, R.; Siler, M.; Antonucci, L.; Po, A.; De Smaele, E.; Ferretti, E., et al. PCAF ubiquitin ligase activity inhibits Hedgehog/Gli1 signaling in p53-dependent response to genotoxic stress. *Cell Death Differ* **2013**, *20*, 1688-1697, doi:10.1038/cdd.2013.120.



# LIST OF FIGURES

- Figure 1: Oncogenic pathways in T-ALL
- Figure 2: Schematic representation of normal T-cell differentiation in humans in relation to the different T-ALL molecular subgroups
- Figure 3: Overview of the canonical HH signalling pathway
- Figure 4: Mechanisms of HH pathway activation in cancer
- Figure 5: Transcripts of HH pathway components are aberrantly expressed in T-ALL cell lines
- Figure 6: Protein expression levels of HH pathway components in selected T-ALL cell lines
- Figure 7: HH pathway components are aberrantly expressed in T-ALL PDX samples
- Figure 8: HH pathway components are aberrantly expressed in Notch1-induced T-ALL murine models
- Figure 9: A subset of T-ALL cell lines and PDX samples are sensitive to HH inhibitor GANT61
- Figure 10: T-ALL cell lines are not sensitive to HH inhibition by cyclopamine
- Figure 11: Signalling pathways modulating sensitivity to HH pathway inhibitor GANT61
- Figure 12: GANT61 sensitizes T-ALL cell lines to Dexa treatment
- Figure 13: GANT61 and Dexa induce a synergistic pro-apoptotic effect in cell lines and PDX samples
- Figure 14: The combination of Dexa plus GANT61 predominantly exerts a pro-apoptotic effect
- Figure 15: Dexa induces heterogeneous modulation of HH signalling targets
- Figure 16: Dexa negatively affects GLI1 transcriptional activity
- Figure 17: RU486 reverts the effects of Dexa on GLI1 transcriptional activity
- Figure 18: Additional synthetic glucocorticoids can inhibit GLI1 function

Figure 19: GLI1 cellular distribution is not affected by Dexa

Figure 20: Dexa promotes GLI1 protein turnover

Figure 21: GLI1 interacts with NR3C1

Figure 22: Dexa treatment enhances GLI1 basal acetylation

Figure 23: HDAC1 activates, while p300 and PCAF repress, GLI1 transcriptional activity

Figure 24: Dexa dynamically regulates the interaction between HDAC1 and PCAF with GLI1

Figure 25: Proposed mechanism for the crosstalk between HH signalling pathway and the glucocorticoid receptor pathway

## **LIST OF TABLES**

Table 1: Genetic alterations in T-ALL

Table 2: Selected ongoing clinical trials for relapsed T-ALL

Table 3: Mechanisms of non-canonical activation of GLI1

Table 4: Primer sequences for Real time RT-PCR reactions

Table 5: Combination index values (CI) for Dexa and GANT61 combinations in T-ALL cell lines

Table 6: Combination index values (CI) for Dexa and GANT61 combinations in PDX-derived cells



# LIST OF ABBREVIATIONS

6-MP	6-Mercaptopurine
ABL1	Abelson murine leukemia viral oncogene homolog 1
AML	acute myeloid leukemia
B-ALL	B-cell lineage acute lymphoblastic leukemia
BCC	basal cell carcinoma
BCL2	B-Cell Lymphoma
BCR	breakpoint cluster region
bHLH	basic helix-loop-helix
BOC	brother of CDO
CAR	chimeric antigen receptor
CD	cluster of differentiation
CDKN2A	cyclin-dependent kinase inhibitor 2A
CDON	cell adhesion molecule-related/downregulated by oncogenes
CHX	cycloheximide
CK2	casein kinase 2
CML	chronic myeloid leukemia
CNS	central nervous system
CPM	cyclophosphamide
DN	double negative
DP	double positive
ETP-ALL	early T-cell precursor ALL
ETV6	ETS variant 6
FBXW7	F-box and WD repeat domain-containing 7
FLT3	fms related tyrosine kinase 3
GAS1	growth-arrest specific 1
GATA3	GATA Binding Protein 3

GC glucocorticoid  
GLI2R/3R GLI2/3 repressor forms  
GSK3- $\beta$  glycogen synthase 3 $\beta$   
HAT histone acetyltransferase  
HD heterodimerization domain  
HDAC1 histone deacetylase  
HES1 hairy and enhancer of split-1  
HH hedgehog  
HH-C hedgehog carboxy-terminal  
HHIP HH interacting protein  
HH-N hedgehog amino-terminal  
HOX homeobox  
ICN intracellular domain of NOTCH1  
IGF1R insulin-like growth factor  
IL-7R interleukin-7-receptor  
IP immunoprecipitation  
JAK Janus kinase  
KIF7 kinesin-like protein 7  
LEF1 lymphoid enhancer binding factor 1  
LMO LIM-only domain  
LYL1 lymphoblastic leukemia associated hematopoietic regulator 1  
MB medulloblastoma  
MM multiple myeloma  
mTOR mammalian target of rapamycin  
MTX methotrexate  
MYC avian myelocytomatosis viral oncogene homolog  
NKX2 NK2 homeobox  
NUP214 nucleoporin 214  
PCAF p300/CBP-associated factor

PDX patient-derived xenografts  
PEST proline, glutamic acid, serine, threonine-rich domain  
PGR prednisone good responders  
PHF6 plant homeodomain factor gene 6  
PI propidium iodide  
PI3K phosphoinositide 3-kinase  
PKA protein kinase A  
PPR prednisone poor responders  
PTCH1 patched1  
PTEN phosphatase and tensin homolog  
PTPN11 protein phosphatase non-receptor type 11  
RAS rat sarcoma viral oncogene homologs  
RUNX1 runt related transcription factor 1  
SMO smoothed  
SP single positive  
STAT signal transducer and activator of transcription  
SUFU suppressor of Fused  
TAL1 T-cell acute lymphoblastic leukemia 1  
T-ALL T-cell acute lymphoblastic leukemia  
TLX1/HOX11 T-cell leukemia homeobox 1  
USP7 ubiquitin specific peptidase 7  
WT1 Wilms Tumor 1  
 $\beta$ TrCP  $\beta$ -transducin repeat-containing protein

